

Analyzing Biological Activity of Drugs

Inter- and Intracellular Signaling Analysis
within an Organotypic Co-Culture System

Dissertation

**der Mathematisch-Naturwissenschaftliche Fakultät
der Eberhard Karls Universität Tübingen**

zur Erlangung des Grades eines
Doktors der Naturwissenschaften
(Dr. rer. nat.)

vorgelegt von
Michael Schmohl
aus Nürtingen

Tübingen 2011

Tag der mündlichen Prüfung: 30.11. 2011

Dekan:	Prof. Dr. W. Rosenstiel
1. Berichterstatter:	Prof. Dr. S. Stevanović
2. Berichterstatter:	Prof. Dr. S. Laufer

Acknowledgement

This thesis was prepared at the Natural and Medical Sciences Institute at the University of Tübingen-NMI in the department of biochemistry headed by Dr. Thomas Joos.

Initially I would like to thank my advisor **Prof. Dr. Stefan Stevanović** for the supervision of this thesis. I would like to acknowledge **Prof. Dr. Stefan Laufer** for the agreement to supervise my thesis as the 2nd examiner.

I gratefully thank **Dr. Thomas Joos** and **Dr. Nicole Schneiderhan-Marra** for giving me the opportunity to do this thesis at the NMI and for providing me with great support throughout all work stages.

Special thanks go to **Dr. Manfred Schmolz, Dr. Gerburg Stein, Kathrin Hefner and Michael Blum** at the EDI GmbH for providing me with valuable sample material, complementary data sets and for their scientific support.

I would like to thank **Dr. Jochen Schwenk** at the KTH Royal Institute of Technology, Stockholm for giving me the chance to join his lab in summer 2010 for a exciting time abroad. In this context I would also thank the **European Molecular Biology Organization EMBO** for their financial support during this stay.

Many thanks also go to my **friends and colleagues** at the NMI, for their assistance, help and for the good working atmosphere.

I deeply thank **my parents and my brother Jörg** for their encouraging support, love and trust in me throughout my life. And finally I dearly thank **Mareike** for her love, patience and for a wonderful time together.

Table of Contents

List of Abbreviations	X
List of Figures	XII
List of Tables	XIV
Abstract	XV
1. Introduction	1
1.1. Model systems in drug development.....	1
1.2. The co-culture model of the human gut	3
1.3. Receptor Tyrosine Kinase associated signaling processes	5
1.4. Mediators of the immune response.....	6
1.4.1. Cells of the immune system.....	7
1.4.2. Cytokines/Chemokines	9
1.4.3. Soluble receptors and cell adhesion molecules	10
1.4.4. In vitro activation of immune cells	11
1.5. Antiphlogistic drugs.....	11
1.5.1. Corticosteroids.....	11
1.5.2. NSAIDs	12
1.5.3. Tacrolimus	12
1.6. Multiplexed Sandwich Immunoassays	13
1.6.1. Suspension-bead arrays	13
1.6.2. Bead arrays for signaling pathway analysis	14
2. Research Objectives.....	16
3. Materials and Methods	17
3.1. Materials	17
3.1.1. Sandwich Immunoassays	17
3.1.2. Antibodies and proteins	17
3.1.3. Expendable items	17
3.1.4. Buffers	18

3.1.5.	Devices and Software.....	18
3.1.6.	Chemicals and Reagents.....	19
3.1.7.	Whole blood donors.....	20
3.2.	Suspension bead arrays	20
3.2.1.	Coupling antibodies to microspheres.....	20
3.2.2.	Multiplexed Assay Panels.....	21
3.3.	Cell culture methods	23
3.3.1.	Intracellular RTK-Signaling Analysis.....	23
3.3.2.	Cell culture in transwell® Inserts	24
3.3.3.	Immunohistochemistry.....	25
3.3.4.	Co-culture experiments.....	25
3.3.5.	Whole blood culture assays.....	27
3.4.	Data analysis	27
3.4.1.	The IPA® knowledge base	27
3.4.2.	Hierarchical Clusteranalysis	27
4.	Results.....	28
4.1.	Sandwich Immunoassay Development.....	28
4.1.1.	Cross-Reactivity.....	29
4.1.2.	Titration of detection antibody concentration	30
4.1.3.	Optimization of Assay-Recovery.....	32
4.1.4.	Assayperformance.....	33
4.2.	Caco-2 monolayer as a model for the intestinal barrier	34
4.2.1.	Impact of proinflammatory cytokines on the epithelial barrier	35
4.2.2.	Effect of proinflammatory cytokines on cell junctions.....	36
4.2.3.	Effect of proinflammatory mediators on chemokine release	37
4.2.4.	Intracellular signaling analysis	38
4.3.	In-vitro analysis of drug effects	44
4.3.1.	Addressing subsets of immune cells.....	45
4.3.2.	Effect of Dexamethasone on immune mediator release	48

4.3.3.	Effect of Prednisolone on immune mediator release	51
4.3.4.	Effect of Ibuprofen on immune mediator release	55
4.3.5.	Effect of Diclofenac on immune mediator release.....	58
4.3.6.	Effect of Tacrolimus on immune mediator release	61
4.3.7.	The co-gut system as a test model for drug candidates.....	64
4.3.8.	Summary of drug effects.....	68
5.	Discussion.....	71
5.1.	Multiplexed Sandwich Immunoassays	71
5.2.	Caco-2 cells as a model of the intestinal barrier	73
5.3.	Analysis of RTK signaling in Caco-2 cells.....	77
5.4.	Analyzing biological activity of drugs.....	80
5.4.1.	Specific activation of immune cells	80
5.4.2.	Analyzing biological drug activity: Corticosteroids	81
5.4.3.	Analyzing biological drug activity: NSAIDs.....	85
5.4.4.	Analyzing biological drug activity: Tacrolimus.....	87
5.4.5.	Effects of drug candidates on the release of immune mediators.	90
6.	Summary and Outlook.....	91
7.	Zusammenfassung und Ausblick.....	93
8.	References	96
9.	Supplementary Material	110
10.	List of Publications.....	117
11.	Akademische Lehrer.....	118
12.	Curriculum Vitae	119

List of Abbreviations

AU	Arbitrary Units
BMBF	Bundesministerium für Bildung und Forschung
BSA	Bovine Serum Albumin
CAMK	Calmodulin-dependent protein kinase
CD	Cluster of Differentiation
COX	Cyclooxygenase
CV	Coefficient of Variation
DMSO	Dimethyl Sulfoxide
EDC	1-Ethyl-3-[3-dimethylaminopropyl]carbodiimide hydrochloride
EDTA	Ethylenediaminetetraacetic Acid
EGF	Epidermal Growth Factor
EGFR	EGF-Receptor
ELISA	Enzyme-Linked Immunosorbent Assay
FDA	Food and Drug Administration
HAMA	Human anti-mouse antibodies
HBSS	Hanks Balanced Salt Solution
HOT	Human Organotypic Testsystems
HuCoCSys	Human organotypic Co-culture Systems
IBD	Inflammatory Bowel Disease
IFN- γ	Interferon gamma
IHC	Immunohistochemistry
IL	Interleukin
IP-10	Interferon gamma-induced protein 10
JNK	C-Jun N-terminal kinase
kDa	kilodalton
LOD	Lower limit of detection
LOQ	Lower limit of quantification
LPS	Lipopolysaccharid
M	molar
MAPK	Mitogen Activated Kinase
MCP-1	Monocyte Chemoattractant Protein-1
MEM	Minimum Essential Medium
MFI	Median Fluorescence Intensity
M Φ	Macrophage
N/A	Not available
NBS	Non-Binding Surface
NF κ B	nuclear factor kappa-light-chain-enhancer of B-cells

NMI	Natural and Medical Sciences Institute
NSAID	Non Steroidal Antiinflammatory Drug
PAMP	pathogen associated molecular pattern
PBMCs	Peripheral Blood Mononuclear Cells
PBS	Phosphate Buffered Saline
PBS-	Phosphate Buffered Saline without Ca ²⁺ /Mg ²⁺
PE	Phycoerythrin
PFA	Paraformaldehyd
PG	Prostaglandin
RT	Room Temperature
RTK	Receptor Tyrosine Kinase
S/N	signal to noise ratio
SAM	Significance Analysis for Microarrays
sdv	standard deviation
SEB	Staphylococcus aureus Enterotoxin B
SEM	Scanning electron microscope
Sulfo-NHS	N-hydroxysulfosuccinimide
TEER	transepithelial electric resistance
Th	T-helper
TLR	Toll-like Receptor
TNF α	Tumor Necrosis Factor alpha
Treg	Regulatory T-cell
TSLP	Thymic Stromal Lymphopietin
Tween 20	Polyethylene glycol sorbitan monolaurate
ULD	Upper limit of detection
w/o	without
α	anti

List of Figures

Figure 1: Phases of the drug development process.....	2
Figure 2: Cell junction complexes of the intestinal epithelium.....	4
Figure 3: Experimental set up of the co-culture model.....	5
Figure 4: Phosphosites of the EGF-Receptor.	6
Figure 5: The regulatory network of the immune system.	7
Figure 6: The Luminex xMAP® technology.....	14
Figure 7: Experimental workflow of drug testing in the co-culture model	26
Figure 8: Multiplexed sandwich immunoassays.	29
Figure 9: Optimization of detection antibody concentration.....	31
Figure 10: Comparison of assay recovery for Panel I.	32
Figure 11: Impact of proinflammatory mediators on TEER.	35
Figure 12: Immunohistochemical analysis of cell junction proteins in Caco-2 cells..	36
Figure 13: Effect of IL-1 β and EGF on RTK phosphorylation.....	39
Figure 14: Effect of IL-1 β and EGF on EGFR phosphorylation	40
Figure 15: Time course of S1047 phosphorylation upon IL-1b treatment.	41
Figure 16: Distribution of signal intensities upon inhibitor treatment.	42
Figure 17: Kinase-inhibitor screening in IL-1 β stimulated Caco-2 cells.....	43
Figure 18: In-vitro analysis of drug effects.	44
Figure 19: Hirarchical Clusteranalysis of immune mediator concentrations.....	47
Figure 20: Release of immune mediators after Dexamethasone application.....	50
Figure 21: Release of immune mediators after Prednisolone application.	54
Figure 22: Release of immune mediators after Ibuprofen application	57
Figure 23: Release of immune mediators after Diclofenac application.	60
Figure 24: Release of immune mediators after Tacrolimus application.....	63
Figure 25: Effect of Dihydroxyguajaretic Acid on the release of immune mediators.	67
Figure 26: The assay development process	72
Figure 27: Pathway model of the crosstalk between IL-1RI and EGFR.	79
Figure 28.: Signaling pathways of glucocorticoid action.....	83
Figure 29: Effects of NSAIDs on immune mediator secretion	86
Figure 30: Effects of Tacrolimus on the release of cytokines and chemokines.	88
Supplementary Figure 1: Titration of detection antibodies in Panel II.	111

Supplementary Figure 2: Titration of detection antibodies in Panel III..... 112
Supplementary Figure 3: Optimization of Spike-in recovery for Panel II+III. 113

List of Tables

Table 1: Immune mediators and their main cellular sources.	9
Table 2: Immune stimulating agents.....	11
Table 3: Antibodies and recombinant proteins	17
Table 4: Expendable items	17
Table 5: Buffers	18
Table 6: Devices and Software.....	18
Table 7: Chemicals and Reagents	19
Table 8: Concentrations of reagents applied in cytokine Panels I-III	22
Table 9 : Concentrations of reagents applied in the soluble receptor panel	23
Table 10: Control samples for drug testing.....	27
Table 11: Analysis of cross-reactivities in Panel I.....	30
Table 12: Performance of multiplexed sandwich assays	33
Table 13: Effect of proinflammatory cytokines on chemokine release.....	37
Table 14: Summary of drug effects in the co-culture model of the human gut.....	70
Table 15: Summary of test substances and measured immune mediatorsTable	80
Supplementary Table 1: Cross-reactivities in Panel II.	110
Supplementary Table 2: Cross reactivities in Panel III.....	110
Supplementary Table 3: InhibitorSelect™ protein kinase Inhibitors.....	114
Supplementary Table 4: Concentration data after immune activation.....	115
Supplementary Table 5: Concentrations data in supernatant controls.	116

Abstract

The human immune system represents a highly complex multi-cellular network that protects the organism against the environment and disease. Within this system, different immune cell types communicate with each other, as well as with healthy and diseased tissues, using an impressive network of immunoregulatory signals. This inherent complexity makes it rather difficult to mimic these processes *in vitro*. Therefore, elaborate *in vivo* like test models are needed. The aim of this study was to characterize a compartmentalized co-culture model of the human gut comprising Caco-2 cells as a model for the gut epithelium and whole blood of different donors representing the immune system.

The characteristics of Caco-2 cells upon treatment with proinflammatory mediators were investigated in detail using immunohistochemistry and functional measurements. The multiplexed analysis of intracellular signaling processes in Caco-2 cells provided a closer look at the alterations that take place after treatment with proinflammatory cytokines. The co-culture system was then applied to analyze the intercellular signaling processes in whole blood upon application of drugs and drug candidates. The test substances were applied onto the top of differentiated Caco-2 monolayers and their effect on the release of inflammatory mediators in the whole blood was analyzed using multiplexed sandwich immunoassays. By using blood from different donors, the individual variations in the immune system could be included in the analysis. The immunomodulatory effects observed for well-characterized substances as well as drug candidates were analyzed and interpreted using bioinformatic database analyses. Among the 23 different analyzed immune mediators 13 revealed concentration dependent changes upon drug treatment.

The combined usage of a human organotypic gut model with a multi-parametric read out system facilitated the testing of drugs and drug candidates in an *in vivo* like environment. This approach has the potential to fill the gap existing between currently used cell culture systems, animal models and clinical trials and may therefore contribute to the drug candidate selection process in future.

1. Introduction

1.1. Model systems in drug development

Despite the tremendous technological progress made in drug screening technologies a large number of drug candidates fail during clinical phases I-III due to a lack of overall activity or a problematic safety profile. This can mainly be traced back to the fact that during the preclinical phase of drug development the test systems used do not necessarily reflect the *in vivo* situation in the human body. Drug candidates originally intended to specifically interfere with a pathologic process often influence other intra- and intercellular signaling pathways that are not available in currently used test models.

Cell culture models, which are widely used in the preclinical phase of the drug development process (**figure 1**) show excellent reproducibility and low assay-to-assay variability. However, since cell lines are derived from modified, degenerated cells they do not entirely reflect the *in vivo* conditions in the human body. Animal models by contrast allow drug testing in a complex multi-cellular environment. However depending on the species used e.g. rodent models, pigs or even apes, they exhibit more or less similarity to the human system and although they can be genetically engineered there are still intrinsic differences between animals and human. Moreover, a distinct diversity among individual human beings further exacerbates the search for appropriate model systems. In consequence a gap exists between currently used *in vitro* models and clinical trials [1].

The immune system consists of a highly complex network of signaling events. The different cells of the immune system communicate with each other, as well as with healthy and diseased organs [2, 3]. This inherent complexity makes it extraordinary challenging to find appropriate cell culture models that sufficiently mimic these conditions. The most often used cellular test systems for the evaluation of drug effects on the immune system are Peripheral Blood Mononuclear Cell (PBMC) preparations or test systems using whole blood (e.g. [4]). In contrast to PBMCs, peripheral whole blood consists of all cellular and sub-cellular components of the immune system and exhibits the following benefits [1]:

1. Presence of erythrocytes, thrombocytes, granulocytes
2. Presence of sub-cellular plasma components
3. Individuality can be incorporated by using blood of different donors
4. Stress caused by preparation procedure is minimized
5. Cells remain in their natural environment
6. No serum supplements are necessary
7. Plastic adherence is minimized

However not all cells contributing to immune reactions are represented in peripheral whole blood. The development of human organotypic co-culture systems (HOT) therefore represents a further approximation to the *in vivo* conditions. The co-cultivation of tissue specific cells with human whole blood allows establishing the crosstalk between the immune cells represented by the whole blood and cells of the adjacent organ. These approaches represent a valuable alternative to animal experiments, have a considerably higher similarity to the *in vivo* situation and are very important tools to bridge the gap between immune reactivity in animal models and humans. Drugs interfering with the complex regulatory network of the immune system lead to changes in the activities of the immune cells and this sometimes leads to dramatic changes in the course of the immune reactions. By co-cultivating whole blood and epithelial cells the entire range of immune-relevant elements can be included [5].

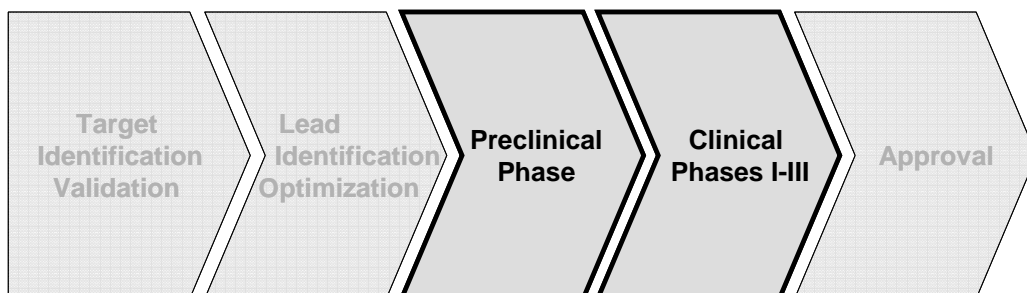


Figure 1: Phases of the drug development process

1.2. The co-culture model of the human gut

The organotypic co-culture model used in this study (**figure 3**) facilitates the testing of drug effects that take place after passage of the intestinal barrier. Therefore, the human Caco-2 cell line is used as a model for intestinal epithelium cells. These cells are cultivated on the top side of membranous transwell® inserts (pore size 0.4µM), fitting into carrier wells, which contain whole-blood. The differentiated Caco-2 cells represent the physiological barrier to orally applied drugs or drug candidates added on top of the epithelium, whereas whole blood of individual donors represents the immune system. Drugs and drug candidates are added onto the Caco-2 monolayer, and their effect on the cells of the immune system can subsequently be analyzed in the whole blood [1, 5]. The addition of immune activating agents like for example bacterial cell wall components (Lipopolysaccharide, Zymosan), superantigens (Staphylococcal Enterotoxine B) and receptor targeting antibodies (anti-CD3, anti-CD28) allows to trigger the immune response in the whole blood. Depending on the stimulus used, different subsets of immune cells can be addressed.

The heterogeneous colorectal adenocarcinoma cell line Caco-2, first characterized by Hidalgo et al. [6] is widely accepted across the pharmaceutical sciences as a *in vitro* model of the human small intestine mucosa [7-9]. Cultivated as monolayers on permeable filters these cells are routinely used to study the intestinal absorption and transepithelial transport of orally administered drugs [10] in accordance with FDA and EMEA guidelines [11]. Upon confluence Caco-2 cells become differentiated and polarized such that they display all major functional and morphological properties of small intestine epithelial cells including the formation of intercellular adhesion complexes, microvilli formation and the expression of small intestine-specific gene products e.g. transporter proteins and enzymes [12].

A schematic overview of the major types of cell junctions connecting intestinal epithelial cells as well as their proteinous components is given in **figure 2**. Tight junctions, consisting of the transmembrane proteins Occludin, Claudin and JAMs and the adapter proteins ZO-1 and Cingulin control the diffusion of many substances between the gut lumen and blood through the extracellular space. Gap junctions allow the exchange of small molecules and ions between adjacent cells and are mainly

composed of connexins. Adherence junctions composed of the transmembrane protein Cadherin and the intracellular adapters Catenin and ZO-1 as well as desmosoms composed of Desmoglein, Desmocollin and Desmoplakin are important for cell-cell and cell matrix adhesion and signaling [13].

Accomplishment of full differentiation of the Caco-2 cells can be assessed microscopically by dome formation [14]. Thus these cells are perfectly suited for the generation of gut epithelial monolayers capable of all known active and passive absorption mechanisms [15], as well as the potential to respond to pathogens and to inflammatory mediators [7].

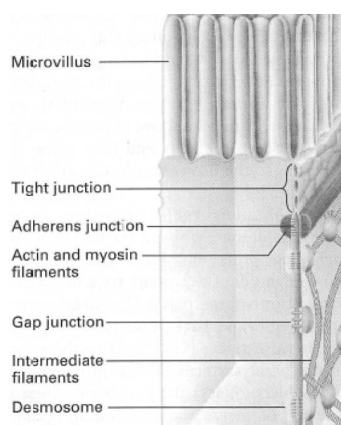


Figure 2: Cell junction complexes of the intestinal epithelium.

Tight junctions control the diffusion of many substances between the lumen and blood. Gap junctions allow the exchange of small molecules and ions between adjacent cells. Adherence junctions and desmosoms are important for cell-cell and cell matrix adhesion and signaling. Adapted from [13].

Proinflammatory mediators like IL-1 β , TNF α and IFN γ which are up regulated during chronic inflammatory conditions of the gut [16-18] have been reported to affect the intestinal barrier function by modulating tight junction permeability [3, 19-24]. In contrast EGF functions as a gastrointestinal mucosal protective factor preventing the oxidant induced disruption of tight junctions [25, 26]. Treatment of Caco-2 monolayer with these proinflammatory cytokines can be used to simulate the altered type of regulation and organ function as it is related to inflammatory processes. Additionally such treatment stimulates the production of immune-regulatory mediators by the epithelial cells [27].

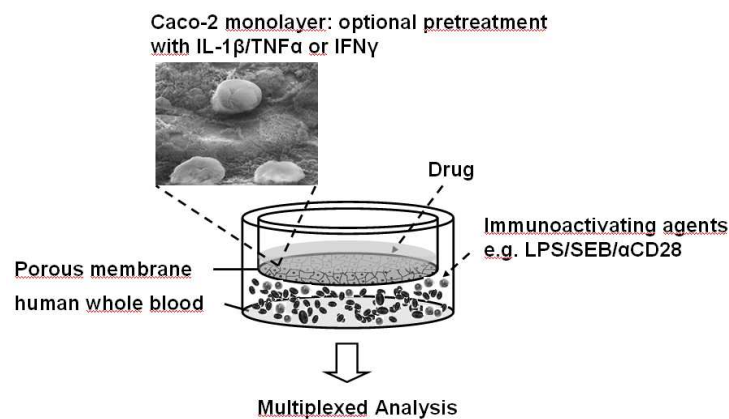


Figure 3: Experimental set up of the co-culture model.

Human CaCo-2 cells are cultivated on top of special culture vessels, fitting as inserts into carrier wells of 24-well culture plates. A filter membrane allows a communication between the two compartments via soluble signaling molecules. Pre-treatment of the Caco-2 cells with proinflammatory mediators allows mimicking alterations in the epithelial barrier function. Drugs and drug candidates are added onto the Caco-2 monolayer, and their effect on the immune response can be analyzed in the whole blood using multiplexed sandwich immunoassays. The addition of immune activating agents like LPS, Zymosan, Staphylococcal Enterotoxine B and receptor targeting antibodies (anti-CD3, anti-CD28) is used to trigger the immune response in the whole blood. SEM picture adapted from www.edigmbh.de

1.3. Receptor Tyrosine Kinase associated signaling processes

Receptor Tyrosine Kinases (RTKs) represent a class of cell-surface receptors that regulate a plethora of cellular processes including cell proliferation and differentiation, cell survival, migration, apoptosis and protein expression [13, 28]. On a structural basis RTKs can be divided into 20 subfamilies which share an intrinsic catalytic tyrosine kinase domain. Examples include the ErbB family, the Insulin receptor family and the PDGF, FGF, VEGF and HGF families [29]. Ligand binding to the extracellular domain leads to receptor dimerization and the subsequent activation of the intrinsic tyrosine kinase activity. This leads to the autophosphorylation of tyrosine residues and the subsequent recruitment of adapter proteins to the receptor which in turn triggers several intracellular signaling pathways e.g. the Ras/MAP-Kinase pathway or the PLC γ pathway. In addition the activation of other intracellular signaling pathways can lead the phosphorylation/dephosphorylation of RTKs by intracellular kinases and phosphatases.

The epidermal growth factor receptor (EGFR) is a member of the ErbB family of RTKs. Changes in expression and aberrant activation of EGFR have been shown to be associated with a variety of cancers [28]. Upon binding of its specific ligands e.g. epidermal growth factor (EGF) and transforming growth factor alpha (TGF α), dimeri-

zation triggers the intrinsic tyrosine kinase activity. This results in the autophosphorylation of Tyrosine residues in the C-terminal domain and the subsequent activation of various downstream signaling molecules. Phosphorylation of intracellular Serine and Threonine residues is thought to represent a mechanism for attenuation of EGFR kinase activity [30]. The EGFR receptor is subject to various intracellular interaction partners regulating the phosphorylation status of intracellular Threonin, Serine and Tyrosine residues with diverse biological effects [31]. **Figure 4** schematically shows the phosphorylation sites that were analyzed in this study as well as their potential interaction partners and downstream effects.

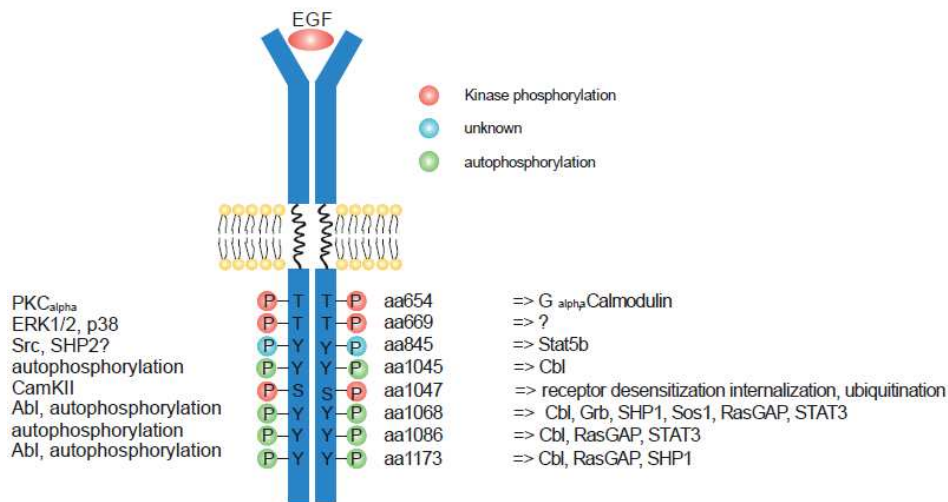


Figure 4: Phosphosites of the EGF-Receptor. Adapted from Oliver Poetz

1.4. Mediators of the immune response

The human immune system represents a highly complex cellular network that protects the organism against diseases. Within this network complex intercellular communication processes are mediated via cytokines and chemokines, surface receptors and antagonists, eicosanoids, complement factors, coagulation factors and even low molecular weight mediators that control the fate and functions of immune cells. Maintenance of the delicate balance at the level of these mediators is essential for health and disruption of homeostasis is implicated in the pathogenesis of a large variety of diseases like for example Inflammatory Bowel Disease (IBD) [17, 32, 33], Sepsis [34], Rheumatoid Arthritis [35] and Arteriosclerosis [36]. **Figure 5** gives an simplified

overview of the major subtypes of immune cells as well as the associated key regulatory signaling processes among them.

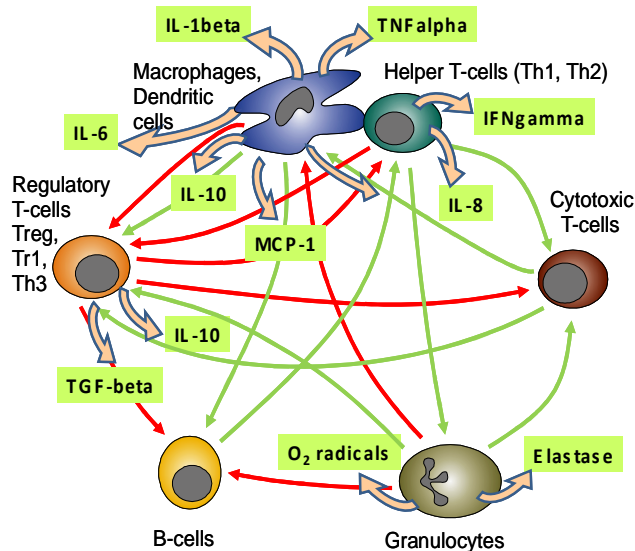


Figure 5: The regulatory network of the immune system. Adapted from [1]

1.4.1. Cells of the immune system

A detailed description of the different subsets of immune cells is given by Murphy *et al.* [37]. Leukocytes are the major players of the immune system. *Macrophages* are the mature tissue-form of the blood circulating *monocytes* and can be found in almost all tissues of the body. Both macrophages and monocytes are phagocytic, recognizing and killing invading pathogens. Moreover, they function as antigen presenting cells (APC) thus contributing to the induction of the adaptive immune response. By secreting soluble signaling molecules like cytokines and chemokines they can activate and recruit other immune cells.

Like the macrophages *granulocytes* are also responsible for the first line killing of invading microorganisms at the site of infection. Three types of granulocytes - *neutrophils*, *basophils* and *eosinophils* can be distinguished of which the neutrophils are the most numerous. They phagocytize invading microorganisms and destroy them using degradative and antimicrobial substances. Eosinophils and basophils are thought to participate in the defense against parasites which are too large for phagocytosis. Mature *Dendritic Cells* are also tissue resident phagocytes. They are present in the blood stream by their immature form. Both forms take up antigens by phagocytosis and macropinocytosis and display these antigens on their surfaces upon degrada-

tion. They are specialized in presenting antigens to lymphocytes thus initiating adaptive immune responses. Macrophages, granulocytes and dendritic cells recognize distinct pathogen associated molecular patterns (PAMPs) via specific pattern recognition receptors. Examples are Toll-like receptors (TLR) or NOD-like receptors. The activation through pattern recognition receptors is a prerequisite for the expression of co-stimulatory molecules on the surface of antigen presenting cells and the subsequent complete activation of naive T-lymphocytes.

B-lymphocytes play an essential role in the humoral immune response. After binding of a specific antigen to the B-cell receptor, the lymphocytes proliferate and differentiate into plasma cells. These cells produce antibodies, which are the secreted form of the B-cell receptor. However, for activation of the B-cell a co-stimulation provided by a T-helper cell is required (except T-cell independent antigens).

T-lymphocytes play a central role in the cell mediated immunity. They can be classified into two major groups CD4 positive and CD8 positive cells. Upon activation by antigen presenting cells CD8⁺ T-cells differentiate into cytotoxic T-cells capable of directly killing pathogen infected cells. CD4⁺ T-cells differentiate into diverse effector types depending on the signals they receive during activation. In particular, the four main subsets Th1, Th2, Th17 and Treg can be distinguished by their cytokine secretion profile.

Th1 cells produce cytokines that activate macrophages, enabling them to destroy incorporated microorganisms more efficiently. In addition, they provide co-stimulatory signals for B-lymphocytes and induce class switching to strongly opsonizing antibody subclasses. *Th2 cells* carry out a similar function of activating B-cells and inducing class switching to other antibody subclasses especially IgE. *Th17 cells* induce local epithelial and stromal cells to produce chemokines that recruit neutrophils to the site of infection. The *regulatory T-cells Treg* represent a heterogeneous subgroup that suppresses T-cell activity thus limiting the immune response.

1.4.2. Cytokines/Chemokines

Cytokines are secreted or membrane-bound structurally diverse proteins with a molecular weight of approximately 25 kDa that are released by various cell types (e.g. leukocytes, fibroblasts, epithelial cells, hepatocytes) usually in response to an activating stimulus. Cytokines induce responses through binding to their specific receptors. They can act in a autocrine, paracrine and endocrine manner [37]. Cytokines play a key role in the modulation of the immune cell activity. They are rapidly synthesized and secreted by immune cells upon stimulation and induce the production of adhesion molecules, oxygen metabolites, nitric oxide and lipid mediators such as prostaglandins, leukotriens and platelet-activating factor [17].

Cytokines are generally grouped in two categories proinflammatory and anti-inflammatory cytokines, although several cytokines do not fit specifically into either one of these categories. Many cytokines have pleiotropic functions and some act in a synergistic manner. In addition they can also be grouped on a structural basis [37] or based on their main cellular source into Th1, Th2, Treg, Th17 and macrophage/monocyte derived cytokines. **Table 1** shows the different immune mediators analyzed in this study as well as their main cellular sources. Th1 cytokines are commonly referred to as proinflammatory while Th2 cytokines mainly induce anti-inflammatory responses [38]. However, the fact that many cytokines have overlapping cellular sources and diverse biological functions hampers an exact classification. Chemokines are a family of small cytokines with a size of 8-10 kDa released in the early phase of an immune response. These chemo-attractant mediators induce directed chemotaxis of susceptible immune cells mainly of monocytes, neutrophils, basophils and T-lymphocytes thus recruiting them to the site of infection [39-41].

Table 1: Immune mediators and their main cellular sources. Adapted from [5]

MΦ /Monocytes	TH1	TH2	TH17	Treg	others
IL-1β	IFNγ	IL-4	IL-17A	IL-10	TARC
IL-6	IL-12p70	IL-5			TSLP
TNFα	IP-10	IL-13			IL-1ra
IL-8					
MCP-1					

1.4.3. Soluble receptors and cell adhesion molecules

In addition to the classical notion of cytokine receptors as transmembrane proteins, many receptors have soluble forms that are released into the extracellular space. They are produced through alternative mRNA splicing or cleavage from the cellular surface (shedding) and released into the extracellular milieu. Due to their ability to bind ligand they can modulate the balance between cytokines and their membrane-bound receptors. On the other hand, soluble receptors can bind their ligands, stabilize them, and may induce cellular responses by association with signaling receptor subunits thus acting as a cytokine agonist [42].

There is evidence that receptor expression and shedding can be regulated by other cytokines and that this plays an important role in the pathogenesis of human diseases [2]. The exact role of the soluble cytokine receptors still remains unclear but it is generally assumed that they are important regulators of inflammation and immunity [43]. The TNF receptor-associated periodic syndrome which occurs in patients with an impaired TNFR1 receptor shedding demonstrates the importance of this immune-regulatory mechanism [44] as well as the finding that sgp130 acts as a negative regulator of the IL-6 induced acute phase response in hepatocytes [45]. Moreover the role of soluble cytokine receptors as regulators of immune events is shown by sIL-2R α which was used as biomarker for T-cell activation lymphoid neoplasms [46].

Cell adhesion molecules play an important role for the recruitment of leukocytes from the blood to the site of inflammation. In addition, soluble forms of these endothelial-derived adhesion molecules can be detected in circulating blood and may serve as biomarkers of the extent of inflammatory response, and endothelial damage [47-49]. For example increased circulating concentrations of the adhesion molecules ICAM-1, and VCAM-1 can be found in the sera of inflammatory bowel disease patients [50]. However, the exact role of soluble cell adhesion molecules remains unclear. It has been suggested that they act as chemotaxins on monocytes [51] or as negative regulators of cell-cell adhesion processes [52].

1.4.4. In vitro activation of immune cells

In order to investigate drug effects on the *in vitro* secretion of inflammatory mediators in whole blood it is necessary to elicit immune cell function by using stimulatory agents. The use of antibodies, bacterial cell wall components, and mitogens is hereby well established [53-55]. The immune stimulating agents applied in this study, their cellular target, as well as their reported effect on mediator release are described in detail in **table 2**.

Table 2: Immune stimulating agents

stimulus	description	Target receptor/cell type	triggered mediators
Zymosan	yeast membrane glycoprotein	TLR2/complement, macrophages/monocytes, granulocytes	TNF α , IL-8 [56-59]
LPS	membrane component of gram-negative bacteria	LBP/ CD14/ TLR4/ MD2, macrophages, monocytes, dendritic cells, epithelial cells, granulocytes	IL-1 β , IL-6, IL-8, IL-12, TNF α , TARC, IFN γ [60-62]
SEB	superantigene	MHCII/ TCR on antigen presenting cells and T-cells	IL-12p70 [63], IL-1 β [64], IL-2, TNF α , IL-6, IFN γ , MCP-1 [65] IL-8
α CD28	anti-CD28 antibody	CD28 , co-stimulatory signal	IFN γ
α CD3	anti-CD3 antibody	CD3 on T-lymphocytes	IFN γ
Poly I:C	double stranded RNA	TLR3 on B-lymphocytes and dendritic cells	IL-6, TNF α , IL-10 [66], IP-10 [67]

1.5. Antiphlogistic drugs

1.5.1. Corticosteroids

Synthetic glucocorticoids like Prednisolone and Dexamethasone mimic natural glucocorticoids and are widely used in the treatment of inflammatory disorders like for example inflammatory bowel disease and rheumatoid arthritis [68, 69]. They are known to systemically inhibit the entire immune response including T-cell activation, adhesion molecule expression, effector cell activation and cytokine production [70]. After binding to the glucocorticoid receptor a pleiotropic range of interactions with intracellular signaling pathways take place. Direct interaction with glucocorticoid response elements (transactivation) leads to an upregulation expression of proteins that are implicated in the resolution of inflammation e.g. Annexin 1, which in turn inhibits the release of arachidonic acid [71-73]. The glucocorticoid receptor can also directly interact with other transcription factors (transrepression) such as NF κ B and AP-1 [74] thus preventing the transcription of proinflammatory cytokines [75, 76].

1.5.2. NSAIDs

Non-steroidal anti-inflammatory drugs (NSAIDs) like Diclofenac, Ibuprofen or Aspirin act as inhibitors of cyclooxygenase isoenzymes COX-1 and COX-2 and are widely used as analgesic, antipyretic and anti-inflammatory drug [77]. COX catalyzes the conversion of arachidonic acid into prostaglandins and thromboxanes. Whereas COX-1 is constitutively expressed in nearly all tissues the expression of COX-2 can be induced in response to hormones, growth factors and proinflammatory cytokines. In addition of the diverse physiologic and pathologic functions prostaglandins exert various functions in the regulation of inflammation and immunity [78]. Prostaglandin D₂ (PGD₂) is a proinflammatory mediator produced and released mainly by mast cells during an allergic response. It has been demonstrated to be a potent chemoattractant for eosinophils, and Th2 cells [79, 80]. Prostaglandin E₂ (PGE₂) is the major prostaglandin involved in pain and inflammation. It is secreted by macrophages, monocytes, and neutrophils upon treatment with inflammatory mediators, whereas lymphocytes do not produce any of the prostanoids [81, 82]. PGE₂ inhibits IL-2 and IFN γ production from T-lymphocytes as well as the release of IL-1 and TNF α by macrophages [83-85]. Prostacyclin (PGI₂) is thought to exert anti-inflammatory action since PGI₂ analogues inhibit IFN γ /IL-6 induced MCP-1, IL-8, RANTES and TNF α production in monocytes [86] and led to an increased IL-10 production in LPS stimulated PBMCs [87].

1.5.3. Tacrolimus

Tacrolimus (FK506) is a macrolidic immunosuppressant drug used for the treatment of graft rejection after allogenic organ transplantations. It has also been shown to be effective in the therapy of ulcerative colitis [88, 89]. The immune suppressive effect of Tacrolimus is facilitated through complex-formation with the immunophilin FKBP12 and subsequent inhibition of Calcineurin. This prohibits the dephosphorylation and activation of NFAT thus inhibiting T-lymphocyte signal transduction [90-92]. T-cells express low intracellular levels of Calcineurin and this renders them more susceptible to inhibition of this pathway [37]. The inhibition of Calcineurin and its substrate NFAT is a major component of the immunosuppressive effect of Tacrolimus, however im-

mune suppression may also be accomplished through inhibition of other Calcineurin substrates or Calcineurin-independent effects [93].

1.6. Multiplexed Sandwich Immunoassays

Protein microarrays have become important tools for large-scale and high throughput applications. This technology enables the simultaneous detection and quantification of multiple parameters in complex biological mixtures like for example plasma [94] or tissue lysates [95]. Protein microarray technology is of major interest for proteomic and diagnostic applications as well as for drug discovery. This technology has been applied for the identification, quantification and functional analysis of proteins [96-99].

Roger Ekins [100, 101] initially described the basic principles of protein microarray technology. According to his “ambient analyte theory” superior sensitivity can be achieved with miniaturized ligand-binding assays. Because of the small number of capture molecules in a microarray spot ligand binding does not significantly alter analyte concentration even in the case of targets of low concentrations and high affinity binding reactions. Therefore, highest signal intensities per area and optimal signal to noise ratios can be achieved.

1.6.1. Suspension-bead arrays

Bead based arrays (e.g. Luminex) employ a set of up to 500 color or size coated microspheres as solid support for the capture molecules. Beads are identified in a flow cytometer and the amount of captured target molecules is quantified on each individual bead. In a first step, antigen-specific capture molecules are immobilized on the individual bead set. Then different bead sets are combined and incubated with the sample of interest. A labeled secondary antibody detects captured analytes and is visualized with an appropriate reporter system. Sensitivity, reliability and accuracy are similar to those observed with standard ELISA procedures. The preferred detection method for bound analytes is fluorescence. Using bead based technology hundreds of samples can be screened within a short time. Throughput and sample volume is no longer a limiting factor [97, 102].

The bead based xMAP® technology (Luminex, Austin, TX, USA) used in this study has experienced rapid adoption across many fields of the life sciences in the past few years. It is based on 100 distinct sets of color coded polystyrene beads, called microspheres (\varnothing 5,6 μ m) each coated with defined capture molecules. The mixture of two internal red-fluorescence dyes in different ratios creates the color code. Within the Luminex compact analyzer, a laser excites the internal dyes with 635 nm, and a second laser excites any green fluorescent reporter dye captured during the assay with 532 nm (**figure 6**). The Luminex LX100 standard instrument allows multiplexing of up to 100 unique assays with a single sample. For each bead set the fluorescence intensity is detected and the median fluorescence intensity (MFI), is determined [103].

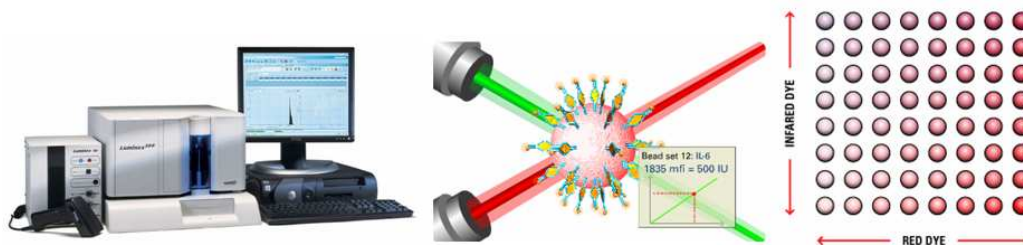


Figure 6: The Luminex xMAP® technology. Adapted from: [103]

1.6.2. Bead arrays for signaling pathway analysis

Inflammation is characterized by a plethora of inter- and intracellular signaling events. Each response arises from a dynamic network of thousands of molecules that are subject to multiple influences [104]. Due to this complexity a complete set of mediators is considered to be of more value than the single analysis of only one mediator [105]. To study these processes on a systemic level appropriate technologies are needed. Suspension bead arrays are perfectly suited for the multiplex analysis of signaling events and drug effects in an inflammatory context. Multiplexed sandwich immunoassays are hereby the most frequently used assay format and they are considered to represent the gold standard.

Using the Luminex platform Hsu *et al.*[106] showed for example that it is possible to discriminate between trauma and sepsis patients by measuring plasma concentrations of 11 different soluble cytokine receptors and cell adhesion molecules. Van Erk and colleagues studied the effect of Diclofenac in obesity associated inflammation [107].

Mogensen *et al.* [108] evaluated the *in vitro* effect of Dexamethasone on the secretion of proinflammatory cytokines in stimulated PBMCs. Torrence *et al.* [109] identified biomarkers to monitor disease status in a mouse model of inflammatory bowel disease.

In addition to the analysis of secreted signaling molecules, the same technology can be used to study intracellular signaling events. In this context the determination of MAP Kinase phosphorylation pattern in Leukocytes upon treatment with mediators of inflammation [110] can be exemplified. Moreover Khan and co-workers [111] demonstrated that suspension bead arrays can effectively be used for phosphoprotein analysis in lymphatic cell lines. Poetz *et al.* [112] applied bead array technology for profiling of EGF Receptor phosphorylation upon growth factor treatment.

2. Research Objectives

Due to the complex nature of the human immune system the development of appropriate *in vivo*-like test models for the preclinical phase of drug development is challenging. Currently used test systems like PBMC preparations, whole blood cultures or even animal models do not sufficiently mimic the *in vivo* conditions found in the human body. Therefore, elaborate *in vivo* like cell culture models are urgently needed.

Embedded in the BMBF funded HuCoCSys project the purpose of this study was the detailed characterization and validation of a novel compartmentalized co-culture model of the human gut. Comprising differentiated Caco-2 epithelial monolayers and human whole blood to represent the immune system this *in vitro* model will be applied to mimic the intestinal resorption of drugs and drug candidates.

Initially the effect of a proinflammatory environment, as observed in the gut of inflammatory bowel disease patients, on the epithelial integrity of functionally differentiated Caco-2 monolayer was investigated in detail using immunohistochemistry and TEER measurements. Moreover, the impact on such proinflammatory treatment on intracellular receptor tyrosine kinase signaling (RTK) will be interrogated using multiplexed phosphoprotein analysis.

Antiphlogistic drugs as well as primarily uncharacterized drug candidates were subsequently added on top side of the epithelium and their differential effects on extracellular signaling processes in the whole blood were analyzed using multiplexed protein microarray technology. For this purpose bead based sandwich immunoassays were developed on the Luminex platform, optimized and applied for the quantification of immune mediators in human plasma. The obtained multiparametric datasets should be analyzed and interpreted using bioinformatic tools.

3. Materials and Methods

3.1. Materials

3.1.1. Sandwich Immunoassays

For the development of multiplexed sandwich immunoassays, commercially available matched pair antibodies and recombinant standard proteins were used. For signal generation commercially available Streptavidin-R-Phycoerythrin was applied.

3.1.2. Antibodies and proteins

Table 3: Antibodies and recombinant proteins

Antibody	Vendor
rabbit-anti-human Claudin 5	Abcam, Cambridge, UK
mouse-anti-human Dsg 2	Acris Antibodies, Herford, Germany
goat-anti-human-E-Cadherin	R&D Systems, Minneapolis, MN, USA
rabbit-anti-human Occludin	Life Technologies, Darmstadt, Germany
mouse-anti-human ZO1	Life Technologies, Darmstadt, Germany
goat-anti-rabbit IgG-Alexa 488	Life Technologies, Darmstadt, Germany
goat-anti-mouse IgG-Cy3	Jackson ImmunoResearch, Newmarket, Suffolk
donkey-anti-goat IgG-Cy3	Jackson ImmunoResearch, Newmarket, Suffolk
human IL-1 β	Miltenyi Biotec, Bergisch Gladbach, Germany
human TNF α	Miltenyi Biotec, Bergisch Gladbach, Germany
human EGF	Merck KGaA, Darmstadt, Germany

3.1.3. Expendable items

Table 4: Expendable items

Material	Vendor
96-well filter plate MultiScreen	Millipore, Billerica, MA, USA
96-well microplate, half area (NBS)	Corning, New York, NY, USA
Luminex xMap TM carboxylated microspheres	Luminex Corp., Austin, TX, USA
1.5 mL reaction tubes	Starlab Ahrensburg, Germany
reagent reservoir, sterile	Brand Wertheim, Germany
cell culture flask T75	Greiner Bio-One, Frickenhausen, Germany
96-well PCR plate	Brand, Wertheim, Germany
96-well cell culture plate	Greiner Bio-One, Frickenhausen, Germany

3.1.4. Buffers

Table 5: Buffers

Chemical	Components
Low Cross Buffer	Candor Biosciences GmbH, Wangen, Germany
Activation Buffer	100mM Na ₂ HPO ₄ , pH 6.2
Coupling Buffer	50mM MES, pH 5.0
Wash Buffer	PBS + 0,05% (v/v) Tween 20
Roche Buffer	50mM Tris HCl; 150mM NaCl; 1% Gelatine (w/v)
Cell Culture Medium	MEM, 20% (v/v) FCS , 1% (v/v) Penicillin/Streptomycin, 1% (v/v) L-Glutamin, 1% (v/v) NEA
RTK Extraction Reagent	Merck KGaA, Darmstadt, Germany

3.1.5. Devices and Software

Table 6: Devices and Software

Device/ Software	Vendor
Cell Counter & Analyzer Casy TT	Innovatis AG, Reutlingen, Germany
Cell Culture Incubator	Binder, Tuttlingen, Germany
centrifuge C5415D, 5417R, 5810	Eppendorf, Hamburg, Germany
centrifuge Universal 25	Hettich, Tuttlingen, Germany
Luminex100	Luminex Corp., Austin, TX, USA
Luminex100 IS 2.2	Luminex Corp., Austin, TX, USA
multichannel pipette	Eppendorf, Hamburg, Germany
Pipetus®	Hirschmann Laborgeräte, Eberstadt, Germany
Roth Micro centrifuge	Carl Roth GmbH & Co, Karlsruhe, Germany
pipettors	Gilson, Middleton, WI, USA
sonification bath Sonorex	Bandelin Electronics, Berlin, Germany
Thermo Mixer Comfort	Eppendorf, Hamburg, Germany
Vacuum station	Millipore, Billerica, MA, USA
Vortex Genie 2	Scientific Industries, Bohemia, NY, USA
Confocal microscope LSM 510 META	Carl Zeiss AG, Göttingen, Germany
Axiovision software	Carl Zeiss AG, Göttingen, Germany
TIGR	Dana-Farber Cancer Institute, Boston, MA, USA.
IPA® web-based knowledge database	Ingenuity Systems, Redwood City, CA, USA
yEd Graph Editor	yWorks GmbH, Tübingen, Germany
Masterplex 2010	MiraiBio, San Fransisco, CA, USA

Microsoft Office 2003	Microsoft (Redmond, WA, USA)
Endnote X1	Thomson Corp. (Philadelphia, PA, USA)
Adobe Illustrator	Adobe INC., San Jose, CA, USA

3.1.6. Chemicals and Reagents

Table 7: Chemicals and Reagents

Chemical	Vendor
DMSO	Sigma Aldrich, St. Louis, MO, USA
EDC	Oxford GlycoSystems, Oxford, UK
sulfo-NHS	Pierce, Rockford, IL, USA
Tris-HCL	Carl Roth GmbH & Co, Karlsruhe, Germany
Horse Serum	Sigma Aldrich, St. Louis, MO, USA
Glycerol	Fluka (Sigma-Aldrich), St. Louis, MO, USA
FCS	Lonza, Basel, Switzerland
Benzonase® Nuclease	Merck KGaA, Darmstadt, Germany
Blocking reagent for ELISA	Roche Diagnostics, Mannheim, Germany
Complete Protease Inhibitor	Roche Diagnostics, Mannheim, Germany
L-Glutamine	Biochrom, Berlin, Germany
PBS	PAA Laboratories GmbH, Pasching, Austria
Tween20	Merck KGaA, Darmstadt, Germany
Penicillin/Streptomycin	Biochrom, Berlin, Germany
Phosphatase Inhibitor Cocktail	Sigma-Aldrich, St. Louis, MO, USA
Trypsin	PAA Laboratories GmbH, Pasching, Austria
MEM Biochrom AG/Berlin	Biochrom, Berlin, Germany
HBSS-	Biochrom, Berlin, Germany
PFA	Carl Roth GmbH & Co. KG, Karlsruhe, Germany
LiquiChip™ System Fluid 10x concentrate	Qiagen, Hilden, Germany
non-essential amino acids (NEA)	Biochrom, Berlin, Germany
InhibitorSelect™ Kinase Inhibitor Library IIII	Merck KGaA, Darmstadt, Germany
KN62, KN93	Merck KGaA, Darmstadt, Germany
Caco-2 adenocarcinoma cells	Deutsche Sammlung von Mikroorganismen und Zellkulturen (DSMZ) Order Number DSM ACC 169
Mounting Medium	Dianova, Hamburg, Germany
LPS	Calbiochem Schwalbach, Germany
SEB	Bernhard Notsch Institut, Hamburg, Germany

Anti-CD28	Beckman Coulter GmbH, Krefeld, Germany
Anti-CD3	R&D Systems, Minneapolis, MN, USA
Zymosan	Sigma-Aldrich, St. Louis, MO, USA
Poly I:C	Life Technologies, Darmstadt, Germany
Diclofenac-Sodium	Sigma-Aldrich, St. Louis, MO, USA
Ibuprofen	Biomol, Hamburg, Germany
Prednisolon-21-hydrogensuccinat	MIBE GmbH Arzneimittel, Brehna, Germany
Dexamethasone	Sigma-Aldrich, St. Louis, MO, USA
Tacrolimus	Selleck Chemicals LLC, Houston, TX, USA
Dihydroxyguajaretic Acid	Intermed Discovery GmbH, Dortmund, Germany

3.1.7. Whole blood donors

Blood donation was done at the project partner EDI GmbH by healthy volunteers through venipuncture right before experimental usage. The ability of the individual donors to respond to the used stimuli was assessed in advance. Non-responders to the stimuli or individuals with chronic disorders, or a surgery in the past three months were excluded as well as persons with infectious diseases in the past two weeks or a immunizations in the past six weeks. The usage of immunomodulating drugs in the past two weeks also disqualified the donors. Blood samples were taken with a syringe prefilled with 1% Heparin. Blood was mixed and used within 30 min.

3.2. Suspension bead arrays

The bead based protein microarrays applied in this thesis were performed with the Luminex¹⁰⁰ microsphere array system.

3.2.1. Coupling antibodies to microspheres

For covalent immobilization of capture antibodies to Luminex carboxylated microspheres 400 μ l of the appropriate bead stock solution (1.25×10^7 beads/ml) were transferred to a Ultrafree-MC filter unit and centrifuged for 1min at 3000 xg to remove supernatant. Beads were washed twice with 300 μ l of Activation Buffer followed by vortexing and spinning. The bead surface groups were activated by addition of 150 μ l Activation Buffer supplemented with 50 mM EDC and 50 mM sulfo-NHS to each cou-

pling reaction and 20 min of incubation at room temperature in the dark with agitation. After spinning and removal of the flow through, beads were washed three times with 400 μ l Coupling Buffer, vortexed, and centrifuged briefly to remove activation reagents.

Subsequently a solution of capture antibody in Coupling Buffer was added to the beads and incubated for 120 min at RT in the dark on a shaker. The coupling concentration varied between the different capture antibodies and had to be optimized during assay development. After spinning and removal of flow through the capture coated beads were washed three times with 400 μ l of Wash Buffer, resuspended in Roche Buffer +0.05% sodium-azide and transferred to an Eppendorf cup. The beads were stored at 4°C in the dark. To determine recovery the antibody coated beads were diluted 1:500 in Roche Buffer + 0.05% Tween20 and vortex for 10 seconds. 100 μ L were transferred to a microtiter plate (NBS). After 30 min of incubation at RT read out was performed using the Luminex 100 analyzer, Settings: Sample Size 50 μ L, time out 80 s, total beads 10,000. Bead concentration was calculated as follows: beads per μ L = number of beads divided by 30 and multiplied by a dilution factor of 500. The recovery is usually approximately 90%.

3.2.2. Multiplexed Assay Panels

For quality assurance and low inter- and intra-assay variability capture beads, detection antibodies and standard proteins had to be validated ahead of usage. All newly purchased lot numbers were compared to already applied proteins and concentration was adjusted if necessary.

3.2.2.1. Cytokine/Chemokine Panels I-III

Prior to usage of the established multiplexed cytokine/chemokine panels I-III a 96-well filterplate was blocked with 100 μ l per well of Roche buffer for 30 min. The specific capture coated beads of different sets were diluted (1500 beads per well of each bead type) and mixed in Low Cross buffer for the individual multiplexed panels. The recombinant standard proteins were mixed and diluted in Low Cross buffer to 10000 pg/ml, followed by 4-fold serial dilutions in Low Cross buffer. Plasma samples were diluted in Low Cross buffer and 25 μ l of sample or standard were added to each well

of the 96-well filter plate. The dilution factor was optimized and adapted according to sample treatment. Then 25 μ l of bead solution were added to each standard or sample well and incubated for 2 h at RT in the dark on a shaker. After washing twice with 100 μ l per well of Wash Buffer, 30 μ l of a detection antibody mixture (for antibody concentration see **table 8**) in Low Cross buffer were added to each well, followed by 1 h of incubation at RT in the dark on a shaker.

Beads were washed twice with 100 μ l of Wash Buffer and 30 μ l of a 2 μ g/ml Streptavidin-PE solution in Low Cross buffer was added to each well. After 30 min of incubation at RT in the dark on a shaker two wash steps were performed with 100 μ l/well of Wash Buffer and beads were resuspended in 100 μ l per well of Roche Buffer. The assays were analyzed using the Luminex100 analyzer. Settings: sample Size 80 μ L, time-out 60 s, 50 events, bead gate 7000-15000. To convert MFI values in concentration values a 5-parametric fitting of the standard curve was performed. Values below the lower limit of quantification (LOQ) which is calculated by the blank + 10x sdv of the blank were excluded from the analysis. Values exceeding the upper limit of detection (ULD) were also not included.

Table 8: Concentrations of reagents applied in cytokine Panels I-III

Panel I									
Analyte	IL-1 β	IL-6	IL-8	MCP-1	IFN γ	IP-10	TNF α		
Standard [ng/ml]	10	10	10	10	10	10	10		
Det.Ab [μ g/ml]	0,1	0,2	0,1	0,1	0,1	0,5	1		
Panel II					Panel III				
Analyte	IL-4	TARC	IL-17A	TSLP	IL-5	IL-10	IL-1ra	IL-13	IL-12
Standard [ng/ml]	10	10	10	10	10	10	10	10	10
Det. Ab [μ g/ml]	0.1	1	0.5	1	0.5	0.5	2	0.1	0.1
Streptavidin- PE	2 μ g/ml								

3.2.2.2. Soluble Receptor 8-plex Panel

The soluble receptor 8-plex assay used in this study was developed by Xiaobo Yu and Hsin-Yun Hsu at the NMI [113, 114]. The assay procedure for the soluble receptor panel basically is similar to procedure used for the cytokine/chemokine panels. Except that instead of Low Cross buffer Roche buffer is used. The standard protein mix-

ture is 3-fold diluted in Roche buffer supplemented with 10% horse serum. Additionally the number of wash steps is raised to three after each incubation step and 5 µg/ml of Streptavidin-PE are used for signal generation. To convert MFI values in concentration values a 5-parametric fitting of the standard curve was performed. Values below the lower limit of quantification (LOQ) were excluded from the analysis. Values exceeding the upper limit of detection (ULD) were also not included. **Table 9** gives an overview of the standard and detection antibody concentrations used for the soluble receptor assays.

Table 9 : Concentrations of reagents applied in the soluble receptor panel

Soluble Receptor Panel								
Analyte	ICAM-1	VCAM-1	IL-2 R α	gp130	Fas	E-Sele.	TNF-RII	TNF-RI
Standard [ng/ml]	160	80	160	40	200	400	60	9
Det. Ab [µg/ml]	0,4	0,8	0,4	1	0,4	1	0,6	0,8
Streptavidin-PE	5 µg/ml							

3.3. Cell culture methods

Caco-2 cells were thawed carefully, washed with 45 ml pre-warmed cell culture medium, centrifuged at 500 xg for 5 min, resuspended in 4 ml medium and added to a T75 flask containing pre-warmed medium. Cells were cultured at 37°C and 5% CO₂. 80% confluence was reached after 3-4 days. For subculturing cells were washed with 20 ml HBSS⁻ and incubated for 5 min with 5 ml of 1x Trypsin-EDTA solution at 37°C. The reaction was quenched by adding 10 ml of medium. After resuspension, cells were centrifuged for 5 min at 500 xg and excessive supernatant was removed carefully. Cells were resuspended again, separated in medium, counted using a particle counter and seeded at a density of 0.5x10⁶ cells in a T75 culture flask containing 20 ml of pre-warmed medium.

3.3.1. Intracellular RTK-Signaling Analysis

For the stimulation experiments cells were used at passages 20-50. 20x10³ cells per well were seeded onto 96-well cell culture plate containing 200 µl medium per well. After 8 days, differentiation was assessed microscopically. Hereby dome formation was used as a measure for the full accomplishment of enterocyte differentiation.

Cells were starved for 24 h with 180 μ l per well of serum-free medium and treated for different times with 20 μ l per well of serum-free medium containing 10 ng/ml IL-1 β or EGF respectively. For the pretreatment of starved Caco-2 cells with InhibitorSelectTM Protein Kinase Inhibitor Library III, 20 μ l of serum-free medium containing the predicted inhibitors were added to the cells for 1 h, prior to stimulation with 10 ng/ml IL-1 β for 30 min. Total DMSO concentration was 0.1%. For cell lysis, culture medium was aspirated and the cells were rinsed twice with ice cold PBS following addition of 120 μ l per well of pre-cooled RTK-Extraction Reagent. After incubation for 20 min at 4°C with agitation cells were solubilized by repeated pipetting until extracts were clear and non-viscous. For further clearance, the lysates were transferred onto a pre-wetted 96-well filterplate and centrifuged with 1500x g for 5 min at 4°C. A 96-well PCR-Plate was used to collect the lysates. Lysates were frozen immediately at -70°C and sent to the project partner Merck KGaA for the bead based analysis.

For RTK signaling analysis bead based multiplex immunoassays developed by Merck KGaA were applied. The WidescreenTM RTK pTyr 7-plex kit enables the simultaneous determination of the EGFR, IGF-1R, HGFR, ErbB2, PDGFR β , VEGFR2 and Tie-2 phosphorylation status in cell lysates. In addition the WidescreenTM RTK total 7-plex kit was used to detect the total amount of RTKs. The specific phosphorylation pattern of EGFR was examined in detail with a phospho EGFR 9-plex profiler kit. This kit enables the detailed analysis of EGFR phosphorylation at pT654, pT669, pY845, pY1045, pS1047, pY1068, pY1086, pY1173 as well as the determination of total EGFR protein.

3.3.2. Cell culture in transwell® Inserts

All cell culture experiments using membranous transwell® inserts were performed by Kathrin Hefner and Michael Blum (EDI GmbH, Reutlingen, Germany). The Caco-2 cells were cultivated on top side of special transwell® vessels fitting as inserts into a 24-well cell culture plate. 20000 cells in 200 μ l medium were seeded in the upper compartment and grown for 8 days. The basal compartment was filled with cell culture medium. Medium was changed every other day. To assess the grade of differentiation the transepithelial electric resistance (TEER) between the upper and lower compartment was measured. This parameter is mainly determined by the formation

of tight junctions and extracellular matrix. A TEER of $400 \Omega \cdot \text{cm}^2$ was set as a threshold for further usage. In addition the quality of the monolayer in every well was judged microscopically before further proceeding. Dome formation was used as a measure for the full accomplishment of enterocyte differentiation.

3.3.3. Immunohistochemistry

In order to examine the effect of proinflammatory mediators on tight junctions, adherence junctions and desmosoms, Caco-2 cells were grown for 8 days in transwell® inserts as described above and were subsequently stimulated by adding a mixture of 10 ng/ml IL-1 β and 10 ng/ml TNF α or 50 ng/ml IFN- γ in serumfree medium to the basolateral compartment of the transwell® vessel. After 6 h (IL-1 β and TNF α) or 24 h (IFN γ) cells were washed twice with 200 μ l PBS and treated for 10 min with 100 μ l per well of 2% PFA in PBS at RT. Following 15 min of incubation with 100 μ l per well of Triton-X 100 (0.1%) in PBS cells were washed three times with 100 μ l/well of PBS and incubation was performed with 100 μ l per well of PBS + 3% BSA for 60 min to block unspecific binding of the antibodies. Cells were then treated with 80 μ l of primary antibody solution in PBS+ 3% BSA (α -Claudin 5 1:200, α -Dsg 2 1:50, α -E-Cadherin 1:100, α -Occludin 1:100 and α -ZO 1 1:50) over night at 2-8 $^{\circ}$ C. After three wash steps with 200 μ l PBS cells were incubated with 80 μ l per well of the corresponding fluorescent labeled secondary antibodies (diluted 1:600 in PBS+ 3% BSA) for 60 min at RT in the dark. Cells were washed three times and the filter-grown monolayer were cut out of the inserts and placed together with 8 μ l Mounting Medium on top of a glass slide. The slides were stored at 2-8 $^{\circ}$ C in the dark until microscopic analysis.

3.3.4. Co-culture experiments

The experimental workflow of the co-culture experiments is schematically depicted in **figure 7**. Caco-2 cells were grown for 8 days in transwell® inserts and differentiation was judged microscopically and by TEER measurements. If primed monolayers were required 10 ng/ml IL-1 β and 10 ng/ml TNF α were added to the basal compartment for 6 h. The dissolved test substance was applied on top side of the epithelium and the transwell® inserts were transferred to a 24-well cell culture plate containing heparinized whole blood of three different donors. Controls received either drug dilu-

ent (diluent control) or medium (stimulation control). After 1 h of incubation to allow passage of the epithelium experimental inflammation was elucidated by application of either LPS/SEB/anti-CD28 or Zymosan or Zymosan/anti-CD3/anti-CD28, or anti-CD3/anti-CD28 or Poly I:C in serumfree medium to the lower chamber of the compartmentalized model. Unstimulated controls received medium (cell control).

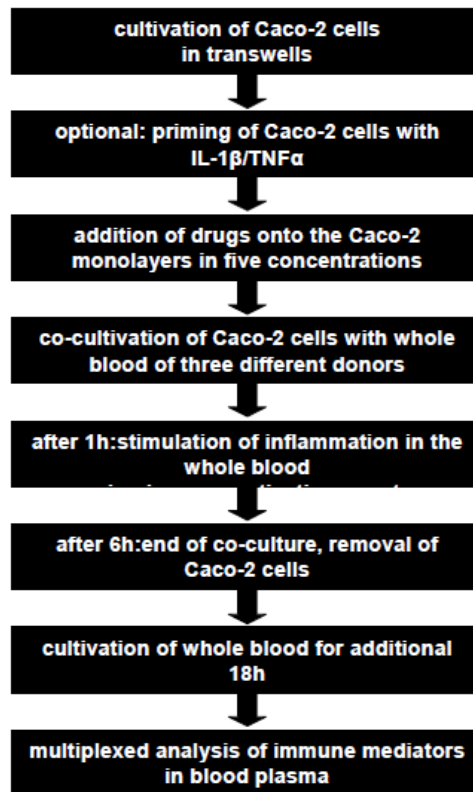


Figure 7: Experimental workflow of drug testing in the co-culture model

The co-culture was stopped after 6 h and the transwell® inserts were removed. The stimulated whole blood was further cultivated for 18 h. After 24 h of total incubation, the blood plasma of duplicate wells was pooled and stored at -20°C until multiplexed analysis. **Table 10** summarizes the control samples generated for each test substance and each blood donor. To enable a direct comparison of the dose response curves obtained for different blood donors the determined analyte concentrations were normalized to the concentrations found in the diluent control. The resultant ratio is termed **Stimulation Index**.

Table 10: Control samples for drug testing

designation	Drug-Solvent	Stimulating Agents
Stimulatory control	-	+
Solvent control	+	+
Cell control	-	-

3.3.5. Whole blood culture assays

For drug tests in whole blood cultures, the test substance was dissolved in DMSO and diluted in medium supplemented with DMSO. Different concentrations were directly injected into heparinized whole blood of two different donors. Final DMSO concentration was 0.1 %. Control cells received the drug diluent (diluent-control) or medium (cell-control and stimulatory-control). After 1h of incubation inflammation was induced by addition LPS/SEB/anti-CD28 in medium. Unstimulated controls received medium. After 24 h of incubation, blood plasma from duplicate wells was pooled and stored at -20°C until further analysis.

3.4. Data analysis

3.4.1. The IPA[®] knowledge base

For the analysis of the generated intracellular and extracellular signaling data the IPA[®] knowledge base developed by Ingenuity Systems was used. This web-based software application utilizes on a highly structured database of literature-extracted signal transduction pathways. This tool enables the analysis of already known pathways as well as the evaluation of uncharacterized pathways in a biological context.

3.4.2. Hirarchical Clusteranalysis

Cluster analyses was carried out using MultiExperiment Viewer (MeV Version 4.0 <http://www.tm4.org>) [115]. Analyte concentrations below the lower limit of quantification (LOQ) cannot be determined with acceptable statistical confidence. For cluster analysis these data were replaced by the concentration value of the LOQ. If the measured value was above the upper limit of detection (ULD) these data points were replaced by the value of the ULD. To scale the data ahead of cluster analysis the

analyte concentrations were median centered and log2 transformed, to yield data values in the range of +/- 3. Subsequently the heatmap was generated (parameters: Euclidean distance, complete linkage). Hierarchical clustering (HC) uses the distances between different objects for forming subgroups (clusters). Euclidean distance is the 'ordinary' distance between two points in the multidimensional space. It can be described as:

$$d(x, y) = \left(\sum_i (x_i - y_i)^2 \right)^{\frac{1}{2}}$$

The distance between any two objects is defined by the distance measure. However, it is necessary to define a linkage function to specify how the distance between clusters with more than one element is determined. For complete linkage clustering the distance between two clusters, is computed as the distance between the two farthest objects within these clusters. The linkage function is described by the following expression, where $d(x, y)$ is the distance between objects x and y :

$$D(X, Y) = \max_{x \in X, y \in Y} d(x, y)$$

For significance analysis the samples were assigned into 6 groups according to their treatment and then multiclass SAM (significance analysis of microarray) analysis was carried out to identify analytes which exert statistically different concentration levels.

4. Results

4.1. Sandwich Immunoassay Development

Prerequisite for the development and validation of multiplexed sandwich immunoassays is the compatibility of all assay components as well as the fact that the simultaneous measurement of multiple analytes in one test requires compatibility of analyte dilutions. For this study, a panel of plasma parameters was selected based on their known involvement in inflammatory processes. For each selected analyte commercially available antibodies together with their corresponding recombinant antigens were purchased. After an initial test in a singleplex assay format, cross reactivities

among the proteinous assay components had to be determined. Antibodies which were identified to cross react with other assay components had to be replaced or excluded since they critically impair the ability to multiplex the assays. Further important quality parameters for the development process were dynamic range, sensitivity, specificity, reliability and robustness as well as limits of detection (LOD) and quantification (LOQ) [116]. **Figure 8** gives an overview of the cytokine and chemokine assays developed in the context of this study.

4.1.1. Cross-Reactivity

Prerequisite for the simultaneous measurement of multiple parameters in one experiment is the exclusion of cross-reactivities among:

- capture- and detection antibodies
- capture antibodies and analytes
- analytes and detection antibodies.

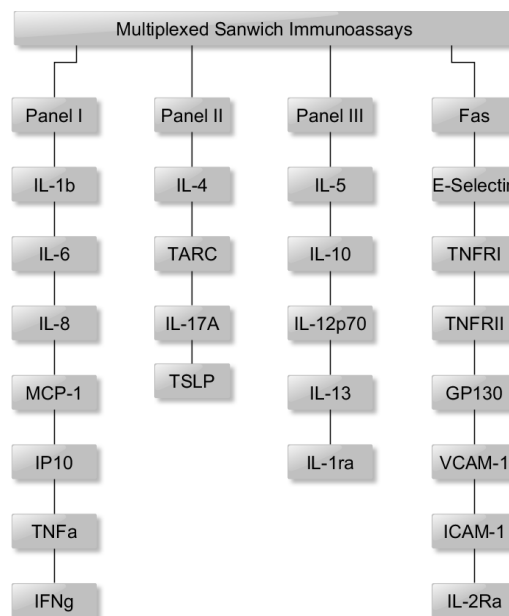


Figure 8: Multiplexed sandwich immunoassays.

Assays for 16 cytokines and chemokines were developed, and grouped into three different multiplexed panels. In addition, an existing 8-plex panel targeting soluble receptors and cell adhesion molecules was used for sample analysis.

Cross-reactivities between capture and detection antibodies were assessed by incubation of all capture antibody coated beads with a mixture of all corresponding detec-

tion antibodies in the absence of any standard protein. Cross-reactions between capture antibodies and analytes were determined by incubation of all capture beads with separate standard proteins in the presence of all detection antibodies. Cross-reactivities between standard proteins and detection antibodies were determined by incubation of all beads with all analytes and separate detection antibodies. As shown in **table 11** no cross-reactivity occurred in Panel I. Cross-reactivities were evaluated for Panel II and III in an analogous manner with comparable results (**supplementary table I and II**).

Table 11: Analysis of cross-reactivities in Panel I.

Cross-reactivities were evaluated between capture and detection antibodies **A**, capture antibodies and analytes **B**, analytes and detection antibodies **C**. Displayed are median fluorescence intensities (MFI). All standard proteins were used at 10000 pg/ml. The cut off threshold was set to 40 MFI.

A: all beads, no analyte, separate detection antibodies

detection	capture coated beads						
	IL-1 β	IL-6	IL-8	IFN γ	MCP-1	IP-10	TNF α
IL-1 β	3	2	2	2	3	3	3
IL-6	2	2	3	2	2	3	3
IL-8	2	2	27	2	2	4	3
IFN γ	2	2	3	2	14	3	3
MCP-1	2	2	3	2	2	4	3
IP-10	2	1	2	3	2	5	4
TNF α	2	2	3	2	3	3	3

B: all beads, separate analytes, all detection antibodies

analyte	capture coated beads						
	IL-1 β	IL-6	IL-8	IFN γ	MCP-1	IP-10	TNF α
IL-1 β	11137	19	28	3	17	4	5
IL-6	6	15311	27	4	21	5	5
IL-8	4	21	22477	4	21	5	5
IFN γ	4	17	30	14356	23	4	5
MCP-1	4	19	29	4	10177	4	5
IP-10	5	20	29	4	22	20670	5
TNF α	4	16	28	3	19	9	7036

C: all beads, all analytes, separate detection antibodies

detection	capture coated beads						
	IL-1 β	IL-6	IL-8	IFN γ	MCP-1	IP-10	TNF α
IL-1 β	13476	2	2	2	2	4	3
IL-6	4	14437	4	9	3	7	3
IL-8	3	3	22465	3	3	6	3
IFN γ	3	9	2	13103	9	7	5
MCP-1	3	3	3	3	10656	6	4
IP-10	2	5	6	4	3	20608	6
TNF α	3	5	35	2	2	5	6929

4.1.2. Titration of detection antibody concentration

The optimal detection antibody concentration has a major influence on the sensitivity of the assay. Usually antibody concentrations need to be increased with the level of multiplexing. However to minimize unspecific binding and to optimize the signal to noise ratio (S/N) the antibody concentration should be kept as low as possible. This

is also financially important since consumption of detection antibody represents a substantial cost factor.

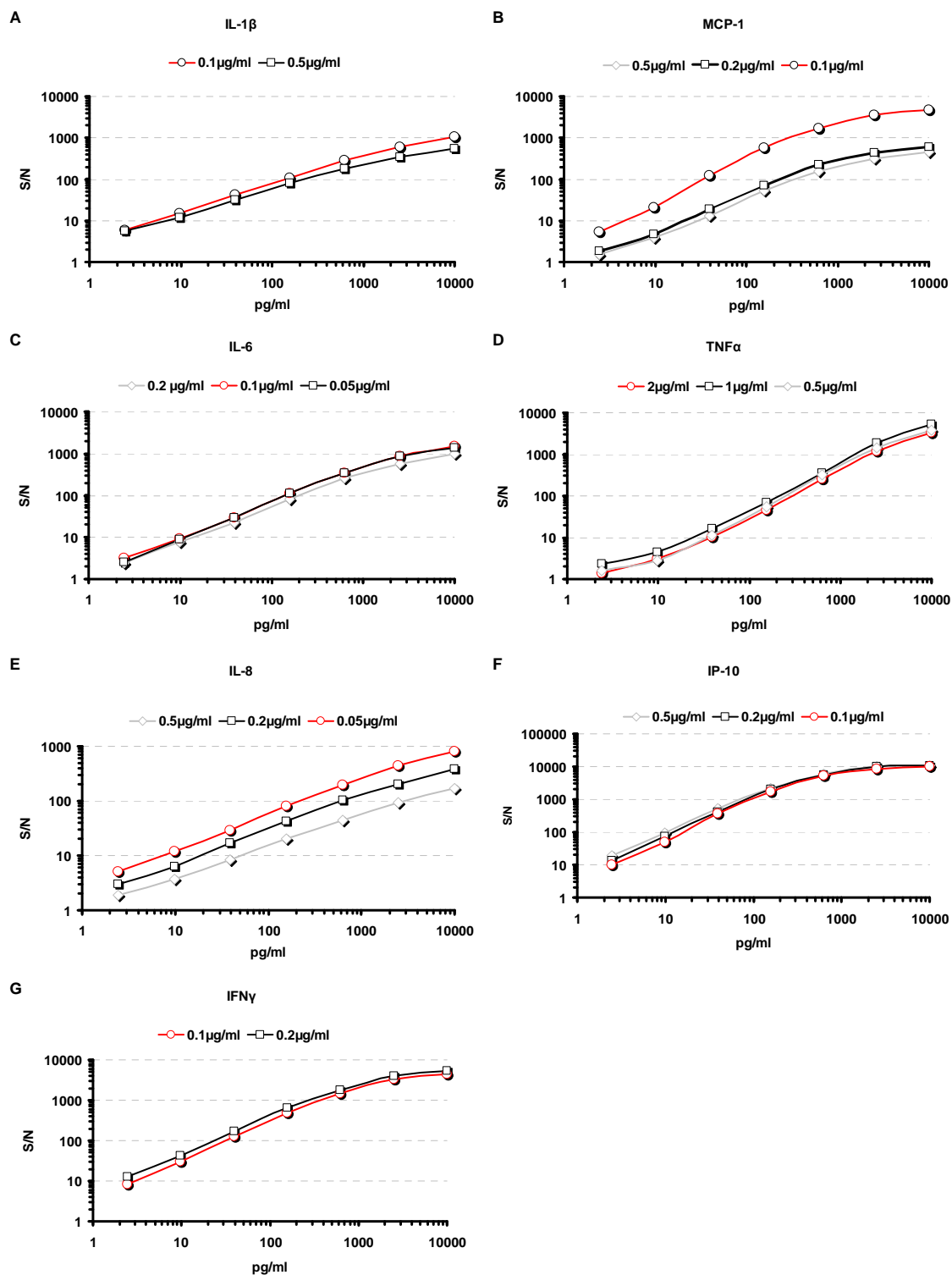


Figure 9: Optimization of detection antibody concentration. Shown are signal to noise ratios (S/N) calculated by dividing the obtained MFI signals by the measured blank value. Curves of the finally selected antibody concentrations are depicted in red. **A** IL-1 β , **B** MCP-1, **C** IL-6, **D** TNF α , **E** IL-8, **F** IP-10, **G** IFN γ .

Figure 9 shows the obtained results from the titration experiments exemplarily for Panel I. The results for the Panels II-III are depicted in **supplementary figure 1-2**.

4.1.3. Optimization of Assay-Recovery

It is necessary to adapt the standard dilution matrix to the sample type, in order to yield the maximal possible accuracy and to avoid systematic errors. This is done by spiking defined concentrations of analyte into a sample and determination of the recovery.

$$\text{Recovery}[\%] = \frac{\text{measured amount}}{\text{added amount}} * 100$$

Measured values between 80-120% of the spiked concentration are considered of sufficient accuracy. Different matrices were tested as standard diluent and scored with respect to the analysis of human plasma samples. A comparison between Roche buffer + 0.05% Tween20 and LowCross buffer is shown in **figure 10** and **supplementary figure 3**. Most of the obtained recovery values were in the acceptable range of 80-120% when LowCross buffer was used as assay matrix. Therefore, this buffer was selected as standard curve diluent for the Panels I-III.

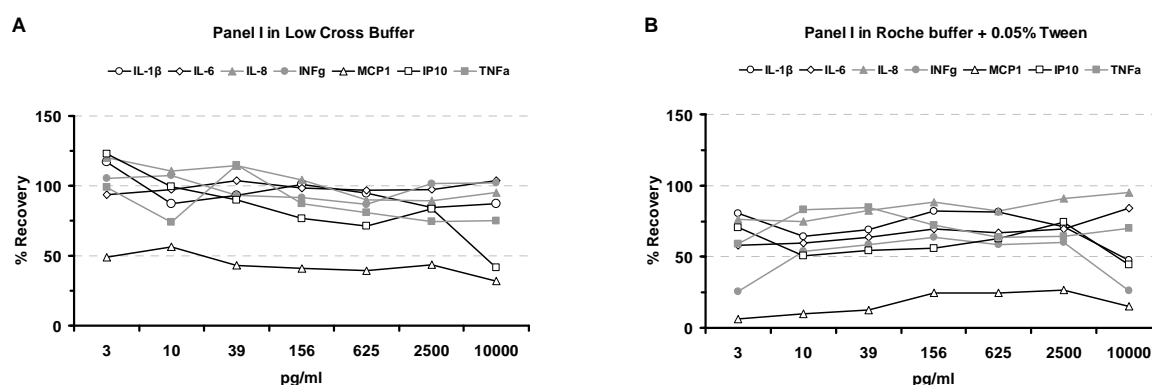


Figure 10: Comparison of assay recovery for Panel I. Standard proteins were spiked into human heparin plasma in the indicated concentrations. In parallel standard curves were determined in LowCross buffer (**A**) and Roche buffer +0.05% Tween (**B**). The measured MFI signals in human plasma were converted into concentration values using a 5-parametric fitting of the detected standard curve and percental recovery was determined on the basis of the initially added concentrations. Shown are the results obtained with Low Cross buffer and Roche buffer +0.05% Tween used as standard dilution matrix.

4.1.4. Assayperformance

After the development process was completed, the assays were applied for the multiplexed analysis of plasma samples generated in the co-culture model. In addition to the newly developed cytokine and chemokine Panels I-III, an already established 8-plex soluble receptor panel was used for plasma sample analysis over a time span of 2.5 years. **Table 12** summarizes the corresponding assay specific quality parameters [116] determined from the standard curves of 20 individual assays. Assay precision is indicated by the coefficient of variation (%CV) which is the standard deviation divided by the mean and expressed as a percentage. Whereas intra-assay variation measures the variability between replicate measurements in the same experiment, inter-assay variation expresses the variation between different experiments.

Table 12: Performance of multiplexed sandwich assays

Panel	Analyte	LOD [pg/ml]	LOQ [pg/ml]	detection Range [pg/ml]	Intra-CV [%]	Inter-CV [%]
I	IL-1b	4.1	11.8	2.4-10000	4	23
	IL-6	1.4	4.0	2.4-10000	4	20
	IL-8	0.1	0.4	2.4-10000	4	14
	IFN γ	1.6	4.9	2.4-10000	8	19
	TNF α	18.5	30.9	2.4-10000	7	21
	MCP-1	6.6	15.8	2.4-10000	5	18
	IP-10	1.0	2.5	2.4-10000	7	20
II	IL-4	4.7	14.4	2.4-10000	6	20
	IL-17	1.8	4.7	2.4-10000	6	18
	TSLP	2.1	6.5	2.4-10000	4	17
	TARC	4.6	10.8	2.4-10000	6	9
III	IL-13	71.3	150.7	2.4-10000	8	16
	IL-1ra	29.6	93.3	2.4-10000	6	25
	IL-5	0.6	1.4	2.4-10000	6	15
	IL-10	1.5	3.0	2.4-10000	4	14
	IL-12p70	7.4	23.4	2.4-10000	12	17
Soluble Receptors	IL-2Ra	361.6	717	300-200000	4	10
	E-Selectin	448.2	1534.5	500-400000	4	19
	Fas	7.7	23.3	300-200000	3	14
	ICAM-1	165.2	487.7	300-200000	8	18
	TNF-RI	4.1	9.1	10-9000	4	20
	TNF-RII	9.1	17.4	100-60000	4	15
	VCAM-1	27.2	54	100-80000	5	16
	gp130			50-40000	4	12

The intra-assay variation was calculated as the mean of the %CVs from duplicate measurements over eight different concentrations in a single assay. The inter-assay

variation is calculated by the mean of the %CVs from duplicate measurements across eight concentrations and 20 different assays. For the detection of low abundant analytes in complex biological samples it is crucial to accurately detect target molecules even at low concentrations. The sensitivity of each individual assay is expressed by the lower limit of detection (LOD) and the lower limit of quantification (LOQ). Whereas the LOD indicates the lowest accurately detectable amount of analyte in the sample, the LOQ refers to the lowest concentration of analyte that can be quantified with statistical confidence. LOD and LOQ are calculated as described below.

$$LOD = mean_{blank} + 3 \cdot SD_{blank}$$

$$LOQ = mean_{blank} + 10 \cdot SD_{blank}$$

The sensitivities of the majority of the analytes were in the lower pg/ml range except for IL-1ra and IL-13. The intra-assay CV of all assays was below 10% and the inter-CV below 20% for most of the measured analytes. In summary, the developed assays showed good intra- and interassay precision. These results demonstrate that a constant assay performance over 2.5 years of measurements was achieved.

4.2. Caco-2 monolayer as a model of the intestinal barrier

In this study Caco-2 monolayers were used as a organotypic model of the intestinal epithelium. Cells were treated with IL-1 β , TNF α or IFN γ to characterize the effect of immune mediators on the epithelial barrier. The effect on the permeability of the Caco-2 monolayer as well as the localization of cell junction molecules was assessed by TEER measurements and immunohistochemistry respectively. In addition to its role as physical barrier the gut epithelium also functions as a sensory organ against intestinal pathogens and forms a regulatory unit with the cells of the immune system. The required intercellular crosstalk is thereby established via the secretion of inflammatory mediators [1]. In order to analyze the capability of the differentiated Caco-2 monolayer to respond to inflammatory stimuli, cells were treated with IL-1 β , TNF α or IFN γ and the release of immune mediators was assessed using sandwich immunoassays. For a more detailed understanding of the cellular mechanisms that take place after treatment with proinflammatory mediators, the effect of IL-1 β , TNF α and IFN γ on intracellular receptor tyrosine kinase (RTK) signaling was studied using mul-

tiplexed bead arrays. Treatment with the gastrointestinal protective factor EGF was thereby used in control stimulations [117].

4.2.1. Impact of proinflammatory cytokines on the epithelial barrier

Elevated levels of proinflammatory cytokines elucidate an increase in epithelial tight junction permeability [19-21]. To validate this effect for differentiated Caco-2 monolayer cells were incubated with either 10ng/ml IL-1 β and TNF α [20, 24] or 50 ng/ml IFN γ [118, 119] for 6 h or 24 h in the lower compartment of transwell® culture vessels and transepithelial electric resistance (TEER) was determined. Control cells were handled identically and received serum free medium without the addition of cytokines. **Figure 11** shows the obtained results.

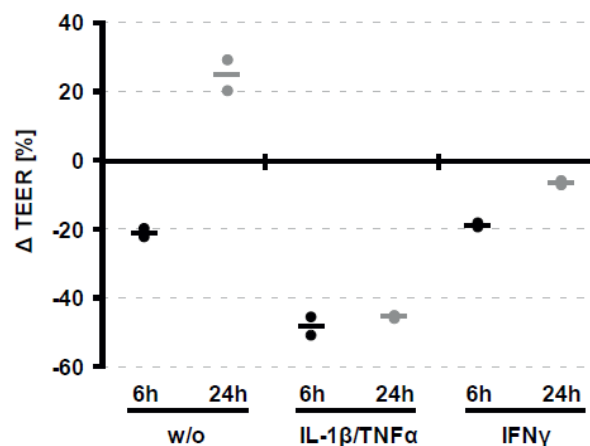


Figure 11: Impact of proinflammatory mediators on TEER.

Differentiated Caco-2 monolayers were treated with either 10 ng/ml IL-1 β /TNF α or 50 ng/ml IFN γ for 6 h or 24 h respectively from the basal side of transwell® vessels. Depicted are percental changes in TEER of duplicate experiments, relative to the TEER values before treatment ($\approx 400 \Omega \cdot \text{cm}^2$). Control cells received medium.

Incubation with IL-1 β /TNF α lead to a decrease in TEER of 48.4% after 6 h with no further reduction after 24 h. In comparison the control cells also revealed a 21.2% decrease of the TEER value after 6 h and a slight increase of 24.6% after 24 h. When cells were treated with IFN γ no difference to controls after 6 h of incubation was detected, however after 24 h of IFN γ treatment the TEER values were clearly lower than those of the control cells.

4.2.2. Effect of proinflammatory cytokines on cell junctions

The impact of IL-1 β /TNF α and IFN γ on the localization of cell adhesion molecules was analyzed by immunohistochemistry. Therefore, Occludin, ZO-1, Claudin 5, Dsg 2 and E-Cadherin were selected as representatives of tight junctions, adherens junctions and desmosomes. Differentiated Caco-2 monolayer were treated with either 10 ng/ml IL-1 β /TNF α for 6 h or with 50 ng/ml IFN γ for 24 h from the basal side of the chambered set up and immunohistochemical analysis was performed using a confocal laser-scanning microscope. As shown in **figure 12** the tight junction proteins Occludin and ZO-1 were clearly located at the cellular borders. Whereas Occludin showed up to be equally distributed along the plasma membrane ZO-1 appeared to be concentrated at the interfaces of three adjacent cells. Incubation with IL-1 β /TNF α or IFN γ lead to a reduction of fluorescence signal for both proteins. Occludin and ZO-1 were found to be co-localized (not shown). Dsg 2 was also found to be localized at the cellular borders and both treatments reduced fluorescence intensity relative to the untreated controls. Claudin-5 and E-Cadherin were found to be localized at the cellular borders. However, proinflammatory treatment did not alter fluorescence intensities.

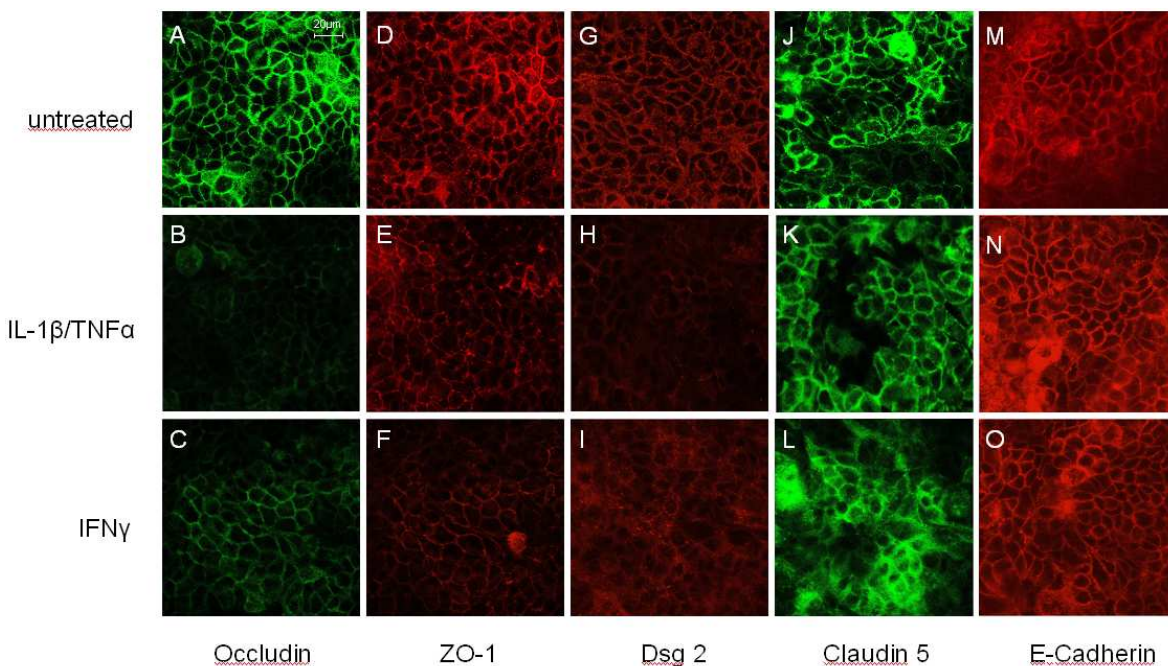


Figure 12: Immunohistochemical analysis of cell junction proteins in Caco-2 cells. Differentiated Caco-2 monolayers were treated with either IL-1 β /TNF α for 6 h or with IFN γ for 24 h from the basal side of transwell® culture vessels. Controls received medium. Occludin (**A-C**), ZO-1 (**D-F**), Claudin 5 (**J-L**), E-Cadherin (**M-O**) as well as Dsg 2 (**G-I**) were stained with specific primary antibodies and visualized with the corresponding secondary antibodies.

4.2.3. Effect of proinflammatory mediators on chemokine release

Proinflammatory cytokines are known to trigger the production of immunoregulatory mediators by the epithelial cells [27]. Thus a crosstalk between the epithelial cells and cells of the immune system is established. To study the ability of Caco-2 cells to respond to proinflammatory cytokine treatment by the release of immune mediators, differentiated monolayer were treated with either 10 ng/ml IL-1 β /TNF α or 50 ng/ml IFN γ in the lower compartment of the compartmentalized model. Supernatant was collected after 6 h or 24 h of incubation. In an additional experiment medium of the lower compartment was exchanged and cells were further incubated for 18 h. Subsequently the concentration of IFN γ , TNF α , IL-1 β , IL-6, TSLP, IP-10, IL-8 and MCP-1 were measured in the cell culture supernatant of the lower chamber using multiplexed sandwich immunoassays. The results are listed in **table 13**. The measured concentrations of IL-1 β , TNF α and IFN γ after treatment with these mediators revealed that no significant passage effect occurred when medium was exchanged after 6 h.

Table 13: Effect of proinflammatory cytokines on chemokine release.

Differentiated Caco-2 cells were treated with the indicated concentrations of IL-1 β /TNF α or IFN γ from the basal side of transwell® vessels and IL-8 (**A**), IP-10 (**B**, **D**) and MCP-1 (**C**) were analyzed in cell culture supernatant using multiplexed sandwich immunoassays. Supernatant was either directly analyzed after 6 h or 24 h, or medium was changed after 6 h of treatment and analyzed after additional 18 h of incubation.

Treatment	conc. [ng/ml]	incubation	concentration [pg/ml]					
			IL-8	MCP-1	IP-10	IL-1b	TNFa	IFNg
IL-1 β /TNF α	w/o	6h+18h	<LOQ	101	155	<LOQ	<LOQ	<LOQ
	10	6h+18h	20	350	2030	<LOQ	<LOQ	<LOQ
	w/o	24h	<LOQ	36	68	<LOQ	<LOQ	<LOQ
	10	24h	105	5465	3245	15043	18076	<LOQ
	w/o	6h	<LOQ	19	33	<LOQ	<LOQ	<LOQ
	10	6h	69	3990	2286	14172	22333	4
IFN γ	w/o	6h+18h	<LOQ	101	155	<LOQ	<LOQ	<LOQ
	50	6h+18h	<LOQ	42	543	<LOQ	<LOQ	6
	w/o	24h	<LOQ	36	68	<LOQ	<LOQ	<LOQ
	50	24h	<LOQ	149	1382	<LOQ	<LOQ	8667
	w/o	6h	<LOQ	<LOQ	33	<LOQ	<LOQ	<LOQ
	50	6h	<LOQ	23	115	<LOQ	<LOQ	9052

Basal treatment of the Caco-2 monolayer with 10 ng/ml IL-1 β and TNF- α resulted in elevated IL-8 concentrations after 6 h and 24 h. Exchange of medium and further culturing for 18 h yielded only low concentrations of IL-8. The concentration of IP-10 was significantly increased after treatment with IL-1 β /TNF α in all experimental set ups with a concentration of 3245 pg/ml after 24 h. Treatment with IFN γ lead to a concentration dependent increase of IP-10 secretion and the highest concentration

(1382 pg/ml) could be found in the supernatant after 24 h. After 6 h the measured concentrations were relatively low (115 pg/ml). Medium exchange and cultivation for additional 18 h revealed that the main IFN γ secretion takes place after medium exchange. IL-1 β /TNF α stimulation induced a strong MCP-1 secretion. The measured concentration was about 4000 pg/ml after 6 h and about 5500 pg/ml after 24 h. In contrast to treatment with IL-1 β /TNF α the Caco-2 cells showed no alterations in the IL-8 and MCP-1 secretion levels after IFN γ treatment. The concentrations of IL-6 and TSLP were all below detection limit (not shown). Taken together secretion of the chemokine mediators IL-8, IP-10 and MCP-1 could be measured upon treatment with IL-1 β and TNF α . The results indicate that treatment with IL-1 β /TNF α leads to clear enhancement of chemokine release in the lower compartment during the first 6 h of incubation. In comparison treatment with IFN γ triggered IP-10 but not IL-8 and MCP-1 secretion. After 24 h of incubation IP-10 level was significantly higher than after 6 h.

4.2.4. Intracellular signaling analysis

4.2.4.1. Multiplexed analysis of RTK phosphorylation

Differentiated Caco-2 monolayers were treated with 10 ng/ml of TNF α , IL-1 β or EGF respectively for different times. Cell lysates were analyzed using RTK pTyr and RTK total 7-plex kits to determine the phosphorylation status of EGFR, IGF-1R, HGFR, ErbB2, PDGFR β , VEGFR2 and Tie-2 as well as the total protein amount of each analyte. **Supplementary figure 4** shows the distribution of average concentrations for total RTK proteins across 15 independent cell culture experiments measured in triplicates. Whereas significant levels of EGFR (974-1579 pg/ml), HGFR (1356-2106 pg/ml) and ErbB2 (1330-1867 pg/ml) could be detected in the cell lysates, relatively low concentrations of IGF1R (98-158 pg/ml) were observed. PDGFR, VEGFR and Tie-2 could not be detected.

IL-1 β and EGF treatment led to a time dependent alteration of EGFR and ErbB2 phosphorylation (**figure 13**) while all other measured RTKs revealed no signal alterations compared to unstimulated controls. Stimulation with EGF led to maximum EGFR phosphorylation after 5 min and 240 min whereas after treatment with IL-1 β signal increased steadily and reached the peak after 60 min followed by a decline. ErbB2 phosphorylation showed only minor alterations after EGF treatment whereas

after IL-1 β treatment signal decreased from 10 min to 60 min, followed by an increase at 240 min. No significant alterations in the phosphorylation status of all analyzed RTKs were detected after TNF α treatment (data not shown).

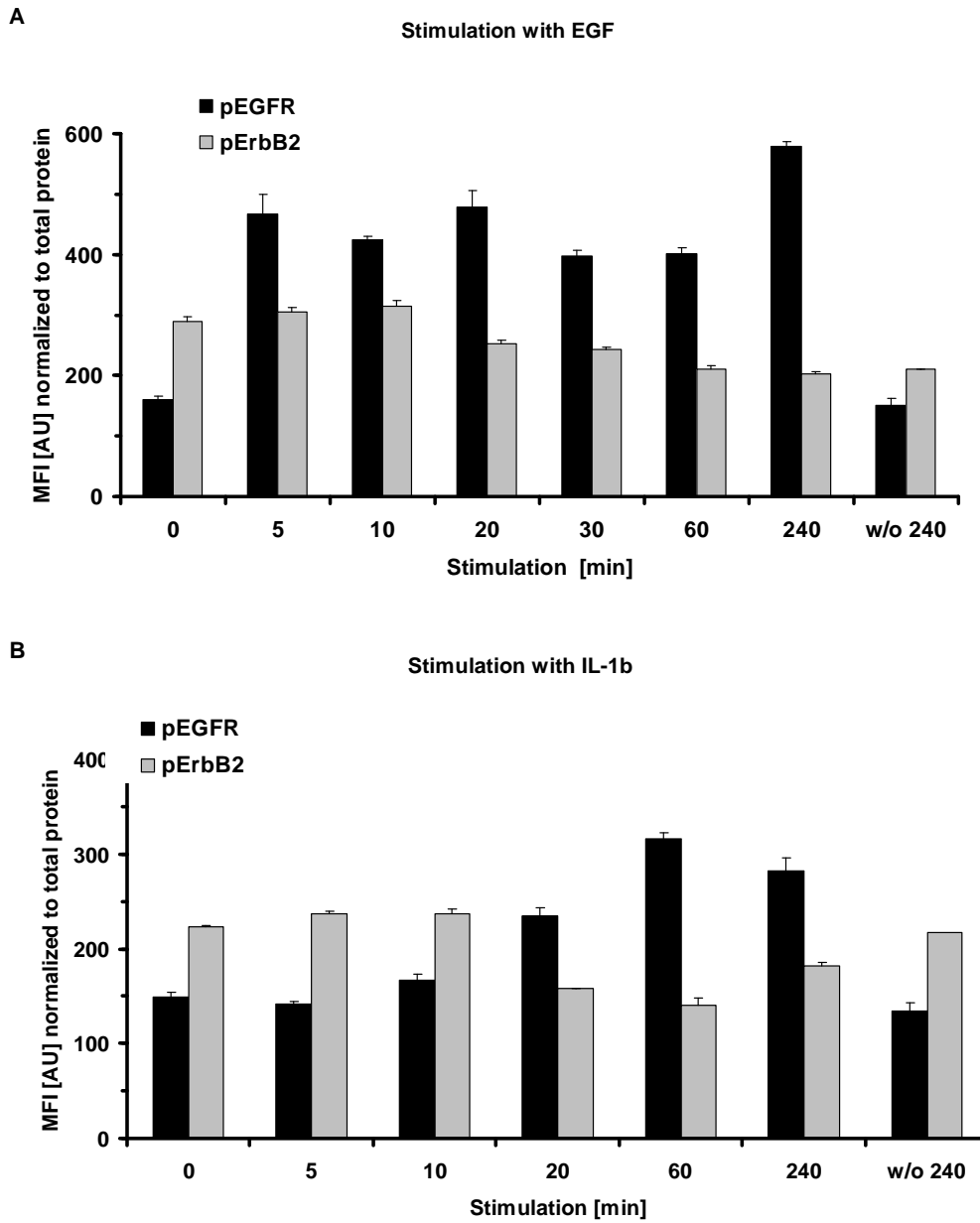


Figure 13: Effect of IL-1 β and EGF on RTK phosphorylation. Differentiated Caco-2 monolayer were starved for 24 h and subsequently treated with 10 ng/ml EGF (**A**) or IL-1 β (**B**). Serum free medium was added to control wells. Cell lysates were analyzed using RTK pTyr and total 7-plex kits. The graph shows averaged MFI values +sdv from triplicate measurements normalized to total RTK signals.

4.2.4.2. Mapping of EGFR phosphorylation

Alterations in the stimulation dependent phosphorylation pattern of EGFR were analyzed in more detail using a phospho-EGFR 9-plex profiling kit. This kit enabled the simultaneous analysis of 8 different phosphosites of the EGF receptor as well as the total amount of EGFR protein.

Starved Caco-2 monolayers were treated for increasing time periods with 10 ng/ml of either IL-1 β or EGF, followed by cell lysis and multiplexed analysis. Control cells received medium and were incubated for identical time intervals ahead of cell lysis.

Figure 14 shows the time dependent distribution of signal intensities for total EGFR protein and the phosphosites pY845, pY1068 and pY1047 after IL-1 β or EGF treatment. For each time point signals were referenced to the signals measured in the corresponding control cells. When cells were treated with 10 ng/ml IL-1 β alterations in phosphorylation at Y845, Y1068 and S1047 were observed. Whereas Y845 and Y1068 showed a comparably small range of fluorescence signals and no clear time dependent tendency, a wide range of signal intensities was detected for S1047.

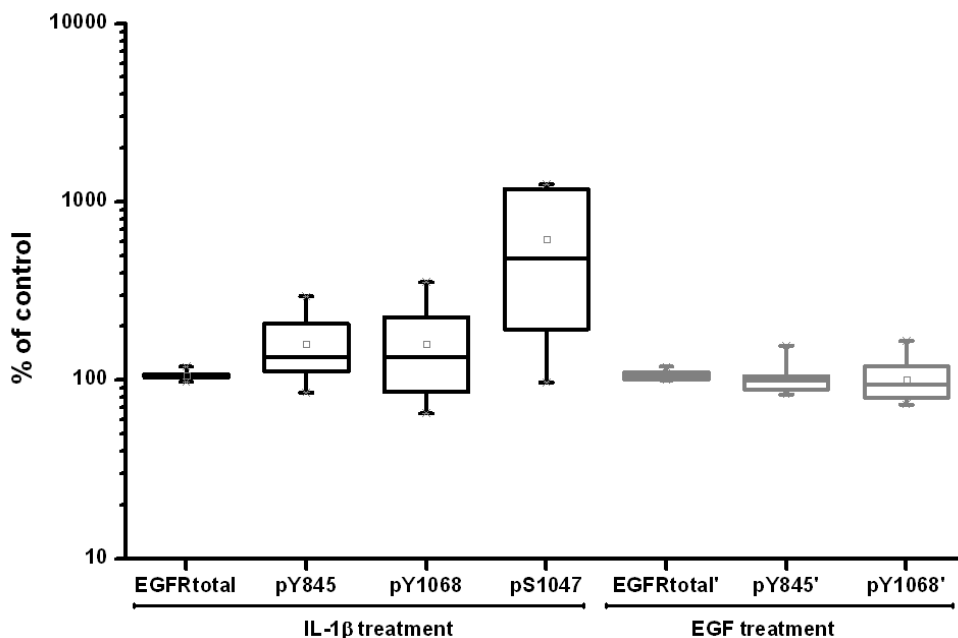


Figure 14: Effect of IL-1 β and EGF on EGFR phosphorylation

Starved Caco-2 cells were treated with 10 ng/ml IL-1 β or EGF for 0, 10, 20, 30, 40, 50, 60, 80, 100, 120, 240 min followed by cell lysis and multiplexed analysis using the Phospho-EGFR 9plex profiling kit. Experiments were performed in biological duplicates. Measurements were performed in technical duplicates. Mean signal intensities were calculated from all data and visualized in box blot diagrams. Shown are signal intensities upon time dependent treatment relative to control stimulations without stimulus application. Boxes indicate the median and the 25th and 75th percentile. The 5th and 95th percentiles are represented by whiskers. Additionally the mean (square) and the 1st and 99th percentiles (crosses) are shown.

When cells were treated with 10 ng/ml of EGF signals for Y845 and Y1068 were almost similar to those of the respective controls with only marginal time dependent alterations. No phosphorylation signal was detected for S1047 after EGF treatment and for the phosphosites Y1045, Y1086, Y1173, Y654, and T669 after both treatments. The time course of signal intensities for the phosphorylation of S1047 after IL-1 β application is shown in **figure 15**. IL-1 β stimulation led to increasing signals from 0 min to 30 min followed by steady decline reaching base level after 80 min and no further increase in the period of observation. Based on these results focus was set on the detailed analysis of the phosphorylation at S1047 and the identification of potentially involved signaling pathways.

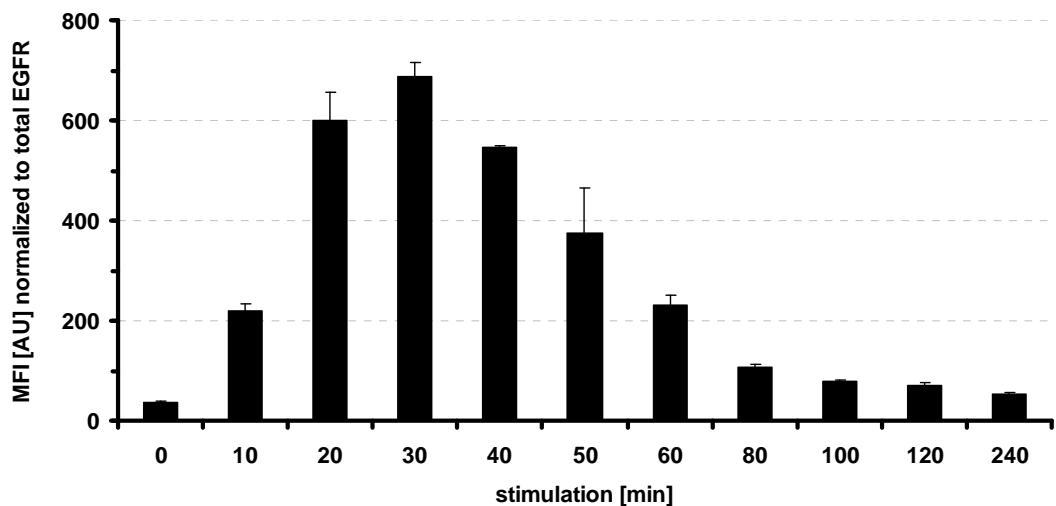


Figure 15: Time course of S1047 phosphorylation upon IL-1 β treatment. Differentiated Caco-2 monolayers were starved for 24 h and subsequently treated with 10 ng/ml IL-1 β for the indicated time intervals. Control wells received serumfree medium. Shown are mean MFI signals +sdv averaged from two independent cell culture experiment each measured in duplicates. Signals were normalized to total EGFR signal.

To identify the relevant intracellular pathways leading to the IL-1 β induced phosphorylation of EGFR at S1047 the InhibitorSelectTM Protein Kinase Inhibitor library III was used. This library consists of 84 inhibitors directed mainly against CMGC, CAMK, AGC and STE families of protein kinases. In addition the library was complemented with the two CamKII inhibitors KN62 and KN93. A detailed list of the applied kinase inhibitors is shown in **supplementary table 3**. Caco-2 cells were cultivated in 96-well cell culture plate until differentiation was reached. Cells were starved and the prediluted 86 kinase inhibitors were added to each well to reach a final concentration of 10 μ g/ml. Final DMSO concentration was 0.1%. After 1 h 10 ng/ml IL-1 β

were added and cells were incubated for 30 min to trigger maximum S1047 phosphorylation. After that immediate cell lysis was performed. The experiment was done in biological duplicates. Bead based analysis was done with the phospho-EGFR 9-plex kit.

The distribution of MFI signals across 86 independent cell culture experiments is shown in **figure 15** for total EGFR, pT845, pT1068 and pS1047. Whereas the signals remained relatively constant for total EGFR, pT845 and pT1068, inhibitor treatment lead to a wide range of MFI signals for pS1047 compared to control cells. Treatment with four inhibitors of p38 α (SB 239063, SB 203580, p38MAPK Inhibitor VI and VIII), three inhibitors of IKK-2 (IKK Inhibitor XI, VI and VII), and one inhibitor of WEE1 (Wee1 Inhibitor) lead to a significant decrease of S1047 phosphorylation (**figure 17**). For data analysis a signal decrease of $\leq 50\%$ compared to control stimulations was defined as cut off threshold. No phosphorylation signal could be detected for the aminoacids Y1045, Y1086, Y1173, Y654, and T669.

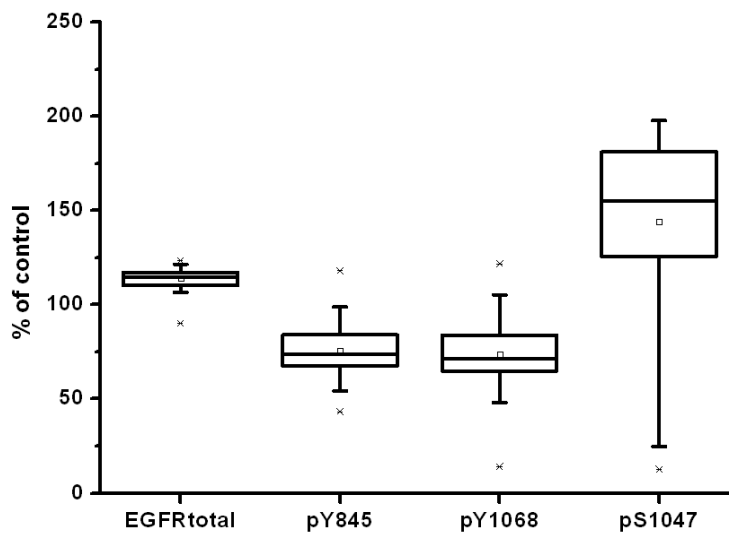


Figure 16: Distribution of signal intensities upon inhibitor treatment.

Starved Caco-2 cells were treated with 86 different kinase inhibitors (10 $\mu\text{g/ml}$ InhibitorSelectTM protein kinase inhibitors in DMSO) for 1 h followed by 30 min of stimulation with IL-1 β (10 ng/ml). Cell lysates were analyzed for total EGFR expression and 8 phosphorylation sites (Phospho-EGFR 9-plex kit). Experiments were performed in biological duplicates. Measurements were performed in technical duplicates. Mean signal intensities were calculated from all data and visualized in box blot diagrams. Shown are signal intensities upon inhibitor treatment relative to control stimulations without inhibitor application. Boxes indicate the median and the 25th and 75th percentile. The 5th and 95th percentiles are represented by whiskers. Additionally the mean (square) and the 1st and 99th percentiles (crosses) are shown.

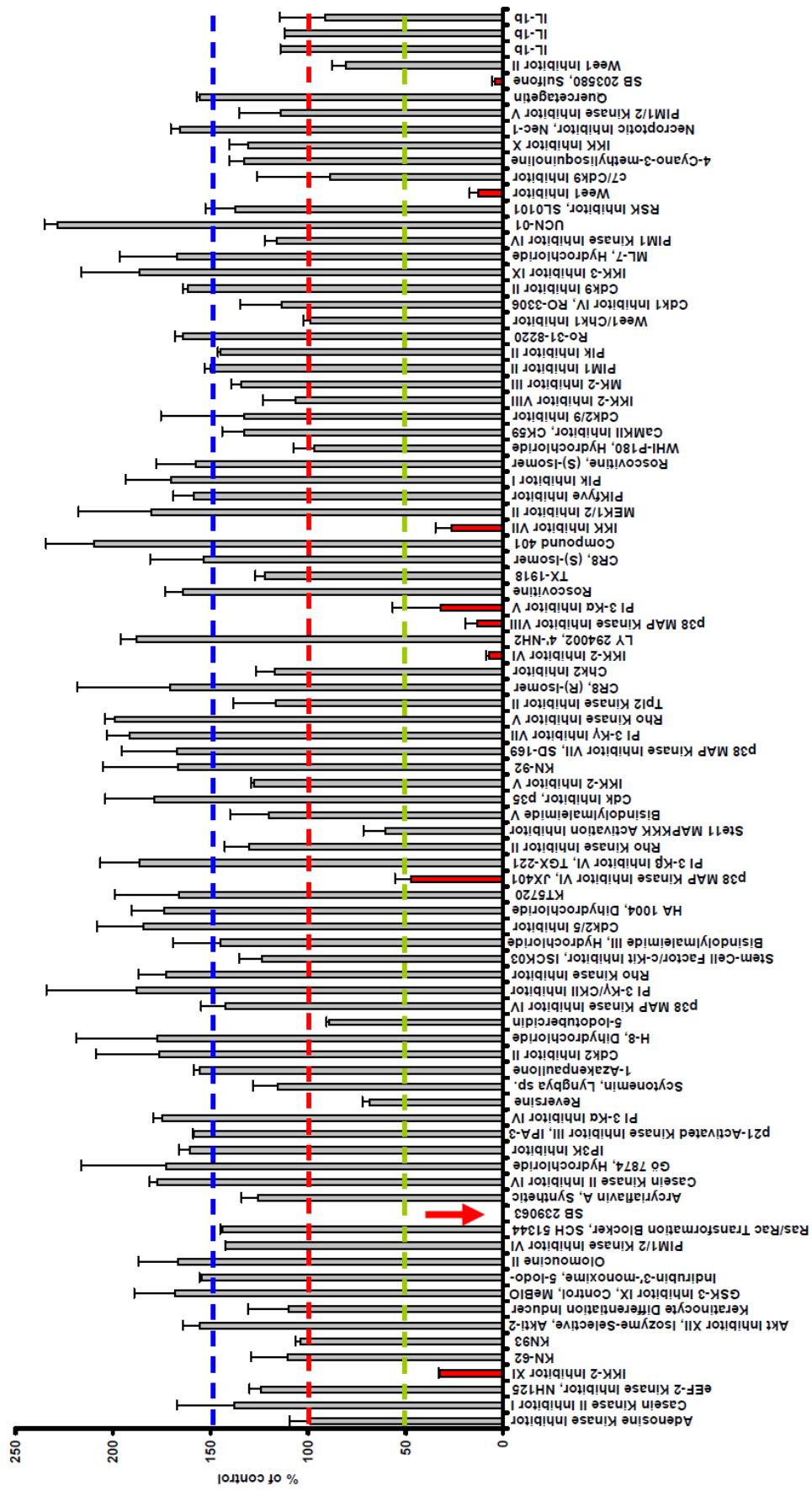


Figure 17: Kinase-inhibitor screening in IL-1 β stimulated Caco-2 cells. Cells were cultured in 96-well plates upon differentiation was accomplished. After starvation for 24 h cells were treated with 10 μ g/ml InhibitorSelect™ protein kinase inhibitors for 1 h followed by application of 10 ng/ml of IL-1 β for 30 min to trigger maximum S1047 phosphorylation. Final DMSO concentration was 0.1%. Medium + DMSO was added to control wells 1 h ahead of stimulation with IL-1 β . Cell lysates were analyzed using the phospho-EGFR 9-plex kit. Shown are percent signal intensities for S1047 phosphorylation upon inhibitor treatment relative to control stimulations. Data were normalized to total EGFR signals. Each bar represents the average of two independent cell culture experiments and duplicate measurements. Specific inhibition of S1047 phosphorylation (red bars \leq 50% compared to control wells) were observed upon treatment with inhibitors of p38 α , IKK-2 and WEE1.

4.3. In-vitro analysis of drug effects

In this study the initially described co-culture model of the human gut (see **chapter 1.2**), consisting of differentiated Caco-2 monolayers and heparinized whole blood was used to analyze the biological activity of well characterized antiphlogistic drugs and mainly uncharacterized natural products. An overview of the experimental setting is given in **figure 18**.

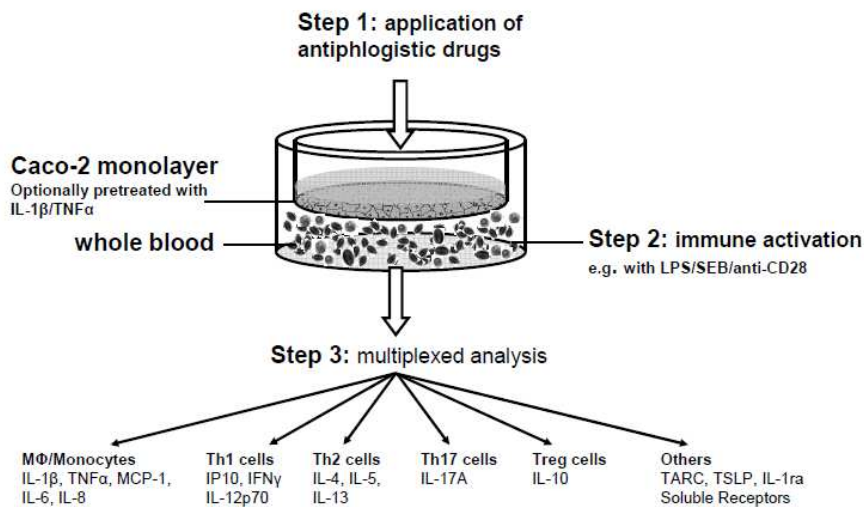


Figure 18: In-vitro analysis of drug effects.

Step 1 antiphlogistic drugs are applied on Caco-2 epithelia in a co-culture set up with human whole blood. **Step 2** inflammation is induced by injection of immune activating agents into the whole blood containing compartment. **Step 3** immune mediators of different subgroups are quantified in blood plasma using multiplexed sandwich immunoassays.

Differentiated Caco-2 cells were treated with five concentrations of the drugs Dexamethasone, Prednisolone, Diclofenac, Ibuprofen and Tacrolimus. Optionally the Caco-2 epithelia were treated with IL-1 β and TNF α ahead of drug application to mimic inflamed conditions. Then the Caco-2 monolayers were co-cultivated with heparinized whole blood. Three different healthy blood donors were tested in parallel for each drug. Experimental inflammation was elucidated in the whole blood by the application of the immune stimulating agents. After co-cultivation the Caco-2 monolayers were removed and the whole blood was further cultivated followed by multiplexed analysis of immune mediator concentrations in blood plasma. In particular the macrophage/monocyte associated mediators IL-6, IL-8, IL-1 β , TNF α , MCP-1, the Th1 associated mediators IFN γ and IP-10, the Th2 associated cytokines IL-4, IL-5 and IL-13, the regulatory cytokine IL-10, the Th17 associated mediator IL-17A as

well as soluble receptors, cell adhesion molecules and receptor antagonists were included in the analysis.

Prior to the drug testing experiments different immune stimulating agents (described in detail in **section 1.4.4**) were tested for their ability to induce immune response and their resultant secretion profile. On this basis well-characterized anti-inflammatory drugs and uncharacterized natural products should then be tested in the co-culture model.

4.3.1. Addressing subsets of immune cells

Whole blood of different donors was stimulated with either one of the stimulatory agents or mixtures LPS/SEB/anti-CD28, Zymosan, Zymosan/anti-CD3/anti-CD28, Poly I:C and anti-CD3/anti-CD28 in a co-culture set up with differentiated Caco-2 monolayers but without drug application. The concentration of immune mediators was subsequently measured in the blood supernatant. The obtained dataset was analyzed using hierarchical cluster analysis (complete linkage clustering, Euclidian Distance). Significance analysis was carried out using the SAM tool of the MeV 4.0 software. The underlying concentration data is shown in **supplementary table 4**. TSLP and IL-12p70 could not be detected in the test samples. These analytes were therefore excluded prior to clustering.

As can be seen in **figure 19** a clear distinction between the assigned treatment groups and the untreated control group is possible. Whereas all measured cytokines and chemokines were found to be differentially up regulated in the six sample groups no significant difference between treated and untreated samples was found for the soluble receptors and cell adhesion molecules. The tested samples clustered in accordance with their treatment, despite of the large differences between the individual blood donors concerning the expression level of the measured analytes (**supplementary table 4**). Moreover, the macrophage/monocyte associated analytes IL-6, IL-8, MCP-1, IL-1 β and TNF α are grouped together in the same cluster as well as the Th2 associated Cytokines IL-4 and IL-13.

Application of Zymosan leads to up regulation of the macrophage/monocyte associated mediators IL-6, IL-8, IL-1 β and TNF α . Elevated secretion of T-cell associated mediators could not be observed. In contrast stimulation with anti-CD3/anti-CD28 antibodies activated the T-cell specific mediators IL-10, IFN γ , IL-17A, IL-5, IP-10, TARC and IL-4 but not the macrophage/monocyte specific cytokines and chemokines. Treatment with Zymosan/anti-CD3/anti-CD28 effectively stimulated macrophage/monocyte and T-cell associated mediator secretion. This treatment led to an increased IL-13 secretion whereas IP-10 could not be detected. IP-10 could be selectively activated by Poly I:C treatment, however all other mediators could not be detected after this treatment. Combined treatment with LPS/SEB and anti-CD28 resulted in a broad immune activation including all macrophage/monocyte associated and T-cell associated mediators.

The tested immune activators allow to selectively activate different immune cell populations regardless of the immunologic diversity of the individual blood donors. Based on these results antiphlogistic substances can be tested in the co-culture model in different experimental set ups. For the further experiments, LPS/SEB/anti-CD28 was selected as stimulating agent. The stimulation of whole blood with immunoactivating agents did not cause significant alterations in the level of soluble receptors and cell adhesion proteins compared to the untreated controls. Therefore, these analytes were not included in the analysis of drug effects.

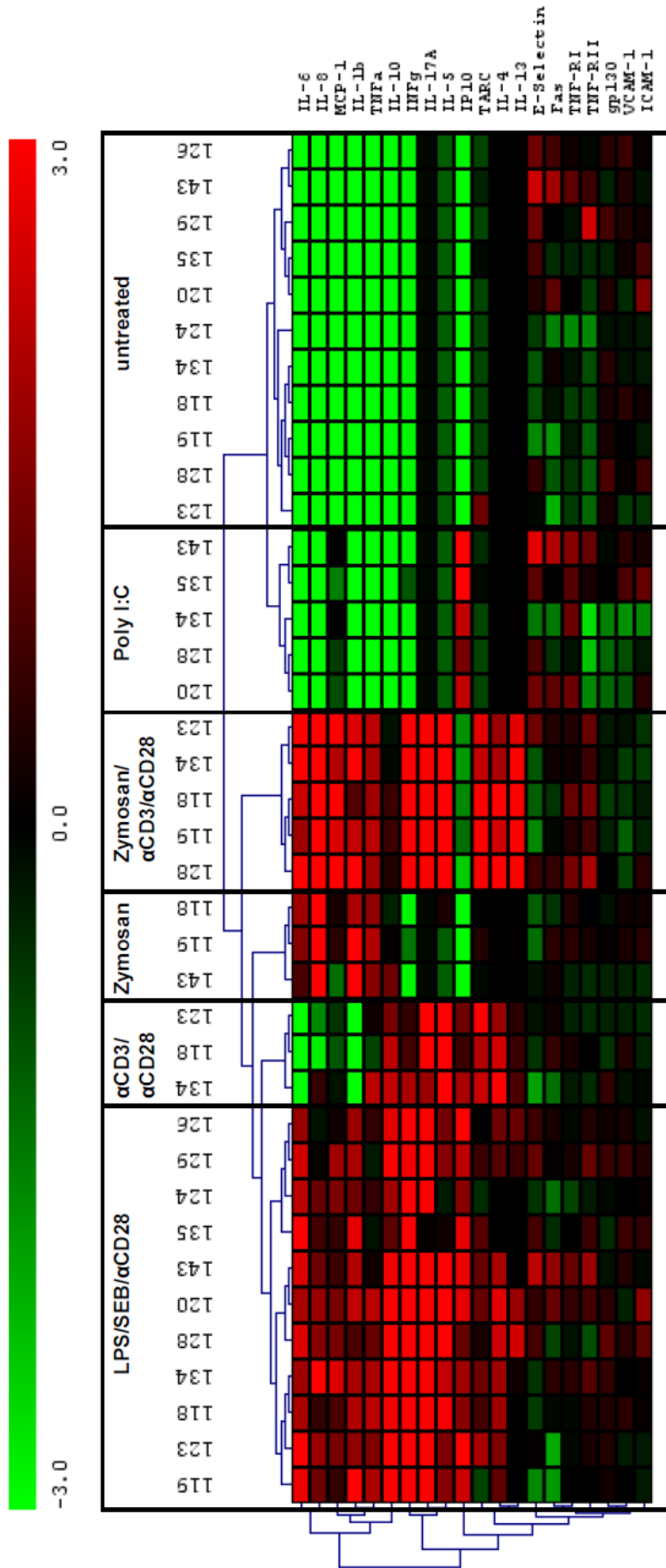


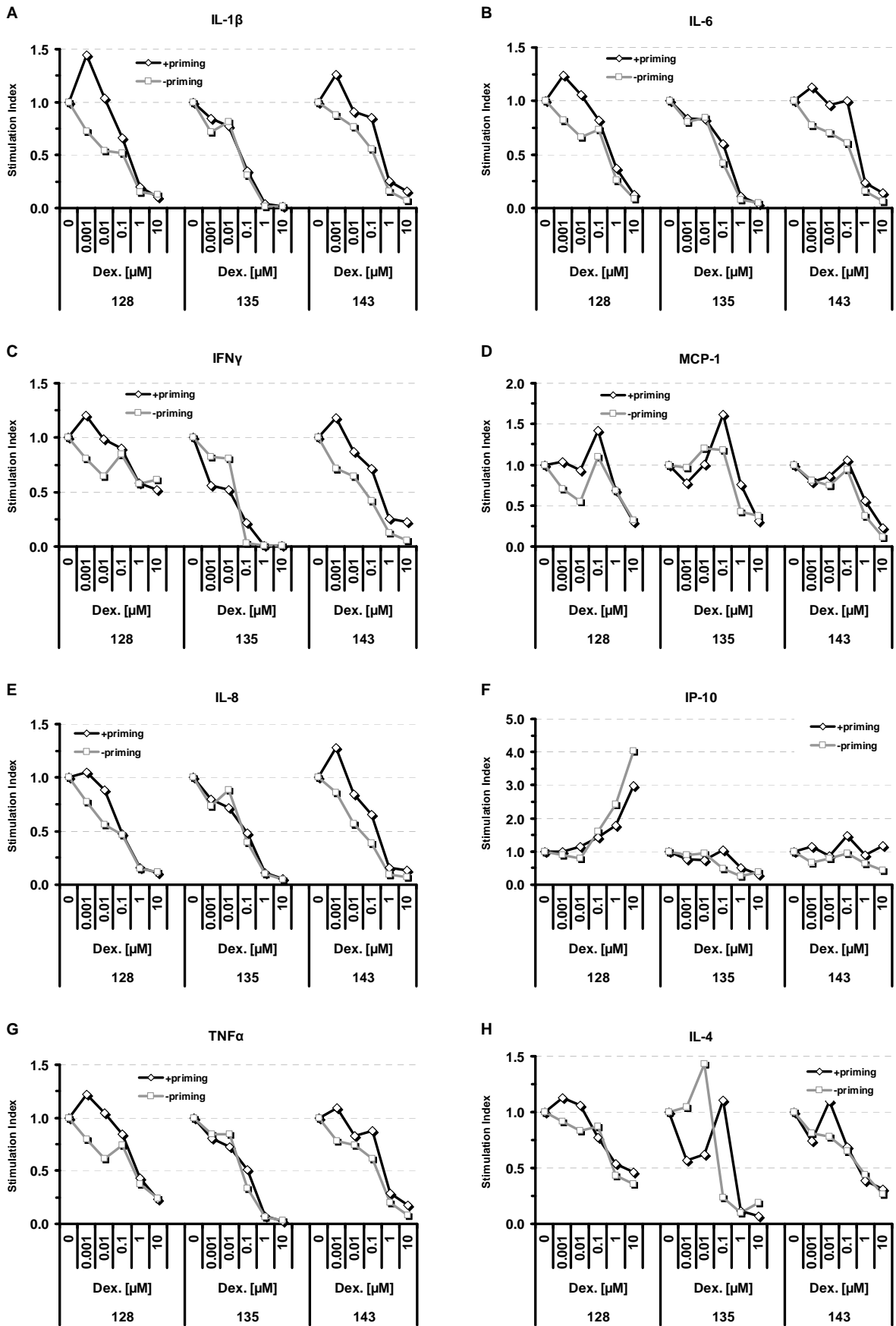
Figure 19: Hierarchical Clusteranalysis of immune mediator concentrations. Heparinized whole blood of different donors (indicated by their ID numbers) was treated with the indicated immune activating agents or mixtures in a co-culture set up with differentiated Caco-2 monolayers. Caco-2 cells were removed after 5 h and the whole blood was further cultivated for 18 h. The content of duplicate wells was pooled and the blood plasma was analyzed using multiplexed sandwich immunoassays. The measured analyte concentrations were median centered, log2 transformed and analyzed using hierarchical cluster analysis (complete linkage clustering, Euclidian Distance). Significance analysis was done using the SAM tool of the MeV 4.0 software. 13 cytokines/chemokines were found to be differentially up regulated in the 6 treatment groups. No significant differences could be observed in the concentrations of Fas, gp130, TNFRI, TNFRII, E-Selectin, ICAM1 and VCAM-1 between the treatment groups and the control group.

4.3.2. Effect of Dexamethasone on immune mediator release

Dexamethasone was initially tested in the co-culture model. The resultant dose response curves for each measured analyte are shown in **figure 20**. Depicted are relative concentration data referenced to the concentrations measured in the diluent control samples (stimulation index). The underlying cytokine/chemokine concentrations of the corresponding diluent controls are listed in **supplementary table 5** together with the basal levels of immune mediators measured in the unstimulated control samples (cell control).

Application of Dexamethasone led to a strong concentration dependent inhibition of the macrophage/monocyte associated mediators IL-1 β , IL-6, TNF- α and IL-8 for all three tested donors with comparable curve shapes. For MCP-1 an initial induction at low concentrations followed by a strong concentration dependent suppression could be observed. The Th1 associated mediators showed partially opposing curve shapes. Whereas Dexamethasone treatment led to a concentration dependent decline of IFN γ concentrations for all tested donors, the concentration of IP-10 was strongly induced for donor 128, inhibited for donor 135 and remained unaffected for donor 143. IL-10, a Treg associated cytokine was also inhibited in a concentration dependent manner. The Th2 associated cytokines IL-4, IL-5 and IL-13 revealed an inhibitory effect of Dexamethasone. However, the magnitude of the IL-13 inhibition varied between the tested individuals. The Th17 associated mediator IL-17A as well as IL-1ra were strongly inhibited by Dexamethasone treatment for all three tested individuals. TARC showed heterogenous curve shapes.

In principle, comparable curve shapes could be observed when Caco-2 monolayer were pre-incubated with 10 ng/ml of IL-1 β /TNF α ahead of usage in the co-culture system. However, the stimulation indices of the macrophage/monocyte associated mediators IL-1 β , IL-6, MCP-1, IL-8 and TNF α were elevated at low and medium drug concentrations for donors 128 and donor 143 while for all other mediators no clear effect of the pretreatment with IL-1 β /TNF α could be found.



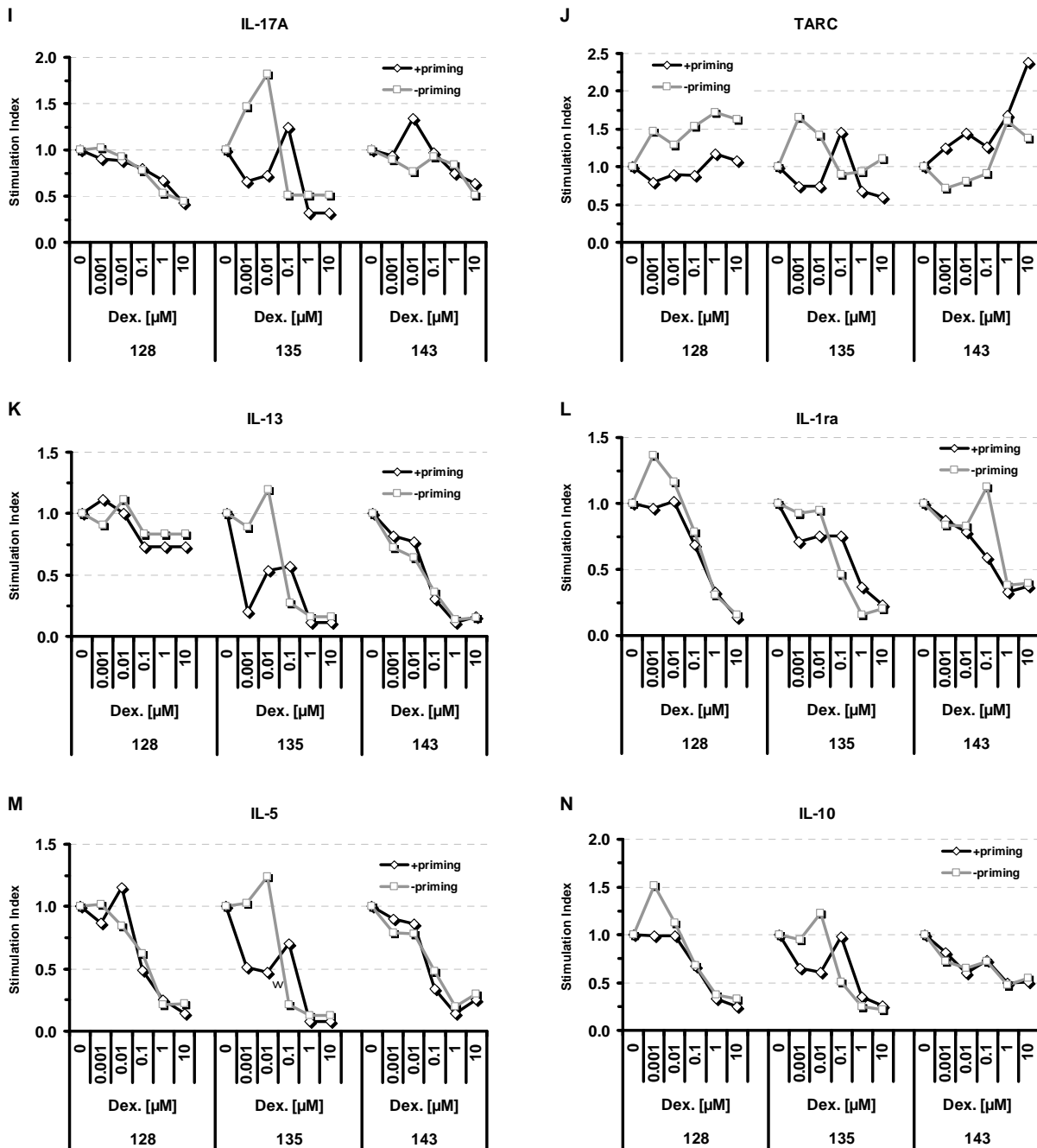


Figure 20: Release of immune mediators after Dexamethasone application.

The indicated concentrations of Dexamethasone were applied on top of differentiated Caco-2 monolayers. Prior to usage Caco-2 cells were either primed (squares) with IL-1 β /TNF α for 6 h or used unprimed (diamonds). Caco-2 cells in transwell inserts were transferred to culture vessels filled with heparinized whole blood of three different healthy donors (indicated by their ID-numbers). After 1 h LPS/SEB/anti-CD28 was injected in the blood containing lower compartment. After 6 h of co-cultivation the Caco-2 monolayers were removed and the whole blood was further incubated for 18 h. 14 different cytokines/chemokines were quantified in the blood plasma using sandwich immunoassays. Depicted are stimulation indices of single experiments. **A** IL-1 β , **B** IL-6, **C** IFN γ , **D** MCP-1, **E** IL-8, **F** IP-10, **G** TNF α , **H** IL-4, **I** IL-17A, **J** TARC, **K** IL-13, **L** IL-1ra, **M** IL-5, **N** IL-10.

4.3.3. Effect of Prednisolone on immune mediator release

Prednisolone was tested under similar experimental conditions using both primed and unprimed Caco-2 cells. The resultant dose response curves for each measured analyte are shown in **figure 21**. Depicted are relative concentration data referenced to the concentrations measured in the diluent control samples (stimulation index). The underlying cytokine/chemokine concentrations of the corresponding diluent controls are listed in **supplementary table 5** together with the basal levels of immune mediators measured in the unstimulated control samples.

In the unprimed set up Prednisolone exhibited a concentration dependent inhibitory effect on the release of the macrophage/monocyte associated mediators IL-1 β , IL-6, TNF α and IL-8. However, the response pattern differed between the tested blood donors. Whereas the donors 134 and 118 displayed clear inhibitory effects upon drug treatment, donor 120 showed inconsistent curve shapes with no clear tendency. Only a minimum inhibitory effect could be found for the IL-8 secretion of donor 118, while high concentrations of Prednisolone induced MCP-1 secretion of this donor. The two other donors showed minor alterations in the levels of MCP-1.

Prednisolone treatment led to a concentration dependent decline of the IFN γ secretion for the donors 134 and 118, whereas the release of IP-10 was induced for donor 118. No alterations were found for the IP-10 secretion of donor 134. Donor 120 showed a discrete curve shape with a decrease at low and medium drug concentrations followed by an increase at higher concentrations for both Th1 associated analytes. The Treg associated mediator IL-10 did not show any dose dependent effect. The measured concentrations of the Th2 associated mediators IL-4 and IL-5 showed heterogeneous response curves upon corticosteroid treatment for the donors 134 and 120 whereas the release of IL-5 was tendentially inhibited for donor 118. Due to its low secretion levels, IL-13 could only be quantified in the plasma of the donors 134 and 120. Whereas donor 134 showed an unsteady trend a concentration dependent inhibition was measured for donor 120. With respect to the measured IL-17A concentrations, Prednisolone was ineffective for the donors 134 and 118. Donor 120 showed a moderate inhibitory effect. IL-1ra was only measured in the plasma of two donors with tendentially inhibitory effects.

In contrast to the results obtained for Dexamethasone, priming of Caco-2 monolayers with IL-1 β and TNF α resulted in clear differences relative to the unprimed set up. Priming of the epithelial cells led to an altered mediator release and differences in curve shapes. For the donors 118 and 134 a clearly increased release of the mediators IL-1 β , IL-6, IFN γ and TNF α in comparison to the unprimed set up could be detected. Notably no inhibitory effect of Prednisolone could be found. Donor 120 showed lower analyte levels when primed monolayers were used. IP-10 was induced by Prednisolone for donor 118 like in the unprimed set up but with a increased curve slope. Clear differences between the two set ups were also measured for IL-8. Here the chemokine levels were clearly decreased when primed monolayer were used. Donor 118 exhibited elevated IL-4 concentrations in comparison to the unprimed set up with no distinct drug effect. Elevated secretion levels were also found for IL-5 in the blood of the donors 120 and 118. All other measured analytes revealed only minor difference between the primed and unprimed experimental set ups.

In accordance with the relevant literature [120] the measured inhibitory effect of Prednisolon was remarkably lower than the effect Dexamethasone. Inhibitory effects were mainly observed for the macrophage/monocyte associated mediators. In contrast to the Dexamethason tests the use of primed Caco-2 monolayers led to alterations in curve shapes and mediator concentrations for these analytes.

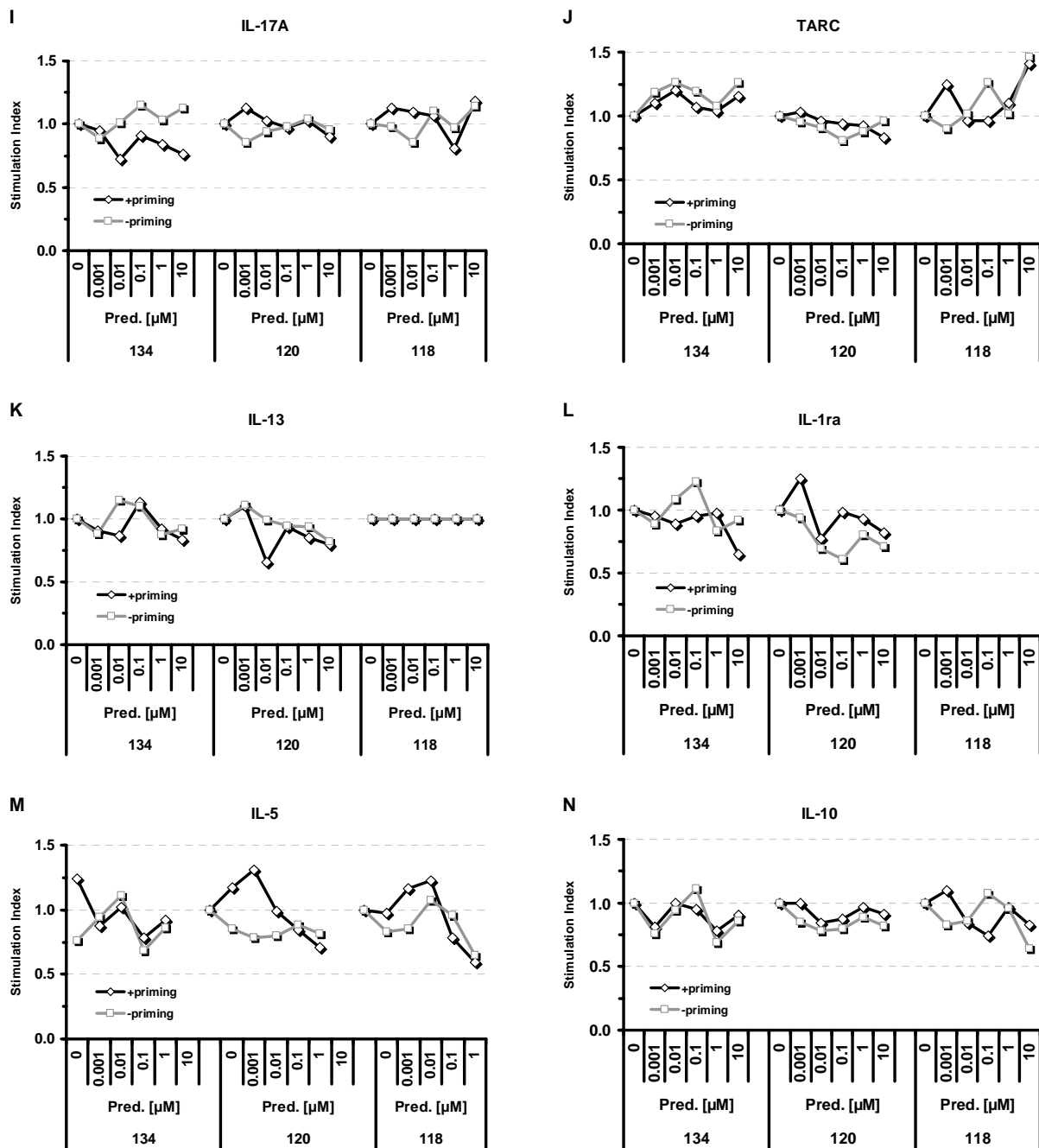


Figure 21: Release of immune mediators after Prednisolone application.

The indicated concentrations of Prednisolone were applied on top of differentiated Caco-2 monolayers. Prior to usage Caco-2 cells were either primed (squares) with IL-1 β /TNF α for 6 h or used unprimed (diamonds). Caco-2 cells in transwell inserts were transferred to culture vessels filled with heparinized whole blood of three different healthy donors (indicated by their ID-numbers). After 1 h the whole blood in the lower compartment was stimulated by LPS/SEB/anti-CD28 injection. After 6 h the Caco-2 cells were removed and the whole blood was further incubated for 18 h. Immune mediators were quantified in plasma. Depicted are stimulation indices of single experiments. **A** IL-1 β , **B** IL-6, **C** IFN γ , **D** MCP-1, **E** IL-8, **F** IP-10, **G** TNF α , **H** IL-4, **I** IL-17A, **J** TARC, **K** IL-13, **L** IL-1ra, **M** IL-5, **N** IL-10.

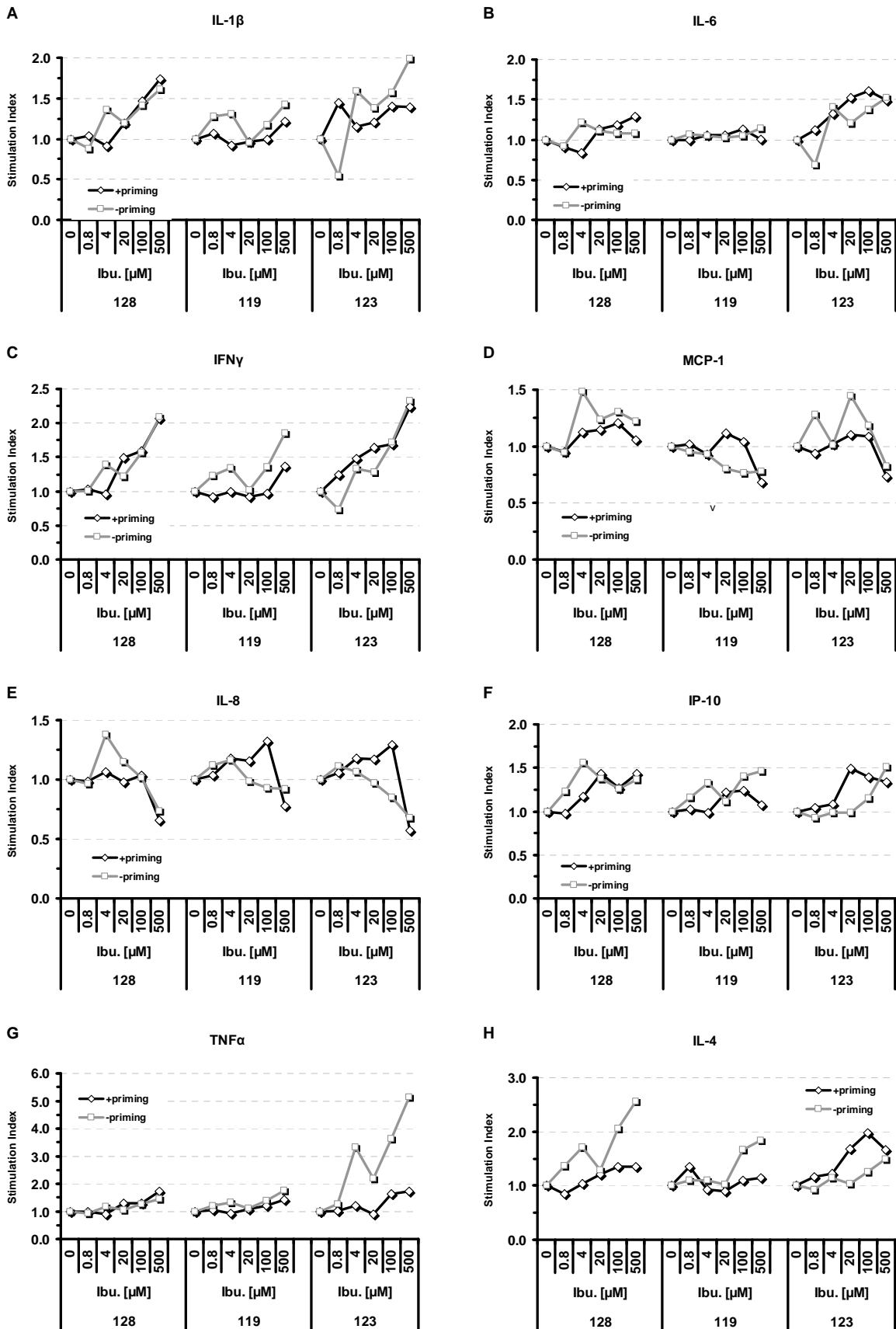
4.3.4. Effect of Ibuprofen on immune mediator release

Ibuprofen as a representative of NSAIDs was also tested in the co-culture model. The dose response curves for each measured analyte are shown in **figure 22**. Depicted are relative concentration data referenced to the concentrations measured in the diluent control samples (stimulation index). The underlying cytokine/chemokine concentrations of the corresponding diluent controls are listed in **supplementary table 5** together with the basal levels of immune mediators measured in the unstimulated control samples.

The macrophage/monocyte associated mediators IL-1 β , and TNF- α were stimulated by Ibuprofen in a concentration dependent manner. Only the blood of donor 123 responded to Ibuprofen treatment with an increased IL-6 release while the two other blood donors remained unresponsive. IL-8 was inhibited and MCP-1 showed heterogeneous curve shapes with a moderate inhibitory effect for donors 119 and 123.

The Th1 associated mediators IFN γ and IP-10 were both induced by Ibuprofen for all tested donors. The Treg associated cytokine IL-10 showed no clear alterations for donors 128 and 123 in comparison to the untreated reference. For donor 119 a slight inhibition was observed. The Th2 associated cytokines IL-4 and IL-5 were induced upon drug treatment for all three blood donors whereas IL-13 showed inconsistent curve shapes with no clear tendency. The release of the Th17 associated cytokine IL-17A was clearly inhibited by Ibuprofen in a concentration dependent manner for all three blood donors. TARC was inhibited in the blood of donors 128 and 123 whereas the TARC levels of donor 119 were below detection limit. No alterations could be detected for IL-1ra in the plasma of two blood donors tested.

When primed Caco-2 cells were used comparable results were found with minor alterations in the shapes of the dose response curves. Whereas donor 123 responded to Ibuprofen treatment with a strong TNF α induction in the unprimed set up the response was more moderate when Caco-2 cells were primed before drug application. For the same donor the concentrations of IL-17A and IL-8 decreased comparably slow at low and medium drug concentrations with a sudden decrease when the highest drug concentration was applied.



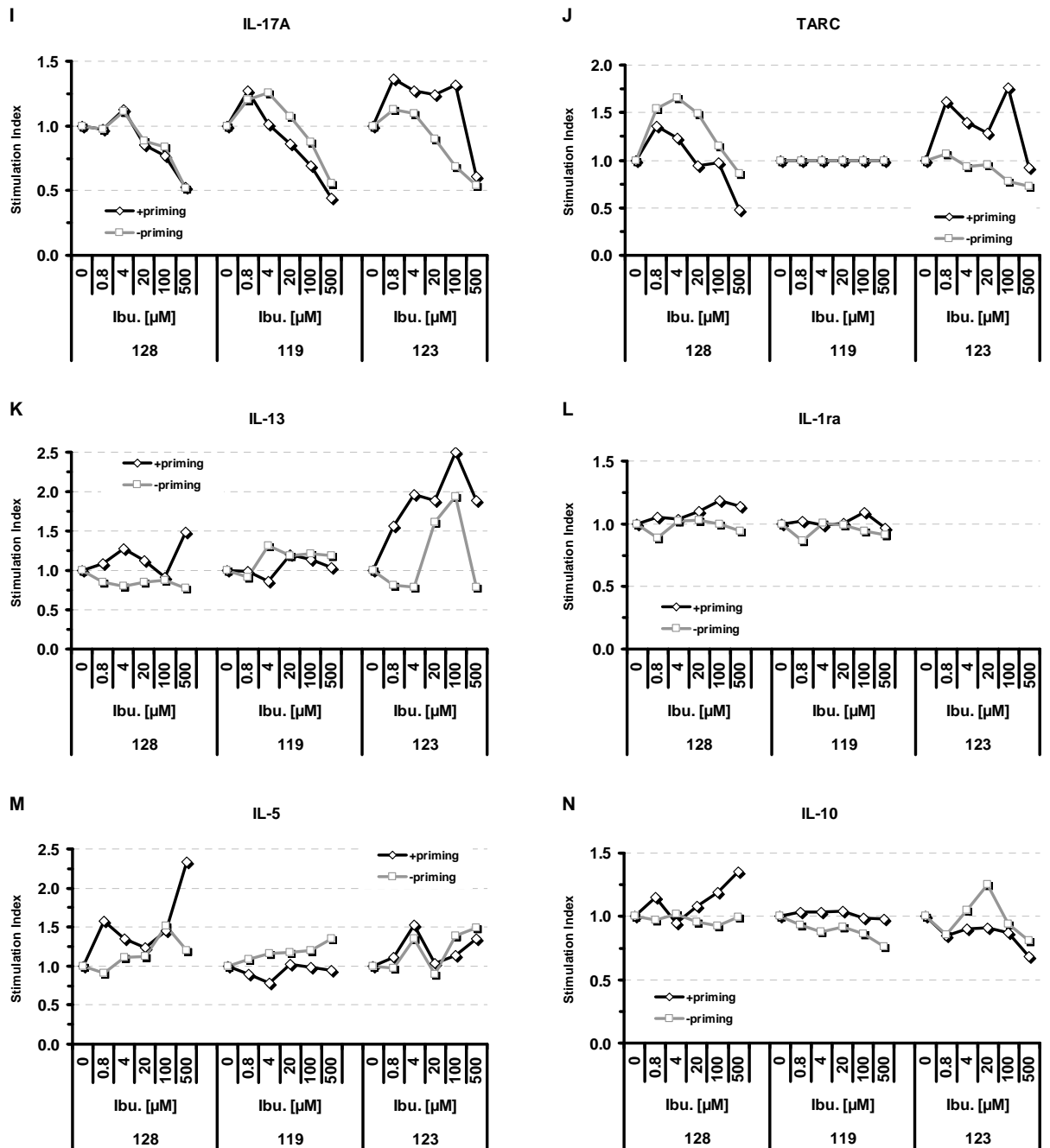


Figure 22: Release of immune mediators after Ibuprofen application.

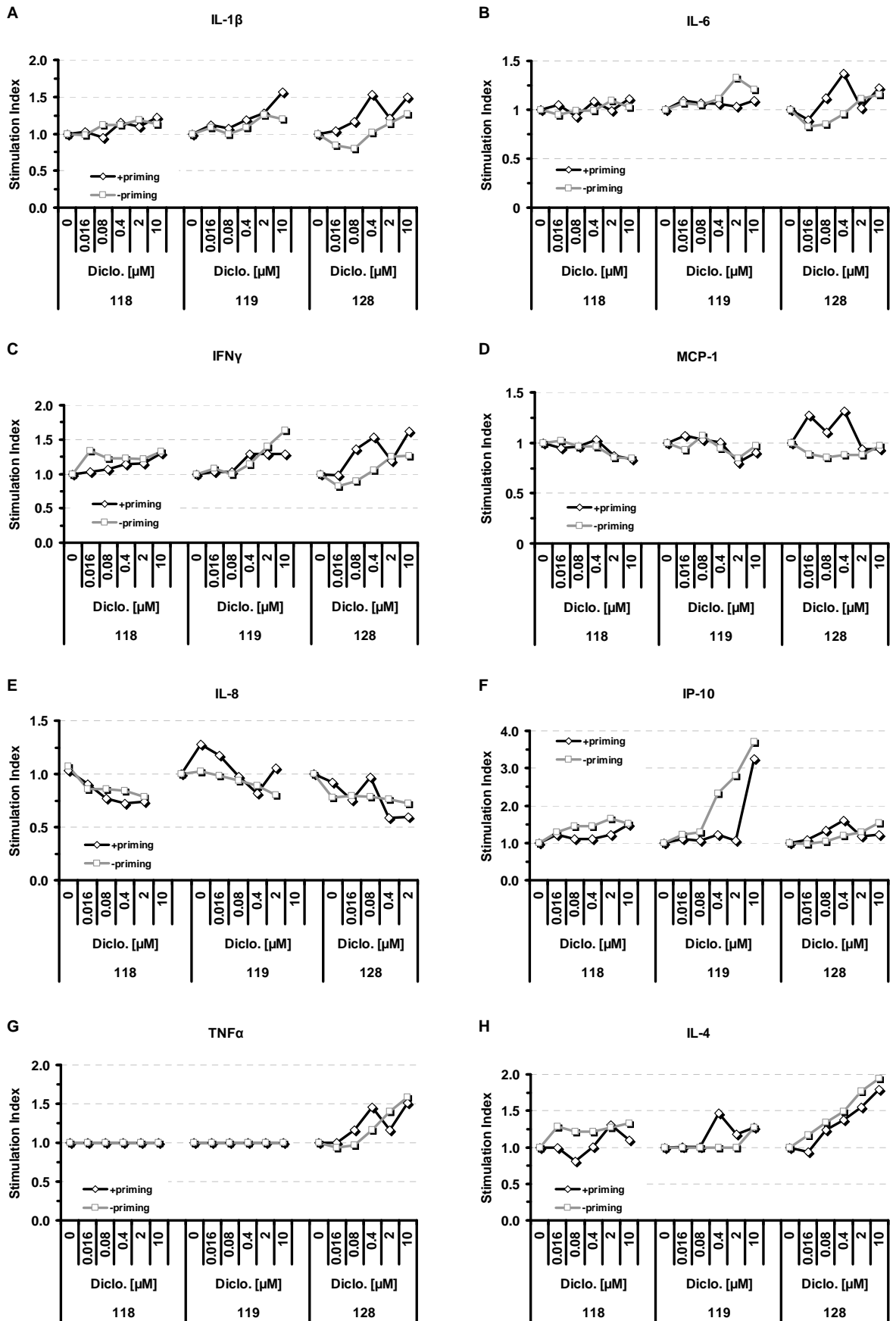
The indicated concentrations of Ibuprofen were applied on top of differentiated Caco-2 monolayers. Prior to usage Caco-2 cells were either primed (squares) with IL-1 β /TNF α for 6 h or used unprimed (diamonds). Caco-2 cells in transwell inserts were transferred to culture vessels filled with heparinized whole blood of three different healthy donors (indicated by their ID-numbers). After 1 h the whole blood in the lower compartment was stimulated by LPS/SEB/anti-CD28 injection. After 6 h Caco-2 cells were removed and the whole blood was further incubated for 18 h. Immune mediators were quantified in plasma. Depicted are stimulation indices of single experiments. **A** IL-1 β , **B** IL-6, **C** IFN γ , **D** MCP-1, **E** IL-8, **F** IP-10, **G** TNF α , **H** IL-4, **I** IL-17A, **J** TARC, **K** IL-13, **L** IL-1ra, **M** IL-5, **N** IL-10.

4.3.5. Effect of Diclofenac on immune mediator release

Next the immune modulating effect of Diclofenac was tested. The results are shown in **figure 23**. Depicted are relative concentration data referenced to the concentrations measured in the diluent control samples (stimulation index). The underlying cytokine/chemokine concentrations of the corresponding diluent controls are listed in **supplementary table 5** together with the basal levels of immune mediators measured in the unstimulated control samples (cell control).

Similar to Ibuprofen the macrophage/monocyte associated mediator IL-1 β was concentration dependently stimulated by Diclofenac application but to a much lower extent. TNF α was stimulated for donor 128, whereas the measured concentrations for the other donors exceeded the upper limit of detection and could therefore not be quantified. IL-6 was tendentially stimulated for donors 119 and 128 and MCP1 showed small inhibitory effects for the donors 118 and 119. IL-8 was moderately inhibited for all three tested donors.

The Th1 associated mediators IFN γ and IP-10 were both induced in a concentration dependent manner. As already observed for Ibuprofen the Treg associated cytokine IL-10 showed no clear alterations in comparison to the untreated reference. However, for donor 128 a moderate induction could be observed. The Th2 associated cytokine IL-4 was induced by drug treatment especially for donor 128. Donor 119 showed only a slight increase in IL-4 concentration. The same was true for IL-5. Here donor 128 responded strongly whereas the two other donors showed heterogeneous curve shapes. IL-13 could only be quantified in the blood of donor 128 with heterogeneous curve shapes. All three donors showed a strong concentration dependent inhibition of IL-17A release by Diclofenac. In contrast the mediators TARC and IL-1ra showed no clear tendency. IL-1ra was induced by low drug concentrations whereas higher drug levels led to a decrease. When Caco-2 cells were primed prior to usage in the co-culture the results were in a similar range with slight modifications.



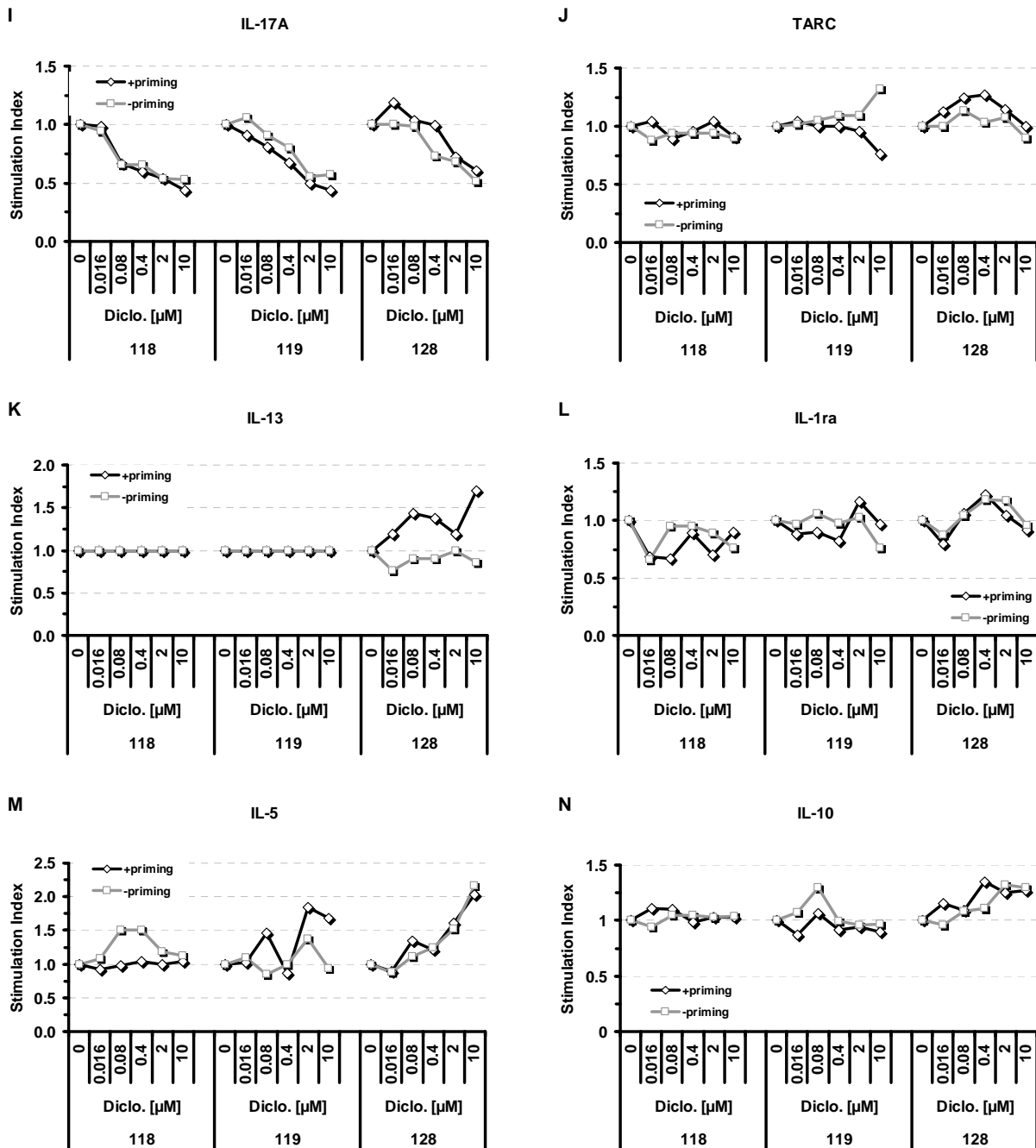


Figure 23: Release of immune mediators after Diclofenac application.

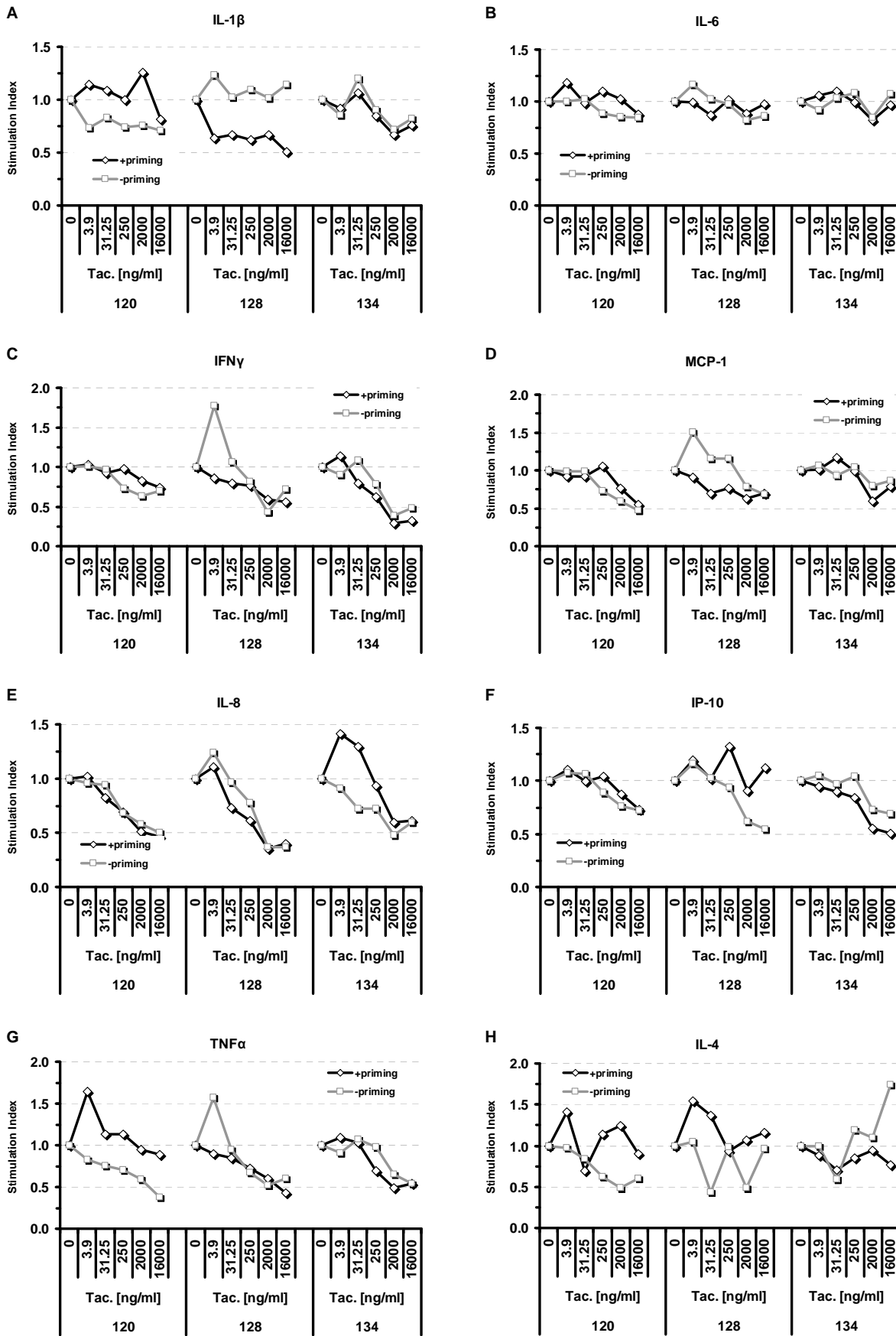
The indicated concentrations of Diclofenac were applied on top of differentiated Caco-2 monolayers. Prior to usage Caco-2 cells were either primed (squares) with IL-1 β /TNF α for 6 h or used unprimed (diamonds). Caco-2 cells in transwell inserts were transferred to culture vessels filled with heparinized whole blood of three different healthy donors. After 1h, the whole blood in the lower compartment was stimulated by LPS/SEB/anti-CD28 injection. After 6 h, the Caco-2 monolayers were removed and the whole blood was further incubated for 18 h. Immune mediators were quantified in plasma. Depicted are stimulation indices of single experiments. **A** IL-1 β , **B** IL-6, **C** IFN γ , **D** MCP-1, **E** IL-8, **F** IP-10, **G** TNF α , **H** IL-4, **I** IL-17A, **J** TARC, **K** IL-13, **L** IL-1ra, **M** IL-5, **N** IL-10.

4.3.6. Effect of Tacrolimus on immune mediator release

Tacrolimus is a representative of the macrolide immune suppressants and was tested in addition to the Corticosteroid or NSAID class of drugs. The results are shown in **figure 24**. Depicted are relative concentration data referenced to the concentrations measured in the diluent control samples (stimulation index). The underlying cytokine/chemokine concentrations of the corresponding diluent controls are listed in **supplementary table 5** together with the basal levels of immune mediators measured in the unstimulated control samples (cell control).

When unprimed Caco-2 monolayers were used, increasing concentrations of Tacrolimus clearly inhibited the release of IL-8, MCP-1, IL-6 and TNF α . The secretion of IL-1 β was slightly inhibited for donor 134 whereas the two other donors remained unresponsive. The same donor showed only a weak response with respect to IL-6 release with a sudden increase at the highest concentration.

A clear inhibition could also be detected for the Th1 associated mediators IFN γ and IP-10 for all three donors. Moreover Tacrolimus application stimulated the release IL-13 for all three donors. The release of IL-5 was induced for donors 128 and 134 in a concentration dependent manner, while IL-4 showed heterogeneous curve shapes and no clear tendency. Similar to the tested NSAIDs, Tacrolimus led to a strong decline of IL-17A release. The Treg associated mediator IL-10 as well as TARC was also inhibited by increasing Tacrolimus concentrations. Tendency inhibition could be observed for the IL-1ra release of the two donors 128 and 134. Like for the other test substances priming of the Caco-2 cells prior to use only partially affected the dose response curves. Interestingly the IL-1 β release of the donors 120 and 128 was clearly affected when primed monolayer were used.



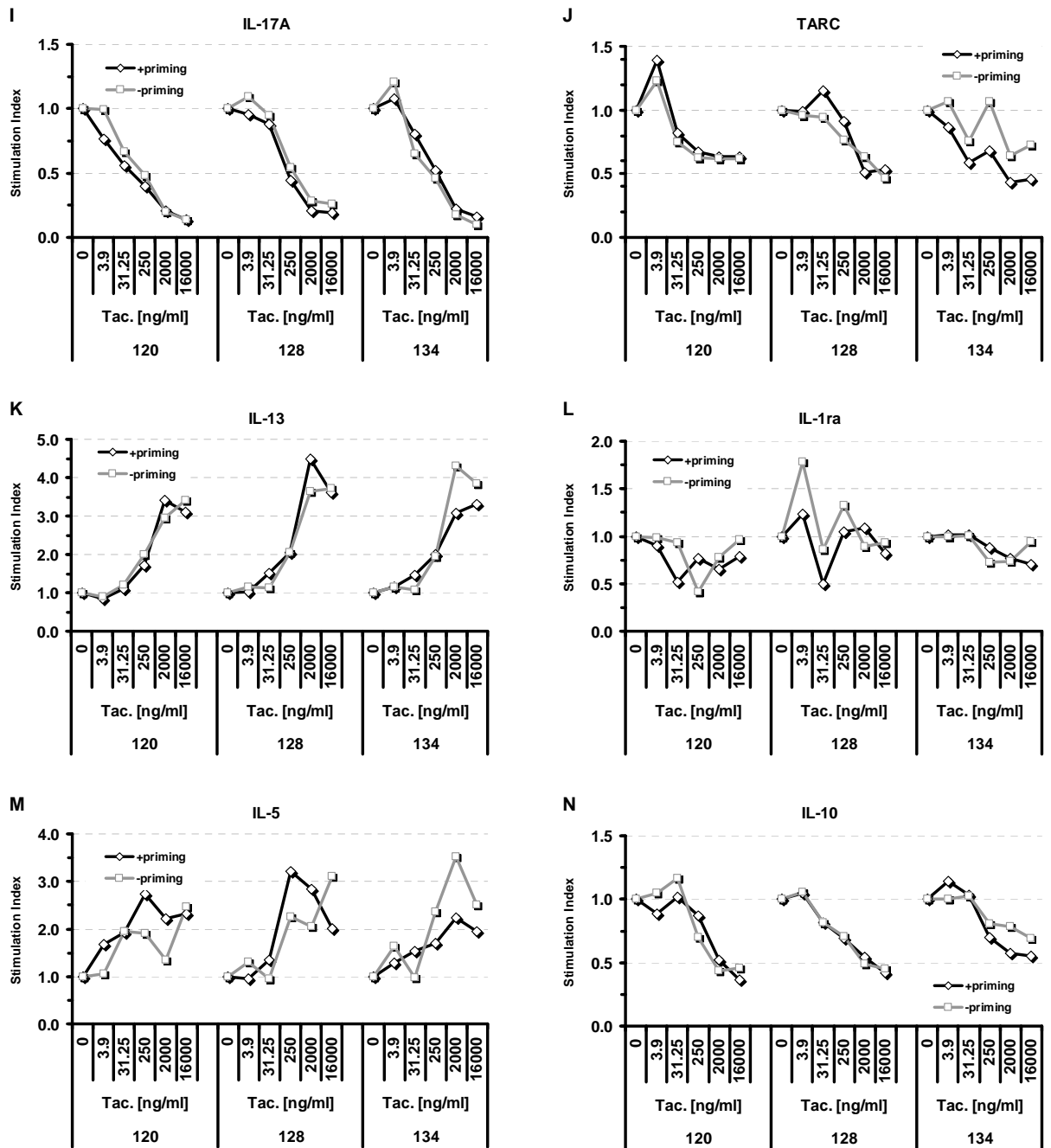


Figure 24: Release of immune mediators after Tacrolimus application. Tacrolimus was applied to IL-1 β /TNF α pretreated (diamonds) or unprimed (squares) Caco-2 monolayer in the indicated concentrations. Caco-2 cells in transwell inserts were transferred to culture vessels filled with heparinized whole blood of three different healthy donors (indicated by their ID-numbers). After 1 h the whole blood in the lower compartment was stimulated by LPS/SEB/anti-CD28 injection. After 6 h the Caco-2 cells were removed and the whole blood was further incubated for 18 h. Immune mediators were quantified in plasma. Depicted are stimulation indices of single experiments. **A** IL-1 β , **B** IL-6, **C** IFN γ , **D** MCP-1, **E** IL-8, **F** IP-10, **G** TNF α , **H** IL-4, **I** IL-17A, **J** TARC, **K** IL-13, **L** IL-1ra, **M** IL-5, **N** IL-10.

4.3.7. The co-gut system as a test model for drug candidates

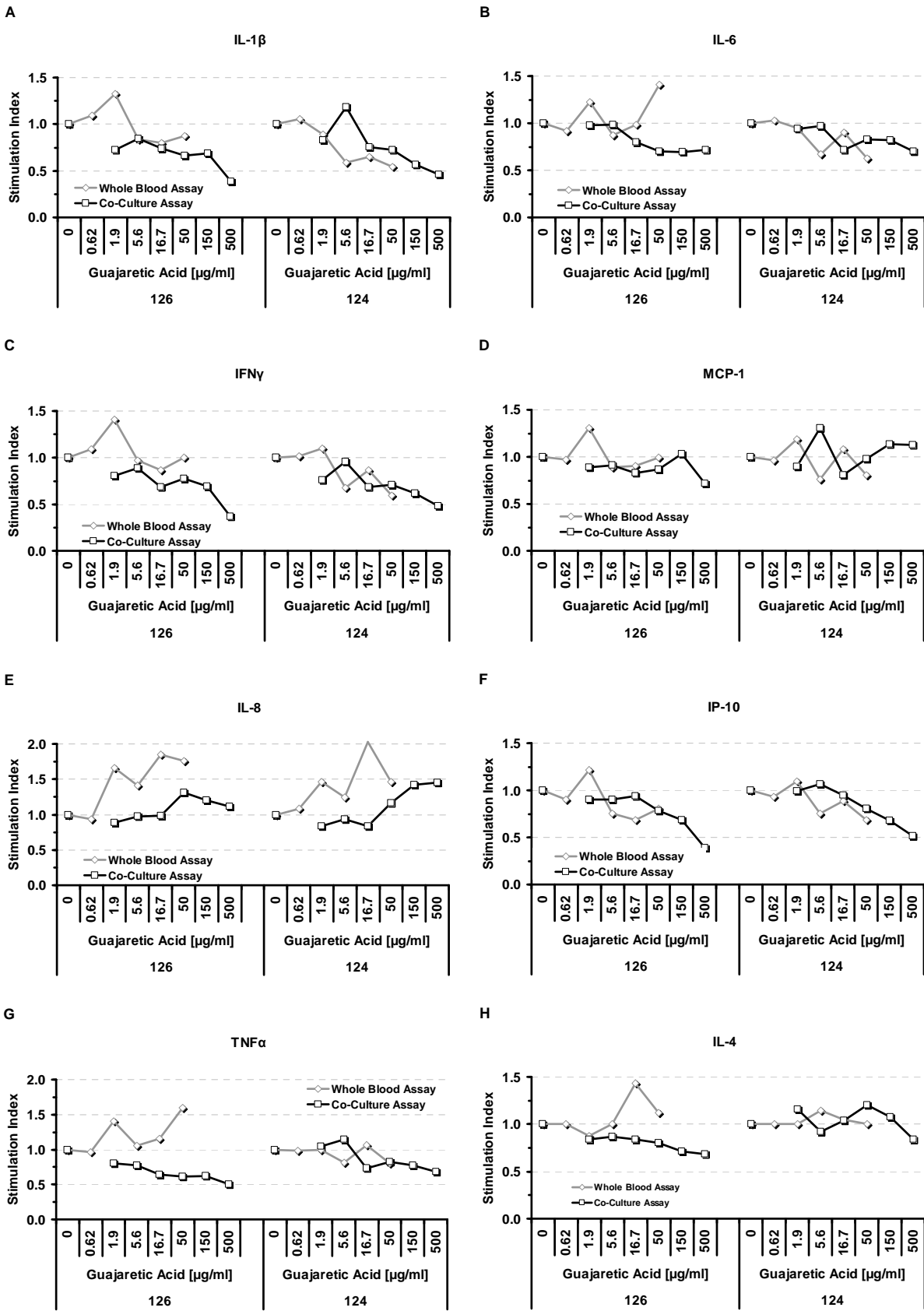
The presented co-culture model consisting of differentiated Caco-2 monolayer and whole blood of different donors combined with a multi-parameter read out system is perfectly suited to evaluate the immune modulating effect of biologically active substances such as drug candidates and entirely uncharacterized substances. In the course of this thesis different natural products were tested in order to investigate effects on inflammation associated signaling processes. This was done for the purified substance as well as for different crude plant extracts. All substances were provided by the Intermed discovery GmbH. In particular Dihydroxyguajaretic acid (Guaiacum Officinale), Harpagosid (Harpagophytum procumbens) as well as Glycyrrhizin and Glycyrrhetin (Glycyrrhiza glabra) were tested. Here the focus should be on the results obtained for purified Dihydroxyguajaretic acid since neither Harpagosid nor Glycyrrhizin and Glycyrrhetin exhibited significant immune modulating effects in the performed experiments (data not shown).

For a more detailed understanding of the influence of Caco-2 monolayers on drug activity, conventional whole blood assays were performed in parallel to the co-culture experiments. This enabled a direct comparison between the two *in vitro* test systems. **Figure 25** shows the obtained results for the two tested blood donors 126 and 124. Due to the poor solubility of the test substance in aqueous medium concentrations >50 µg/ml could not be tested in the whole blood culture. Depicted are relative concentration data referenced to the concentrations measured in the diluent control samples (stimulation index). The underlying cytokine/chemokine concentrations of the corresponding diluent controls are listed in **supplementary table 5** together with the basal levels of immune mediators measured in the unstimulated control samples (cell control).

The macrophage/monocyte associated mediator IL-1 β was concentration dependently inhibited by the test substance in both assay systems. IL-6 and TNF α showed clear inhibitory effects in the co-culture set up while results differed between the two donors in the whole blood assay. Whereas donor 124 responded in a similar manner than in the co-culture model, an induction was observed for donor 126. The concen-

tration of MCP-1 remained mainly unaffected. The chemokine IL-8 was induced by increasing substance concentrations.

The two Th1 associated mediators IFN γ und IP-10 were clearly inhibited by increasing concentrations in both test-systems. The Th17 associated cytokine IL-17A was moderately inhibited in a concentration dependent manner. The Th2 associated mediators IL-4 and IL-5 remained relatively unaffected. IL-13 was tendentially inhibited at the highest concentration tested. IL-10 as a representative of Treg associated mediators was inhibited as well as IL-1ra. TARC showed heterogeneous curve shapes with no clear tendency. The direct comparison of the two test-systems revealed mainly similar response patterns with infrequent differences in the effective concentrations.



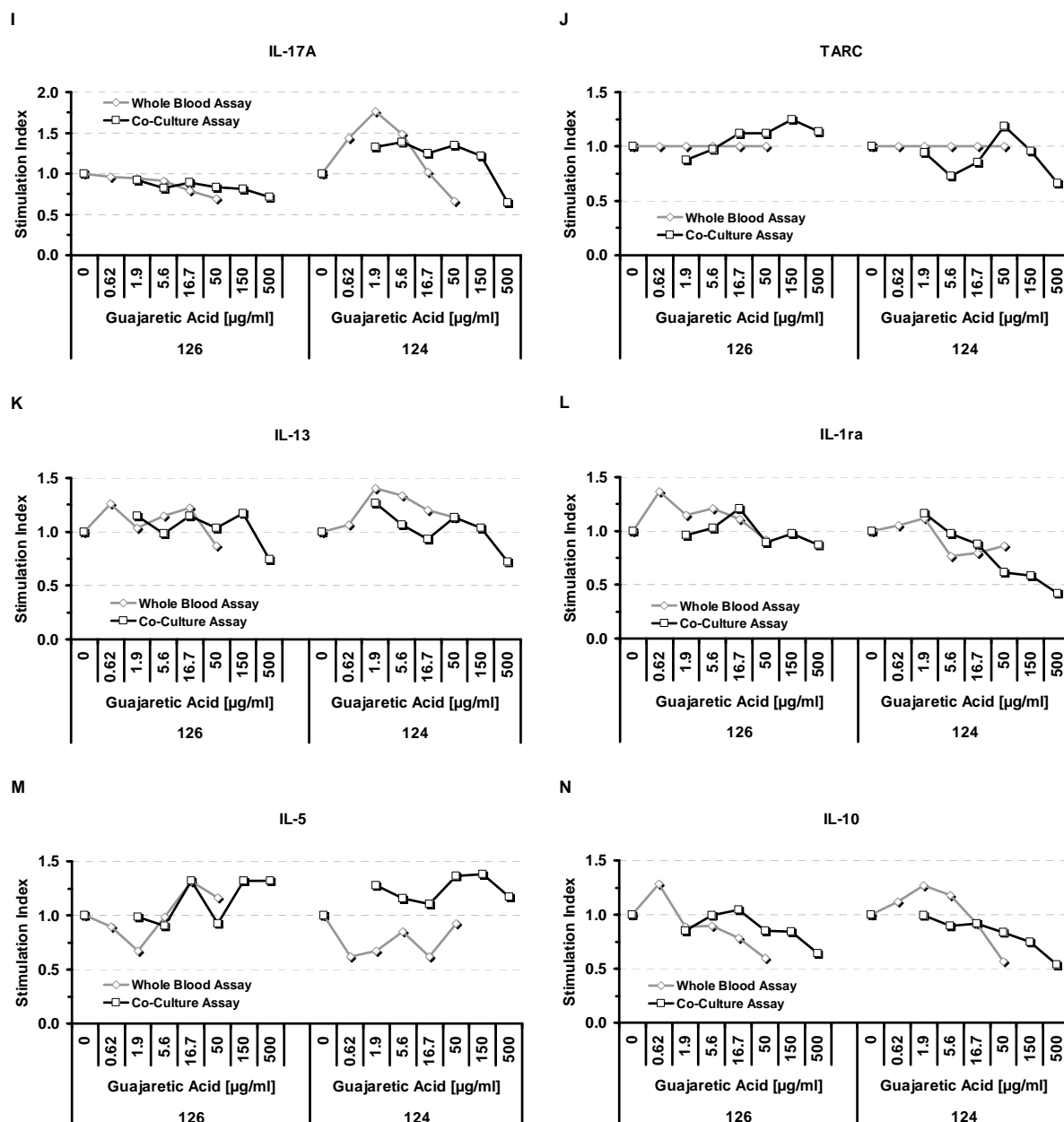


Figure 25: Effect of Dihydroxyguajaretic Acid on the release of immune mediators.

Guajaretic acid was tested in the co-culture model (squares) in the indicated concentrations. After substance application Caco-2 cells in transwell inserts were transferred to culture vessels containing heparinized whole blood of two donors (indicated by their ID-numbers). After 1 h, the whole blood was stimulated by LPS/SEB/anti-CD28 injection. After 6 h Caco-2 cells were removed and the whole blood was further incubated for 18 h. In parallel the test substance was applied to the whole blood cultures (diamonds) followed by LPS/SEB/anti-CD28 injection after 1h and further incubation for 24h. Immune mediators were quantified in plasma of both experimental set ups. Depicted are stimulation indices of single experiments. **A** IL-1 β , **B** IL-6, **C** IFN γ , **D** MCP-1, **E** IL-8, **F** IP-10, **G** TNF α , **H** IL-4, **I** IL-17A, **J** TARC, **K** IL-13, **L** IL-1ra, **M** IL-5, **N** IL-10.

4.3.8. Summary of drug effects

The five drugs Dexamethasone, Prednisolone, Diclofenac, Ibuprofen and Tacrolimus were tested in the organotypic co-culture model of the human gut and their effects on the release of a broad range of cytokines and chemokines was subsequently analyzed in whole blood. For each substance, five different concentrations were tested using blood of three individual blood donors and the immune modulating effects were measured using multiplexed sandwich immunoassays. Pretreatment of the Caco-2 monolayer with IL-1 β and TNF α ahead of drug application enabled us to study the impact of an altered barrier function on drug efficacy. Moreover, the compartmentalized co-culture model was used to investigate the effect of mainly uncharacterized natural products. **Table 14** summarizes the results of the measured drug effects.

Application of Dexamethasone led to a strong concentration dependent inhibition of the macrophage/monocyte associated mediators IL-1 β , IL-6, IL-8, TNF α and a moderate inhibition of MCP-1 for all three tested donors. IFN γ was also inhibited whereas the Th1 associated mediator IP-10 was induced for one donor. The drug also led to a broad inhibitory effect on the Th2 associated mediators IL-4, IL-5 and IL-13, the Th17 associated mediator IL-17A, the regulatory cytokine IL-10 and IL-1ra. In comparison, the corticosteroid Prednisolone showed a much lower inhibitory potency in the co-culture model. The macrophage/monocyte associated mediators were tendentially inhibited, however the effect varied between the tested individuals. Moderate IL-1 β and IL-6 inhibition was observed in the blood of two donors while IL-8 and TNF α were only inhibited in the blood of one donor. No inhibition was detected for MCP-1. IFN γ and IL-5 were inhibited for two donors. All other analytes showed no response or moderate inhibition for only one single donor.

The COX inhibitor Ibuprofen led to a strong to moderate increase in the concentrations of the macrophage/monocyte associated mediators IL-1 β , and TNF α . IL-8 was clearly inhibited and MCP-1 showed moderate inhibition in the blood of two donors and no effect for one donor. IFN γ was strongly induced and IP-10 showed moderate induction in response to the drug. The Th2 associated analytes were moderately induced with the exception of IL-13. IL-17A and TARC were clearly inhibited while IL-10 and IL-1ra showed no effect. Comparable results were found for the second non-

steroidal anti-inflammatory drug Diclofenac. However, effects were less distinctive. IL-1 β and IL-6 were both moderately induced as well as IFN γ and IP-10. IL-4 was induced for two donors and IL-5 for one donor. Concentration dependent inhibition was observed for IL-8 and IL-17 and MCP-1. Moderate induction of TNF α could only be detected for one donor since the concentration exceeded the upper limit of detection in two donors. IL-5 was strongly induced for one donor.

The macrolide immunosuppressant Tacrolimus clearly inhibited the release of IL-8, TNF α , and MCP-1 in a concentration dependent manner. IL-6 was inhibited moderately and IL-1 β was only inhibited in the blood of one donor. Both Th1 associated mediators IFN γ and IP-10 were inhibited as well as IL-17A, IL-10 and TARC. IL-4 was tendentially inhibited for one donor and induced for a second donor. Moderate induction was observed for IL-5 in the blood of two donors. IL-13 was strongly induced by Tacrolimus. And this is in clear contrast to the other tested substances. IL-1ra was inhibited for two donors.

Dihydrohyguajaretic acid moderately inhibited the cytokines IL-1 β , IL-6, TNF α , IFN γ , IL-13, IL-17A, IL-10 and IL-1ra. IP-10 was strongly inhibited while IL-8 was moderately induced by increasing substance concentrations. IL-4 was slightly inhibited for one donor. TARC, MCP-1 and IL-5 showed no distinct effect.

With a few exceptions, priming of the Caco-2 monolayer with pro-inflammatory mediators did not significantly alter the effects of the tested substance. However, curve shifts and altered curve shapes were observed in some occasional instances.

Table 14: Summary of drug effects in the co-culture model of the human gut.

Immune cell subset	Drug	Dexamethasone			Prednisolone			Ibuprofen			Diclofenac			Tacrolimus			Guajaretic Acid		
		128	135	143	134	120	118	128	119	128	118	119	128	120	128	134	126	124	
M Φ /Monocyte-associated	Donor	↘	↘	↘	↘	↘	↘	↘	↘	↘	↘	↘	↘	↘	↘	↘	↘	↘	
	IL-1 β	↘	↘	↘	↘	↘	↘	↘	↘	↘	↘	↘	↘	↘	↘	↘	↘	↘	
	IL-6	↘	↘	↘	↘	↘	↘	↘	↘	↘	↘	↘	↘	↘	↘	↘	↘	↘	
	IL-8	↘	↘	↘	↘	↘	↘	↘	↘	↘	↘	↘	↘	↘	↘	↘	↘	↘	
	TNF α	↘	↘	↘	↘	↘	↘	↘	N/A	↘	↘	↘	↘	↘	↘	↘	↘	↘	
	MCP-1	↘	↘	↘	↘	↘	↘	↘	↘	↘	↘	↘	↘	↘	↘	↘	↘	↘	
Th1-associated	IFN γ	↘	↘	↘	↘	↘	↘	↘	↘	↘	↘	↘	↘	↘	↘	↘	↘	↘	
	IP-10	↘	↘	↘	↘	↘	↘	↘	↘	↘	↘	↘	↘	↘	↘	↘	↘	↘	
Th2-associated	IL-4	↘	↘	↘	↘	↘	↘	↘	↘	↘	↘	↘	↘	↘	↘	↘	↘	↘	
	IL-5	↘	↘	↘	↘	↘	↘	↘	↘	↘	↘	↘	↘	↘	↘	↘	↘	↘	
	IL-13	↘	↘	↘	↘	↘	↘	N/A	↘	↘	↘	↘	↘	↘	↘	↘	↘	↘	
Th17 associated	IL-17A	↘	↘	↘	↘	↘	↘	↘	↘	↘	↘	↘	↘	↘	↘	↘	↘	↘	
Treg associated	IL-10	↘	↘	↘	↘	↘	↘	↘	↘	↘	↘	↘	↘	↘	↘	↘	↘	↘	
others	TARC	↘	↘	↘	↘	↘	↘	↘	N/A	↘	↘	↘	↘	↘	↘	↘	↘	↘	
	IL-1ra	↘	↘	↘	↘	↘	↘	↘	↘	↘	↘	↘	↘	↘	↘	↘	↘	↘	
Legend	↘	strong induction															↘	moderate induction	
	↗	strong inhibition															↗	moderate inhibition	
	↔	no/heterogeneous effect															↔	unquantifiable	
	↖	N/A															↖	N/A	

5. Discussion

5.1. Multiplexed Sandwich Immunoassays

Immunity and inflammation is regulated via a highly complex network of signaling events. Every immunological response arises from the dynamic interplay of thousands of molecules that are subject to multiple influences. A set of mediators is considered to be more valuable compared to any single analysis of only one component when the immune system has to be analyzed [104, 105]. For the analysis of low abundant analytes like cytokines and chemokines in complex biological fluids sensitive, accurate and reliable methods are required. This is usually accomplished using solid phase sandwich immunoassays such as ELISA [121]. However, these methods are characterized by low sample throughput, high reagent consumption, and the single analysis of only one mediator per experiment. In contrast, suspension bead arrays are perfectly suited to perform multiplexed sandwich immunoassays, allowing to measure several dozens of parameters requiring only a minimum amount of sample material.

Appropriate capture and detection antibodies and recombinant standard proteins are required to set up miniaturized and multiplexed sandwich immunoassays. The performance of multiplexed sandwich immunoassays highly depends on these components. The occurrence of cross-reactivities among the antibodies or between antibodies and analytes can lead to non-reproducible assay results. Therefore, any analyte which interferes with the overall performance of the multiplexed assay has to be excluded from the panel. In addition, the assay performance is crucially dependent on the chemical properties of the sample material. The presence of interfering factors like Human Anti Mouse Antibodies (HAMAs), heterophilic antibodies and rheumatoid factors as well as unspecific binding or matrix effects in the tested specimen can lead to imprecision or can cause false positive or false negative results [122]. Therefore, the selection of a suitable assay matrix is of great importance. During inflammatory conditions, cytokines and chemokines can be found in plasma over a wide concentration range and with tremendous inter-individual variability. This span has to be covered by the dynamic range of the applied assays. For that purpose, the sample dilution needs to be carefully selected ahead of the analysis. Moreover, the composi-

tion of the multiplexed assay panels has to be chosen in such a way that analytes that require the same dilution are grouped together.

The statistical analysis of the standard curves and multiplexed data are critical for proper interpretation [121]. This requires the choice of appropriate fitting models as well as the long-term insurance of low intra and inter-assay variability. For each measurement, the limit of detection (LOD) and quantification (LOQ) has to be calculated on the basis of the obtained data. The recommended read out parameter for Luminex measurements are median fluorescence intensities (MFI). The fact that the median represents a data selection method and does not incorporate outliers consequently leads to low intra-assay variability and therefore favors low detection and quantification limits. However, the theoretically calculated LOD and LOQ values have to be judged individually ahead of each data analysis

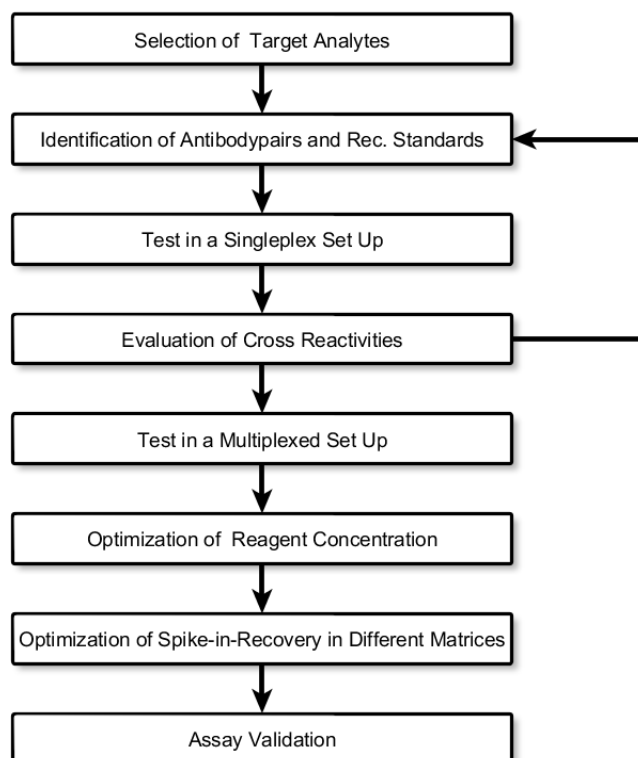


Figure 26: The assay development process

In this thesis multiplexed bead based sandwich immunoassays were developed on the Luminex platform to analyze the concentration of 16 different cytokines and chemokines in parallel. **Figure 26** illustrates the different steps of the assay development process. After the selection of relevant target analytes commercially avail-

able matched pair antibodies and recombinant standard proteins were identified and initially tested in a singleplex set up. In a second step, cross-reactivities between the different antibodies and analytes were assessed. Finally this process, together with the necessity that the analytes had to be grouped together according to the required sample dilution, led to the establishment of the following three multiplexed panels.

- **Panel I** consisting of IL-1 β , TNF α , IL-8, IL-6, MCP-1, IFN γ and IP-10,
- **Panel II** consisting of IL-4, TSLP, TARC and IL-17A,
- **Panel III** consisting of IL-5, IL-10, IL-1ra, IL-12p70 and IL-13

LowCross buffer was chosen as assay matrix since experiments revealed a spike recovery between 80%-120% in human heparinized plasma. Moreover LowCross buffer efficiently reduced cross-reactivities among the assay reagents as well as matrix effects and unspecific binding. In addition to the three cytokine/chemokine panels developed in this study soluble receptors and cell adhesion molecules were separately measured using a 8-plex panel established at the NMI [106, 113].

Most assays showed a linear curve shape over 2-3 orders of magnitude. Assay sensitivity -indicated by the respective LOD and LOQ were in the lower pg/ml range and thus comparable to standard solid phase ELISA assays. All applied multiplexed assays showed excellent repeatability and reproducibility. The intra-assay CV was below 10% and the inter-assay CV range was between 10-25% during a 2.5-year period. In summary, the developed sandwich immunoassays were well suited for detection of immune mediators in stimulated whole blood. The ability to determine multiple analytes in parallel with minimal sample consumption enables the efficient screening of thousands of samples with drastically reduced hands on time and constant quality. Therefore, this technology represents a perfect tool for the analysis of drug effects on the inter-cellular communication via cytokines and chemokines in organotypic cell-culture systems.

5.2. Caco-2 cells as a model of the intestinal barrier

The colorectal adenocarcinoma cell line Caco-2 is widely used across the pharmaceutical sciences to study the intestinal absorption and transepithelial transport of

orally administered drugs in accordance with FDA and EMEA guidelines [10, 11]. To investigate whether an “inflamed gut epithelium” can be simulated *in vitro*, functionally differentiated Caco-2 monolayers were treated with either IL-1 β /TNF α or IFN γ for 6 h or 24 h respectively and the transepithelial electric resistance was used as an indicator of epithelial permeability. The results demonstrated that *in vitro* treatment with pro-inflammatory mediators clearly affects the barrier function of Caco-2 cells. Combined treatment with IL-1 β /TNF α lead to a decrease in TEER after 6 h or 24 h compared to control cells. In contrast, after incubation with IFN γ no difference to controls cells could be measured during the first 6 h of incubation. Interestingly the control cells also exhibited a decrease in TEER after 6h, probably because of stress caused by cell handling. After 24 h, an increase in TEER could be detected in the control cells, which most likely results from further cell differentiation. However, this increase in TEER was not observed when the cells were treated with IFN γ for 24 h.

An intact intestinal epithelial barrier is a crucial factor for preventing paracellular permeation of harmful luminal agents. In this context a “leaky” intestinal barrier function is considered a central pathogenic factor for the onset and flare up of Inflammatory Bowel Disease [123, 124]. The cytokines IL-1 β , TNF α and IFN γ , which are frequently found to be up regulated in the intestinal tissue of IBD patients [16-18] have been reported to affect the intestinal barrier function by modulating tight junction permeability [3, 19-24].

In addition to alterations in TEER, immunohistochemical analysis revealed a significantly altered localization of the tight junction proteins Occluding and ZO-1 after treatment with IL-1 β /TNF α or IFN γ respectively. Whereas in untreated cells Occludin and ZO-1 were located at the cellular borders both treatments significantly reduced fluorescence signal for these proteins. Dsg 2 was also found to be localized at the cellular borders and both treatments affected localization. In contrast both treatments did not affect the localization of the tight junction protein Claudin 5 and the adherence junction protein E-Cadherin.

These observations are in accordance with literature findings. Al-Sadi *et al.* [19] for example showed that treatment of Caco-2 monolayer with IL-1 β leads to a concentration and time dependent decrease in TEER between 6 h and 24 h after treatment.

The maximum drop in TEER was thereby observed at a concentration of 10 ng/ml with no further decrease at higher concentrations. Moreover, they found that IL-1 β causes a significant reduction of Occludin expression as well as disturbance in Occludin junctional localization. Ma and coworkers [20, 24] showed that treatment of Caco-2 monolayer with TNF α significantly decreases TEER in a time and concentration dependent manner. Similar to IL-1 β a concentration of 10 ng/ml was thereby most effective and caused a significant drop in TEER between 12 h and 48 h. The increase in cellular permeability was thereby accompanied by an alteration in ZO-1 expression and junctional localization upon TNF α treatment.

In the present study, the combined treatment with TNF α and IL-1 β resulted in a drop in TEER values during the first 6 h of incubation and this might point to a synergistic effect of the two pro-inflammatory cytokines. Additionally this treatment significantly altered the subcellular localization of Occludin, ZO-1 and Dsg 2. In T84 colonic adenocarcinoma cells Brewer *et al.* [125] showed that treatment with IFN γ results in a decreased TEER together with an internalization of Occludin, and Claudin-1. According to them the localization of ZO-1 and E-Cadherin were not significantly changed upon cytokine treatment. In another study combinatorial treatment with TNF α , IFN γ and IL-1 β was shown to cause a decrease in ZO-1 and Occludin protein expression and an increase in the expression of Claudin-1 in Caco-2 cells together with alterations in the subcellular localization of these proteins [126]. Wang *et al.* [119] demonstrated that the single treatment of Caco-2 monolayer with either 10 ng/ml IFN γ or 2.5 ng/ml TNF α did not cause significant alterations in TEER values. However if both cytokines were combined a significant drop in TEER could be detected. They also found that this treatment resulted in an altered subcellular localization of ZO-1, Occludin and Claudin-1. In the present study, a small drop in TEER was observed after 24 h of IFN γ treatment. Moreover, this treatment prevented a further increase in TEER in comparison to untreated controls. In addition this treatment clearly affected the junctional localization of Occludin, ZO-1 and Dsg 2. The localization of Claudin-5 and Cadherin was not found to be changed proofing the integrity of the epithelial layer.

Gut epithelial cells are known to actively participate in extracellular communication processes via secreted mediators thus forming a regulatory unit with cells of the im-

immune system. They function as a sensory organ and are capable of producing immunoregulatory mediators upon activation signals e.g. cytokines or bacterial stimuli [127, 128]. To analyze the secretion profile of Caco-2 cells in response to pro-inflammatory cytokine treatment, a broad range of immune mediators was measured in cell culture supernatant upon incubation with IL-1 β /TNF α or IFN γ in the basal chamber of the compartmentalized model. In particular, the concentration of IFN- γ , TNF- α , IL-1 β , IL-6, TSLP, IP-10, IL-8 and MCP-1 were determined using sandwich immunoassays. Elevated concentrations of the chemokines IL-8, IP-10, MCP-1 were found upon combined stimulation with IL-1 β /TNF α . A large proportion (\approx 70%) of the secretion occurred during the first 6 h of stimulation. Treatment with IFN γ effectively triggered the release of IP-10 but not IL-8 and MCP-1. After 24 h of incubation IP-10 level was 12-fold higher than after 6 h indicating a slower response to IFN γ than to IL-1 β /TNF α . No detectable concentrations of IL-6 and TSLP were found in both set ups.

These findings confirm previous studies. Sunil *et al.* [129] reported an elevated IL-8 and IP-10 production by intestinal epithelial cells upon treatment with IL-1 β . Schuerer-Maly *et al.* [130] investigated the IL-8 release in Caco-2 cells after IL-1 β , TNF α or IFN γ treatment and found that only IL-1 β induced IL-8 production. Warhurst and colleagues [131] found an increased release of MCP-1 by Caco-2 cells upon stimulation with IL-1 β and TNF α whereas neither the expression of IL-8 nor MCP-1 was influenced by IFN γ treatment. Yeruva *et al.* [132] assessed the expression of IP-10 in Caco-2 cells in response to IL-1 β , TNF α or IFN γ . They found that both IL-1 β and TNF α effectively induced IP-10 expression. According to them IFN γ also triggered the production of this chemokine however with delayed kinetics.

Taken together treatment with the proinflammatory mediators IL-1 β /TNF α or IFN γ effectively altered the barrier function of functionally differentiated Caco-2 monolayers including enhanced permeability and an altered localization of cell junction proteins. It was clearly shown that Caco-2 cells respond to proinflammatory cytokine treatment by the release of chemokines and thus are able to establish a crosstalk with cells of the immune system. These results for the first time demonstrate that the *in vitro* treatment of Caco-2 monolayer with proinflammatory cytokines can be utilized to mimic

the altered epithelial characteristics that can be found in inflammatory bowel disease patients.

5.3. Analysis of RTK signaling in Caco-2 cells

During inflammatory conditions of the gut, proinflammatory cytokines are released into the mucosa and submucosa propagating and sustaining the inflammatory response. In this context, increased concentrations of IL-1 β and TNF α were found to modulate epithelial barrier permeability through the activation of NF κ B signaling [19, 24]. In addition, it was found that EGF prevented oxidative stress induced disruption of tight junctions and that this process is mediated through ERK [25, 26]. Moreover, it is known that a crosstalk exists between MAPK and NF κ B associated signaling pathways [133]. In this study the effect of the proinflammatory cytokines IL-1 β , TNF α and the growth factor EGF on Receptor Tyrosine Kinase signaling in differentiated Caco-2 monolayer was investigated in detail using multiplexed bead array technology.

In a first step, the expression levels of the Receptor Tyrosine Kinases EGFR, IGFR, HGFR, PDGFR, ErbB2, VEGFR2 and Tie-2 were determined together with alterations in their tyrosine phosphorylation status in response to cytokine and growth factor treatment. EGFR, HGFR and ErbB2 were found to be present in the cell lysates. IGFR was present at very low levels and PDGFR, VEGFR and Tie-2 could not be detected. Treatment of Caco-2 cells with EGF and IL-1 β led to time dependent alteration of EGFR and ErbB2 tyrosine phosphorylation. In contrast no alterations in tyrosine phosphorylation could be detected upon treatment with TNF α . This was not expected since Murthy *et al.* [134] described that treatment with TNF α lead to rapid (30min) phosphorylation of EGFR in Caco-2 cells and this event is completely EGFR-ligand independent. Treated cells were no longer susceptible to EGFR ligands and it was assumed that this had an impact on EGF-induced proliferation and migration key processes that promote healing in inflammatory bowel diseases [135, 136].

In further experiments, profiling of eight different phosphorylation sites of EGFR revealed that IL-1 β leads to reproducible time dependent increase in EGFR phosphorylation at Serine1047 over a time span of 30 min followed by a steady signal decline.

This site was not found to be phosphorylated upon EGF treatment. Moreover, treatment with IL-1 β lead to alterations in the phosphorylation at Y845, Y1068 however with no clear and reproducible time dependent pattern. When cells were treated with EGF signals for Y845 and Y1068 were almost similar to those of the respective controls with only marginal time dependent alterations. This was not expected since both sites have been reported to be phosphorylated upon EGF treatment at least in A431 cells [112, 137]. No increase in phosphorylation could be detected for the phospho-sites Y1045, Y1086, Y1173, Y654, and T669 after both treatments. As indicated by the measured total EGFR signals, a very low variability between the different cell culture experiments could be achieved. This clearly demonstrates that the observed signal alterations are the result of ligand induced processes.

In order to identify the intracellular signaling mechanisms that are responsible for the observed S1047 phosphorylation Caco-2 monolayer were treated with 86 different protein kinase inhibitors ahead of stimulation with IL-1 β for 30 min. It was found that the time dependent phosphorylation of the S1047 residue of EGFR could be selectively depleted by four inhibitors of p38 α MAPK and three inhibitors of IKK-2. Signal intensities for the measurement of total EGFR, pT845 and pT1068 remained relatively constant across the 2x86 cell culture experiments. One inhibitor targeting WEE1 was also effective in this regard, however two other compounds targeting the same kinase revealed no effect.

Based on these results extensive literature mining was performed using the Ingenuity pathway analysis platform. In the generated pathway model (**figure 27**) IL-1 β binding to its specific receptor IL-1RI leads to recruitment of MyD88 and Tollip with subsequent addition of IRAK to the receptor complex [138, 139]. IRAK is phosphorylated and interacts with the adaptor TRAF6. IRAK-1 and TRAF6 dissociate from the receptor and form a complex with TAK1, TAB1 and TAB2. This leads to activation of TAK1 which in turn phosphorylates IKK-complex consisting of IKK- α , IKK- β and IKK- γ via NIK [140] resulting in the degradation of I- κ B, and the subsequent activation of NF κ B. Importantly TAK1 also stimulates the activation of the MAP kinases JNK and p38 α via the activation of MKK3/MKK6 or MKK4 [140-146]. p38 α in turn has been reported to phosphorylate EGFR at S1047 in response to TNF α stimulation [133]. Although no information linking IKK-2 with the observed phosphorylation of EGFR could be identi-

fied, IKK-2 recently has been found to directly interact with p38 α thus giving rise to speculations [147]. Countaway *et al.* [117] reported that S1047 is substrate to CAM Kinase II and phosphorylation leads to desensitization and internalization of the receptor. However, in our experiment none of the applied CAMK Inhibitors significantly depleted the IL-1 β induced phosphorylation of S1047. Recently it has also been suggested that phosphorylation at this site might be involved in TNF α induced antiapoptotic signaling [133, 148, 149]. In summary the particular role of the IL-1 β induced EGFR phosphorylation at S1047 is still unclear and further effort is required to identify the relevant downstream effects.

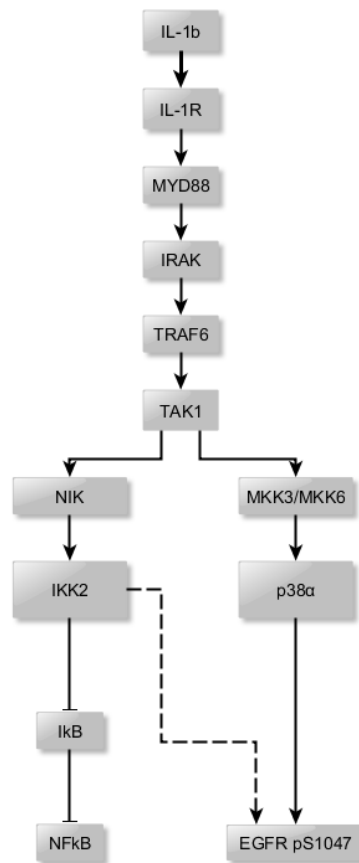


Figure 27: Pathway model of the crosstalk between IL-1RI and EGFR.

Relevant pathway information was identified using the IPA[®] web-based knowledge database (Ingenuity systems). IL-1 β binding to IL-1RI leads to recruitment of MyD88, and IRAK to the receptor. IRAK interacts with TRAF6 forms a complex with TAK1. Activated TAK1 phosphorylates either IKK complex via NIK resulting in the activation of NF κ B or activates JNK and p38 α via MKK3/MKK6. p38 α in turn phosphorylates EGFR at S1047.

5.4. Analyzing biological activity of drugs

Anti-inflammatory drugs, like corticosteroids and non-steroidal anti-inflammatory drugs are widely used in treatment of inflammation nowadays. Drugs administrated via the gastrointestinal tract have to pass different tissue types before entering the blood stream and reaching their final target location. Alteration in pharmacokinetics and the desired drug effect can be the consequence. In this study a organotypic co-culture model consisting of Caco-2 gut epithelial cells and human whole blood (see **chapter 1.2**) was used to study the immune modulating characteristics of antiphlogistic drugs and drug candidates. The substances of interest were applied onto differentiated Caco-2 monolayers in different concentrations and their effect on the secretion of immune mediators was analyzed in the whole blood after activation with immune stimulating agents. In parallel experiments Caco-2 cells were pretreated with IL-1 β and TNF α ahead of drug application in order to mimic the altered epithelial barrier function found during inflammatory conditions of the gut. **Table 15** summarizes the tested substances and the measured read out parameters. The obtained dose response curves for each immune mediator were interpreted on the basis of published observations. Therefore the IPA® Knowledge Base provided by Ingenuity Systems was applied.

Table 15: Summary of test substances and measured immune mediators

test substance					
Dexamethasone	Prednisolone	Ibuprofen	Diclofenac	Tacrolimus	Guajaretic Acid
immune mediators					
M Φ /Monocytes	Th1	Th2	Th17	Treg	Others
IL-1 β , TNF α , MCP-1, IL-6, IL-8	IP-10, IFN γ IL-12p70	IL-4, IL-5, IL-13	IL-17A	IL-10	TARC, TSLP, IL-1ra, Sol. Receptors

5.4.1. Specific activation of immune cells

In preliminary experiments, immune activating substances were added to human whole blood of different donors in a co-culture set up with Caco-2 cells without drug application. The observed release of immune mediators in blood plasma was quanti-

fied using multiplexed sandwich immunoassays. Hierarchical cluster analysis showed that different subgroups of immune cells in whole blood can be selectively activated by application of different stimuli across all blood donor tested.

Zymosan has been reported to trigger TNF α and IL-8 secretion in macrophages, monocytes and granulocytes [56-59]. In addition to these cytokines, Zymosan augmented the production of IL-6, MCP-1 and IL-1 β in this study. Stimulation of T-lymphocytes with CD3- and CD28-receptor targeting antibodies stimulated the secretion of T-cell related mediators IL-10, IFN γ , IL-17A, IL-5, IP-10, TARC and IL-4. As expected the combined application of Zymosan and anti-CD3/anti-CD28 triggered macrophage/monocyte as well as T-cell specific mediators.

LPS is an effective immune stimulus and can be used to trigger the production of IL-1 β , IL-6, IL-8, TNF α , TARC, IFN γ by macrophages, monocytes, and granulocytes [37, 60-62]. The superantigen SEB stimulates the secretion of IL-12p70 [63], IL-1 β [64], TNF α , IL-6, IFN γ , MCP-1 [65] by T-cells and antigen presenting cells. Here these two stimuli together with a anti-CD28 antibody most effectively triggered a broad range of macrophage/monocyte and T-cell specific cytokines and chemokines. Therefore, this mixture was selected for immune activation in the context of drug testing experiments. Although Poly I:C has been reported to stimulate IL-6, TNF α , IL-10, IP-10 [66, 67] in B-cells and dendritic cells only secretion of IP-10 could be observed in whole blood. None of the measured soluble receptors and cell adhesion molecules allowed a clear distinction between stimulated samples and non-stimulated controls. This finding led to the exclusion of these analytes from further experiments.

5.4.2. Analyzing biological drug activity: Corticosteroids

Dexamethasone is one of the most potent synthetic members of the glucocorticoid family of drugs. It is 20-30 times more potent than Cortisone and 4-5 times more potent than Prednisolone [120]. Therapeutic dosages of glucocorticoids vary according to their therapeutic application and drug potency and are between 250-1000 mg Prednisolone equivalent for pulse therapy and 5 mg/day Prednisolone equivalent for long term usage [150]. Standard oral Prednisolone doses for the treatment of active inflammatory bowel disease range from 40-60 mg/day [68]. The bioavailability of

Dexamethasone has been reported to be approximately 80% after oral administration [151]. Oral application of 0.5 mg, or 1.5 mg respectively resulted in plasma levels of approximately 8 ng/ml and 15 ng/ml (0.02 μ M, 0.04 μ M) after 2 h followed by a steady decline with a half life of 4.2-6.6 h [152]. The bioavailability of Prednisolone after oral administration has been reported to be almost 100%. 10 mg Prednisolone orally resulted in a mean peak plasma concentration of 300 ng/ml (0.8 μ M) after 30 min and a mean half-life of 3-4 h [153]. In the context of this study, concentrations of 10-0.001 μ M Dexamethasone and Prednisolone were tested in the co-culture model to cover the relevant *in vivo* plasma levels.

Dexamethasone strongly inhibited the release of the macrophage/monocyte associated mediators IL-1 β , IL-6, IL-8 and TNF α . Moderate inhibition was found for MCP-1. The Th1/Th2 associated mediators IFN γ , IL-4, IL-5, IL-13, the TH17 associated mediator IL-17A, the regulatory cytokine IL-10 and IL-1ra were inhibited in a concentration dependent manner. In comparison, Prednisolone showed a much lower inhibitory potency in the co-culture model. The macrophage/monocyte associated mediators were tendentially inhibited. Moderate IL-1 β and IL-6 inhibition was observed while IL-8 and TNF α were only inhibited in the blood of one donor. IFN γ and IL-5 were inhibited for two donors. All other analytes showed no response or moderate inhibition for only one single donor. Based on these results a model of potentially involved signaling pathways was generated using the Ingenuity pathway analysis platform (**figure 28**).

The immune modulating effects of corticosteroids and their synthetic homologues are facilitated upon binding to the glucocorticoid receptor (GR). The unbound receptor is located in the cytosol. Upon ligand binding the GR-complex exerts its function either by gene regulation in the nucleus or by direct interference with other transcription factors [154]. The transcriptional regulation of anti-inflammatory genes is mediated through binding of the GR to glucocorticoid responsive DNA elements -GREs. For example the enhanced expression of Annexin I inhibits cytosolic phospholipase A₂ thus blocking the release of arachidonic acid, the precursor molecule for the synthesis of eicosanoids [155, 156]. The expression of MAPK phosphatase 1 (MPK-1) is also induced by glucocorticoids [157, 158]. MPK-1 dephosphorylates and inactivates Jun N-terminal kinase thereby inhibiting c-Jun mediated transcription [159].

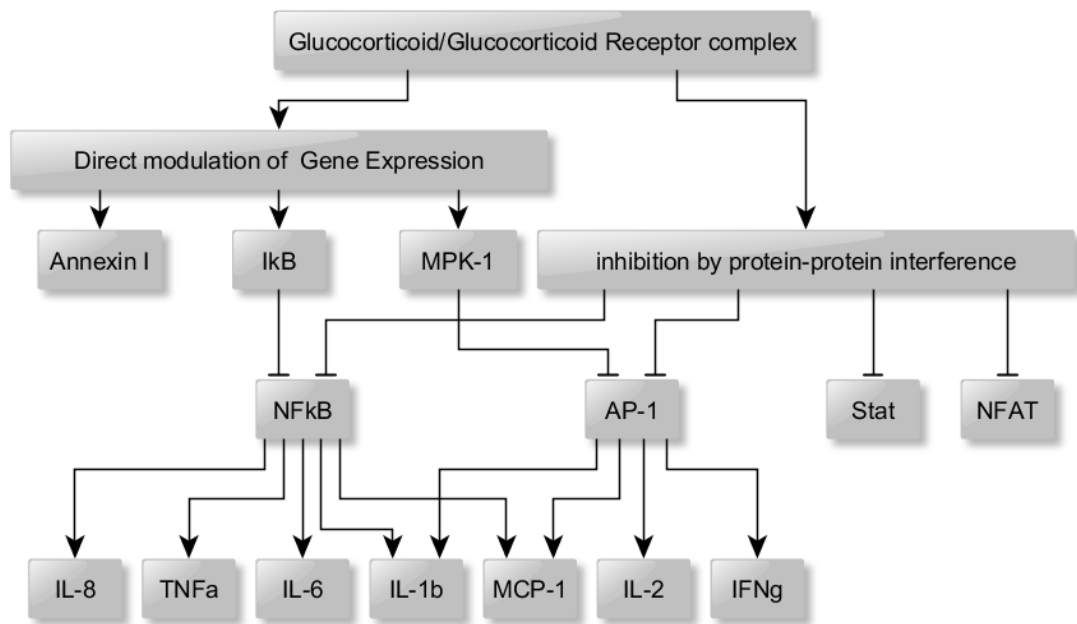


Figure 28.: Signaling pathways of glucocorticoid action

In addition MPK-1 also inactivates all members of the MAPK family including ERK and p38 α kinase [154] thus blocking MAPK mediated inflammatory signaling processes. Direct protein-protein interaction with other transcription factors such as NF κ B [155] and AP-1 (composed of c-jun and fos) leads to a decreased transcription of proinflammatory genes e.g. cytokines [75, 76, 156, 157]. Although it was shown that inhibition of NF κ B can also occur through the transcriptional activation of its cytoplasmic inhibitor I κ B α [158] protein-protein interaction most likely accounts for the majority of the inhibitory effects of glucocorticoids on NF κ B signaling [159, 160]. The glucocorticoid receptor also physically interacts with members of the STAT family of transcription factors such as STAT3 and STAT5 [161].

NF κ B and AP-1 are essential regulators of several cytokine and chemokine genes and inhibition through corticosteroids lead to down regulation of IFN γ [162], IL-8 [155], TNF α [163, 164], IL-6 [73], IL-1 β [161, 165, 166] and MCP-1 [167]. It has also been published that corticosteroid treatment leads to a decrease of IL-17A release in PBMCs and rat lymphocytes together with a decrease in jun phosphorylation [168, 169]. However the exact molecular mechanism underlying this observation is unclear. Conflicting reports were found for the Th2 and Treg associated cytokines. Ramirez *et al.* reported that glucocorticoids lead to enhanced production of IL-4, IL-10 and IL-13 mRNA [170] in rat CD4⁺ lymphocytes. According to Wu *et al.* and Byron *et*

al. [171, 172] the production of IL-4 by human lymphocytes and PBMCs is markedly decreased by hydrocortisone treatment. In mast cells Sewell *et al.* [173] showed that Dexamethasone treatment markedly inhibited IL-4 and IL-5 mRNA production. Agarwal and coworkers [174] reported that Dexamethasone treatment leads to an increased production of IL-4 and IL-10 in tetanus toxoid stimulated PBMCs and that the found Dexamethasone mediated induction of Th2 associated cytokines are primarily the result of the down regulation of Th1 associated cytokines IL-12 and IFN γ . Similar to IL-1 β secretion glucocorticoids also down regulate IL-1ra production in LPS stimulated monocytes [175, 176] thus implicating a complex regulatory interplay between corticosteroids and the IL-1 family members [177].

Heterogeneous results were found in the co-culture model concerning the secretion levels of IP-10. One donor responded to Dexamethasone treatment with a strong concentration dependent increase whereas a second donor showed only moderate inhibition. The third tested donor remained relatively unresponsive. IP-10 is a proinflammatory Th1 associated chemokine expressed mainly in lymphocytes, neutrophils, monocytes, fibroblasts, and endothelial cells upon IFN γ treatment and it has also been found to be inducible by IL-1 β , TNF α and LPS [178-181]. Sunil *et al.* and Tudhope *et al.* reported that Dexamethasone did not down-regulate the expression of IP-10 in Caco-2 gut epithelial cells [129] and bronchial epithelial cells [182]. However, no report was found concerning the effect of corticosteroids on the IP-10 secretion of immune cells.

In this study a broad concentration dependent inhibitory effect of Dexamethasone on the macrophage/monocyte associated mediators IL-1 β , IL-6, IL-8, TNF α , MCP-1, IFN γ , IL-4, IL-13, IL-5, IL-10 as well as IL-17A, IL-10 and IL-1ra was observed. These findings are mainly in accordance with the relevant literature. The experimental design consisting of differentiated Caco-2 epithelial monolayers in co-culture with whole blood of three individual donors incorporated all major cellular components, pharmacokinetic drug properties and the individuality of the immune system in one analysis. All glucocorticoids and their synthetic analogues exert their immune modulating effect through binding to the glucocorticoid receptor. However, the obtained results for Prednisolone demonstrate that there are indeed differences in drug potency and that these could be visualized in the presented co-culture model. Since the bioavailability

of Prednisolone has been reported to be almost 100% we expected that the drug can pass the epithelial barrier and target the immune cells in the whole blood. However the direct comparison with previous experiments performed in conventional whole blood cultures with the same blood donors [183] showed that direct injection of Prednisolone leads to a strong inhibitory effect on macrophage/monocyte as well as Th1/Th2 associated mediators. These findings suggest that the relatively weak anti-inflammatory effect of Prednisolone is not only caused by the in comparison to Dexamethasone 4-5 fold lower drug potency [120] but also by alterations in bioavailability. In this context, it would be interesting to analyze the concentration of Prednisolone in the whole blood compartment after passage of the epithelium.

In the beginning of this study we showed that pretreatment of the epithelial cells with the proinflammatory mediators IL-1 β and TNF α led to a reduced transepithelial electric resistance, alterations in the localization of cell adhesion proteins and chemokine expression by the Caco-2 epithelial cells. However, with a few exceptions the presented data demonstrated that pretreatment with these cytokines did not significantly alter the dose dependent effect of the tested drugs.

5.4.3. Analyzing biological drug activity: NSAIDs

Non-steroidal anti-inflammatory drugs like Ibuprofen and Diclofenac act as non selective inhibitors of cyclooxygenase isoenzymes COX-1 and COX-2 and are routinely used in the clinics to treat pain, fever and inflammatory conditions [77]. Dosages of NSAIDs are routinely adapted to the therapeutic requirements. Daily doses of 500-2000 mg for Ibuprofen and 50-150 mg for Diclofenac are recommended [184]. Ibuprofen is rapidly absorbed, and peak plasma concentrations are reached within 1-2 h depending on the drug formulation. Oral bioavailability has been reported to be approximately 100% [185]. Administration of 400 mg per oral resulted in maximum plasma concentrations of 32 μ g/ml (155 μ M) after 90 min followed by a steady decline with a half life of 3-4 h [186]. Diclofenac shows preferential inhibition of the cyclooxygenase-2 (COX-2) enzyme [187, 188]. Due to first pass metabolism, the bioavailability of Diclofenac is limited to 50–60% [189, 190]. Application of 50 mg per oral resulted in peak plasma concentrations of 1.7 μ g/ml (5.7 μ M) after 1.5-2.4 h followed by a steady decline with a mean half-life of approximately one hour in 20

healthy volunteers [191]. In the context of this study, a concentration range of 10-0.016 μM Dexamethasone and 500-0.8 μM Ibuprofen were tested.

Interestingly application of both drugs led to a concentration dependent increase in IL-1 β , TNF α , IP-10 and IFN γ in the co-culture model. MCP-1 was tendentially inhibited in the blood of two donors. Ibuprofen led to increasing concentrations of IL-4 and IL-5 for all tested donors, whereas Diclofenac enhanced mediator release only in two and one individuals respectively. No significant alterations of IL-13 could be measured. In contrast the mediators IL-8 and IL-17 were clearly inhibited by increasing drug concentrations. IL-10, and IL-1ra showed no clear drug effect and TARC was slightly inhibited. These findings were analyzed using the IPA-knowledge base (Ingenuity Systems). **Figure 29** shows the generated pathway model of NSAID action.

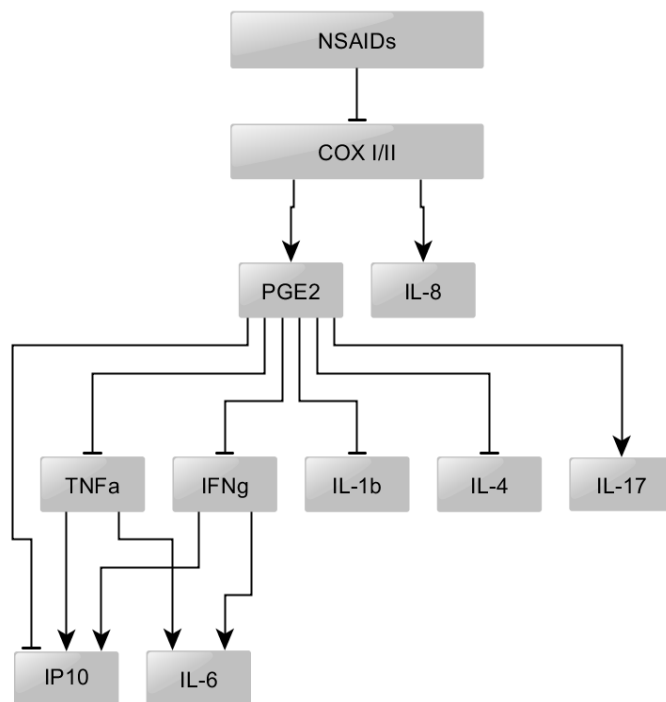


Figure 29: Effects of NSAIDs on immune mediator secretion

PGE₂ which is produced from arachidonic acid via COX mediated catalysis is the major prostaglandin involved in pain and inflammation. It is secreted by macrophages, monocytes, and neutrophils upon treatment with proinflammatory cytokines. PGE₂ inhibits IFN γ and IP-10 production of T-lymphocytes as well as the release of IL-1 β , and TNF α by macrophages [78, 83-85, 192]. PGE₂ is widely viewed as a immune

suppressant and the enhanced release of PGE₂ by macrophages may act as a negative feedback control mechanism, reducing further immune activation [82]. In LPS treated mice, it was shown that inhibition of COX enzymes by Ibuprofen augments the levels of TNF α [193].

These findings strengthen the notion that the observed concentration dependent inhibition of COX enzymes by NSAIDs under inflammatory conditions leads to decreased PGE₂ levels and thus causes an increase in the above mentioned proinflammatory mediators. This again might trigger the release of IP-10 and IL-6 [178, 180, 194-197]. Elevated levels of PGE₂ have been reported to decrease IL-4 release and exhibit a slightly stimulating effect on IL-5 [198]. In this study Ibuprofen induced inhibition of COX isoenzymes exhibited a clear stimulating effect on these mediators. The observed inhibitory effects of Ibuprofen on IL-17A secretion are confirmed by reports showing that PGE₂ leads to an enhanced release of IL-17A in CD4⁺ T-cells and monocytes [199, 200]. Since COX-2 was found to mediate IL-8 production by activated neutrophils [201] the same might be true for this chemokine.

While corticosteroids are routinely used to control symptoms of inflammatory bowel disease there is increasing evidence that non-steroidal anti-inflammatory drugs (NSAIDs) are associated with the onset or the flare-up of IBD [202]. In order to improve the understatement of the relationship between treatment with this drug class and IBD it is necessary to consider the possible pathologic mechanisms involved in the adverse effects of non-selective NSAIDs. This can be done by the use of sophisticated co-culture models. Like for the corticosteroids pretreatment of Caco-2 monolayer with proinflammatory mediators like IL-1 β , TNF α only resulted in minor alterations in the dose response curves of the measured mediators.

5.4.4. Analyzing biological drug activity: Tacrolimus

Tacrolimus (FK506) is a macrolide and mainly used to prevent graft rejection after allogenic organ transplantations. Due to its immunosuppressive effect it can also be used for the treatment of ulcerative colitis [88, 89]. The pharmacokinetic parameters of Tacrolimus vary strongly among individuals. Although rapidly absorbed in the gastrointestinal tract, Tacrolimus has a poor oral bioavailability of approximately 25%

[203, 204]. Peak concentrations in whole blood occur at 0.5-2 h after oral administration [203, 205] followed by drug clearance with a half life between 3.5-40.5 h. Recommended dosages vary among therapeutic applications and are between 0.1 and 0.3 mg/kg/day with target blood concentrations between 5-20 ng/mL (0.02 μ M) (reviewed in [206]). In the present study, a concentration range of 16-0.004 ng/ml was tested in the co-culture experiments.

Tacrolimus application strongly inhibited the production of the macrophage/monocyte associated mediators IL-8, TNF α , and MCP-1. IL-6 was inhibited moderately whereas IL-1 β was inhibited in the blood of only one donor. The Th1 associated mediators IFN γ and IP-10 were inhibited as well as IL-17A, IL-10 and TARC. IL-4 was slightly inhibited for one donor and induced for a second donor. Moderate induction was observed for IL-5 in the blood of two donors. Remarkably IL-13 was strongly induced by Tacrolimus. IL-1ra was inhibited for two donors. Based on the relevant literature **figure 30** summarizes the known effects of Tacrolimus on immune mediator production and release.

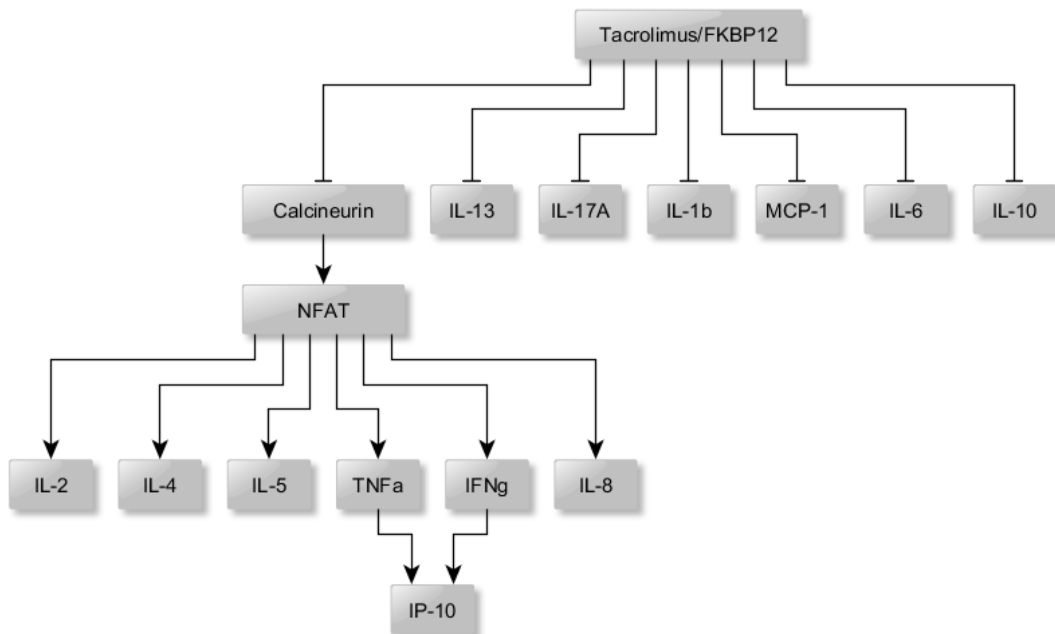


Figure 30: Effects of Tacrolimus on the release of cytokines and chemokines.

The potential target genes for NFAT proteins in diverse cell types as well as additional information about the effect of Tacrolimus or Cyclosporin are reviewed by Rao *et al.* [207]. NFAT plays an essential role in the expression of IL-2. Moreover, binding sites for NFATs have also been found within the promoter regions of several other cytokine genes, including IL-4, IL-5, IL-8, IL-13, TNF α and IFN γ [93, 208]. Since Tacrolimus was shown to decrease the production of IL-1 β , IL-2, IL-4, IL-5, IFN γ , TNF α in PBMCs [209-211] this suggest the participation of calcineurin and NFAT in the expression of these mediators. In addition, it seems likely that the inhibited production of IFN γ and TNF α leads to a reduced release of IP-10 [180, 194, 196, 197].

Tacrolimus also inhibits IL-17A, IL-1 β , MCP-1, IL-6 and IL-10. However, the implicated signaling pathways are not fully characterized yet. Sakuma *et al.* [212] reported that Tacrolimus potently inhibited IL-6 production from PBMCs stimulated with anti-CD3 and anti-CD28 monoclonal antibodies. More recently, it was shown that Tacrolimus inhibits the expression of IL-17A in murine Th17 cells [213] as well as in IL-15 activated PBMCs [214]. In a rat allograft model, Jiang *et al.* [215] showed that Tacrolimus efficiently decreases IL-10 serum levels thus prohibiting graft rejection. With respect to the observed strong increase in IL-13 concentrations Dumont [216, 217] reported augmented IL-13 production by anti-CD3/anti-CD28 stimulated T-cells after Tacrolimus treatment and suggests an inhibitory effect of NFAT on IL-13 expression. Pahl *et al.* [218] showed that Tacrolimus inhibits IL-13 production in TPA/Ionomycin stimulated PBMCs whereas in anti-CD3/anti-CD28 treated cells cytokine production was augmented, thereby giving rise to speculations about the possible mechanistic background of these observations. In activated neutrophils Kohyama *et al.* [219] reported that Tacrolimus suppressed the production of IL-8 and MCP-1. Sasakawa *et al.* [220] showed that Tacrolimus inhibits IL-8 production in activated PBMCs. Okamoto and coworkers [221] showed that AP-1 and κ B-like sites of the IL-8 gene were targets of Tacrolimus sensitive pathways in Jurkat T-cells and suggest that other transcriptional elements besides NFAT sites may be controlled by Tacrolimus sensitive mechanisms.

In summary, it was demonstrated that the immunosuppressive effect of Tacrolimus can be reproduced effectively *in vitro* using the presented co-culture model. Especially for drugs with poor oral bioavailability it is of great importance to use sophisti-

cated test models which are able to mimic intestinal drug absorption mechanisms. For future experiments it would be interesting to test other calcineurin inhibitors e.g. Cyclosporin. Priming of the epithelium with IL-1 β /TNF α had only minor effects on drug potency and overall effectiveness thereby confirming previous findings.

5.4.5. Effects of drug candidates on the release of immune mediators.

Within the scope of this study the presented co-culture model of the human gut consisting of differentiated Caco-2 cells and whole blood of different donors combined with a multi-parametric read out system was applied to evaluate the immune modulating effect of mainly uncharacterized biologically active substances. Different natural products were tested in order to investigate their effects on inflammation associated signaling processes. The tested substances were kindly provided by the Inter-Med Discovery GmbH.

Among the tested substances Dihydroxyguajaretic Acid revealed significant immunomodulating effects. In contrast Harpagosid as well as Glycyrrhizin and Glycyrrhetin were ineffective in this regard. This is interesting since anti-inflammatory activity has already been reported for extracts from *Guajacum Officinale* [222] and the plant was traditionally used for the treatment of inflammatory disorders such as rheumatoid arthritis.

Dihydroxyguajaretic acid effectively inhibited the production of IL-1 β , IL-6 and TNF α in stimulated blood of two donors. Remarkably, it was found that the Th1 associated mediators IFN γ und IP-10 were also clearly inhibited whereas only moderate inhibition could be detected for IL-17A. No clear effect was found for IL-4 and IL-5 whereas IL-13 was slightly inhibited at high concentrations. The regulatory cytokine IL-10 and the IL-1 receptor antagonist IL-1ra were inhibited by increasing concentrations. The observation that not all mediators were inhibited at high concentrations confirms the conclusion that the effect is not caused by toxicity. This is demonstrated by a concentration dependent increase of IL-8. In addition to experiments performed in the co-culture set up Dihydroxyguajaretic acid was simultaneously tested in whole blood cultures using blood of the identical donors. The comparison of the two test systems revealed mainly similar response patterns with infrequent differences in the effective

concentrations. In parts, weaker responses could be observed in the co-culture set up. This can be explained by the altered drug absorption and metabolic processes due to the presence of the epithelial barrier.

In comparison to the results obtained for the well characterized drugs Dexamethasone, Prednisolone, Ibuprofen, Diclofenac and Tacrolimus, the response pattern observed for Dihydroxyguajaretic acid is rather unique. Inhibition of macrophage/monocyte associated mediators IL-1 β , TNF α and IL-6 and the T-cell associated mediators IFN γ , IL-4, IL-13, IL-10 and IL-17A resembles the effects observed for Dexamethasone. Together with the inhibitory effect on IL-1ra this might point to related signaling pathways. However inhibition of IP-10 secretion was only observed for Tacrolimus and the induction of IL-8 suggests independent mechanisms of action. To date signaling pathways and drug targets for Dihydroxyguajaretic acid have not been identified and this might be an interesting starting point for future projects.

6. Summary and Outlook

The human immune system comprises a highly complex network of immunoregulatory signals, which not only involves cells of the immune system but also cells of the surrounding tissues and organs. This inherent complexity together with a distinct diversity among different individuals exacerbates the problems of developing appropriate *in vitro* test systems. Cell lines are the workhorses in the preclinical phase of the drug development process. However since they originate from degenerated cells they can only partially mimic the *in vivo* situation. In contrast animal models allow drug testing in a multi-cellular environment with the limitation that they also differ considerably from the human body. In practice the most often used cellular test systems for the evaluation of drug effects on the immune system are PBMC preparations or test systems using whole blood. However since not all cells contributing to immune reactions are represented in these models the development of more elaborate organotypic co-culture systems represents a closer approximation to the *in vivo* conditions in the human body [5].

Embedded in the BMBF funded project HuCoCSys, the goal of this thesis was the detailed characterization and validation of an established organotypic co-culture model of the human gut. Consisting of differentiated Caco-2 gut epithelial cells and human whole blood this *in vitro* model facilitates the testing of orally applied drugs or drug candidates in an *in vivo*-like environment.

In initial experiments the effect of the proinflammatory mediators IL-1 β , TNF α and IFN γ on the epithelial barrier, was studied using TEER measurements and immunohistochemistry. It was shown that treatment with proinflammatory mediators leads to an increase in epithelial permeability and that this is accompanied by changes in the sub-cellular localization of cell junction proteins. It was demonstrated that Caco-2 cells are capable of secreting the chemokines IL-8, MCP-1 and IP-10 upon treatment with IL-1 β /TNF α and IFN γ . These results indicate that Caco-2 cells can be set to an “inflamed state” in order to mimic the altered barrier function found during inflamed conditions of the gut.

In additional experiments the effects of such a proinflammatory treatment on intracellular Receptor Tyrosine Kinase associated signaling was investigated using multiplexed sandwich immunoassays. It was found that treatment of the Caco-2 cells with IL-1 β leads to a time dependent increase in the phosphorylation of EGFR at Serine 1047. By using a library of protein kinase inhibitors and database mining p38 α and IKK2 could be identified as potential S1047 targeting kinases.

In the context of this thesis three multiplexed sandwich immunoassay panels were developed on the Luminex platform and optimized for the quantification of cytokines and chemokines in human plasma. These assays were applied for the quantification of immune mediators in multiple plasma samples derived from co-culture experiments. Various test substances were added to the top side of Caco-2 epithelial monolayer in different concentrations and their immunomodulatory properties subsequently analyzed in whole blood upon stimulation with immune activating agents. By using blood of different donors the individual variability of the immune response was incorporated in the overall analysis. The combined usage of a multi-parameter read-out system with a sophisticated co-culture model of the human gut enabled the detailed *in vitro* analysis of drug effects.

The comparison of dose response curves obtained for five well characterized drugs Dexamethasone, Prednisolone, Ibuprofene and Tacrolimus with those of the uncharacterized substances allowed to draw conclusions on potential modes of action. This was shown for Dihydroxyguajaretic Acid. In contrast to our expectations, pretreatment of the epithelial monolayer with IL-1 β /TNF α ahead of drug application did not significantly alter the dose dependent effects of the tested substances in the co-culture experiments. Although the Caco-2 monolayers showed an increase epithelial permeability and an altered cell adhesion protein localization the observed impact on drug efficacy was low.

In summary this study showed that the presented co-culture system can be used to evaluate the effects of drugs and drug candidates after passage of the intestinal barrier in a highly standardized *in vivo* like situation. This model has the potential to deliver a more detailed preclinical characterization of desired and undesired drug effects. The large data set generated in the course of this study will provide the basis for the future analysis of the immunomodulatory effects of drug candidates.

7. Zusammenfassung und Ausblick

Das menschliche Immunsystem stellt ein komplexes Netzwerk aus einer Vielzahl verschiedener Zellen und regulatorischen Signalen dar. Neben den Immunzellen sind auch Zellen benachbarter Gewebe an regulatorischen Prozessen beteiligt. Diese inhärente Komplexität erschwert die Entwicklung von *in vitro* Testsystemen die in der Lage sind diese Komplexität mit hinreichender Genauigkeit abzubilden.

Immortalisierte Zelllinien und Tiermodelle werden routinemäßig in der präklinischen Phase der Medikamentenentwicklung eingesetzt. Beide Systeme weisen jedoch deutliche Unterschiede zu den *in vivo* Verhältnissen im menschlichen Körper auf. Das in der Praxis am häufigsten eingesetzte System für die Untersuchung der Wirkung von Medikamenten auf das Immunsystem stellen PBMC Präparationen und Vollblut-Kulturen dar. In diesen Systemen sind jedoch nicht alle an der Immunreaktion beteiligten Zelltypen repräsentiert. In diesem Zusammenhang stellt die Entwick-

lung komplexer organotypischer Co-Kultursysteme eine weitere Näherung an die *in vivo* Verhältnisse dar.

Diese Dissertation entstand im Rahmen des BMBF geförderten Verbundprojekts HuCoCSys. Ziel war die detaillierte Charakterisierung und Validierung eines bereits etablierten organotypischen Co-Kulturmodells des menschlichen Darmes. Die Co-Kultivierung von Caco-2 Kolonkarzinomzellen als Model des menschlichen Dünndarmepithels und Vollblut von verschiedenen Spendern sollte dabei die Untersuchung der Wirkung oral applizierter Medikamente auf das Immunsystem ermöglichen.

In einleitenden Experimenten wurde der Effekt der proinflammatorischen Zytokine IL-1 β , TNF α und IFN γ auf die Integrität der epithelialen Barriere mittels TEER Messungen und immunohistochemischen Analysen untersucht. Dabei konnte gezeigt werden daß die Behandlung der Caco-2 Zellen mit proinflammatorischen Zytokinen zu einer erhöhten Permeabilität des Epithels sowie zu einer geänderten Lokalisation von Zelladhäsionsproteinen führt. Weiterhin konnte gezeigt werden, das die Caco-2 Zellen in der Lage sind auf die Behandlung mit IL-1 β /TNF α sowie IFN γ mit der Ausschüttung der Chemokine IL-8, MCP-1 und IP-10 zu reagieren. Diese Ergebnisse zeigen, daß Caco-2 Zellen in einen „entzündlich veränderten“ Zustand versetzt werden können um die veränderten Eigenschaften der intestinalen Barriere unter entzündlichen Bedingungen *in vitro* nachzubilden.

In weiteren Experimenten wurde die Wirkung proinflammatorischer Zytokine auf intrazelluläre Rezeptor-Tyrosin Kinase vermittelte Signalwege untersucht. Hierfür wurden multiplexe Sandwich Immunoassays eingesetzt. Dabei konnte beobachtet werden, daß die Behandlung von ausdifferenzieren Caco-2 Zellen mit IL-1 β zu einer zeitabhängigen Phosphorylierung des EGF-Rezeptors an Serin 1047 führt. Über die Verwendung einer Kinase Inhibitor Library und einer anschließenden Literaturdatenbank Recherche konnten p38 α und IKK2 als potentielle Serin1047 phosphorylierende Kinasen identifiziert werden.

Im Rahmen dieser Arbeit wurden drei unterschiedliche Luminex basierte Sandwich Immunoassay Panel entwickelt und für die Quantifizierung von Immunmediatoren in

humanem Vollblut optimiert. Diese Assays wurden für die quantitative Analyse von Immunmediatoren in einer Vielzahl humaner Plasmaproben aus Co-Kulturerperimenten verwendet.

Dabei wurden in der Co-Kultur unterschiedliche Konzentrationen der Testsubstanzen auf differenzierte Caco-2 Monolayer gegeben und deren Wirkung in zuvor stimuliertem Vollblut mittels multiplexen Sandwich Immunoassays untersucht. Durch die Verwendung von Blut unterschiedlicher Spender konnte die Individualität des Immunsystems in die Analyse integriert werden. Die Kombination eines komplexen Co-Kultursystems mit der multiplexen Analyse von Immunmediatoren ermöglichte dabei die detaillierte Beschreibung der immunmodulierenden Effekte verschiedener Antiphlogistika und noch uncharakterisierter Naturstoffe. Der Vergleich der Dosis-Wirkungskurven von Dexamethason, Prednisolon, Ibuprofen, Diclofenac und Tacrolimus mit Dihydroxyguajaretsäure ermöglichte es dabei Rückschlüsse auf potentielle Wirkmechanismen zu ziehen.

Entgegen unserer Erwartungen ergaben sich durch die Behandlung der Caco-2 Zellen mit IL-1 β und TNF α vor Medikamentenapplikation keine signifikant veränderten Dosis-Wirkungskurven obwohl in den vorangegangenen Experimenten eine erhöhte Durchlässigkeit des Epithels sowie eine veränderte Lokalisation von Zelladhäsionsproteinen nachgewiesen werden konnte.

Daß im Rahmen dieser Studie eingesetzte *in vitro* Model des menschlichen Darmes ermöglichte die standardisierte Untersuchung der Wirkung oral applizierter Medikamente und Medikamentenkandidaten unter *in vivo* ähnlichen Verhältnissen. Das beschriebene Model stellt eine interessante Ergänzung zu den routinemäßig in der präklinischen Phase eingesetzten PBMC Präparationen, Vollblutassays und Tiermodellen dar. Die im Rahmen dieser Studie generierten Datensätze bilden die Basis für die zukünftige Analyse der immunmodulatorischen Effekte weiterer Wirkstoffe.

8. References

1. Schmolz, M., *Functional drug candidate profiling using complex human organotypic cell culture models: a promising way to reduce clinical drug failure*. Expert Opinion in Drug Discovery, 2007. **2**: p. 1-13.
2. Gustot, T., et al., *Profile of soluble cytokine receptors in Crohn's disease*. Gut, 2005. **54**(4): p. 488-95.
3. Papadakis, K.A. and S.R. Targan, *Role of cytokines in the pathogenesis of inflammatory bowel disease*. Annu Rev Med, 2000. **51**: p. 289-98.
4. Laufer, S., et al., *Human whole blood assay for rapid and routine testing of non-steroidal anti-inflammatory drugs (NSAIDs) on cyclo-oxygenase-2 activity*. Inflammopharmacology, 2008. **16**(4): p. 155-61.
5. Schmolz, M., Joos, T., *HOT Cell-Culture Models*. Discovery Technology, 2008: p. 18-21.
6. Hidalgo, I.J., T.J. Raub, and R.T. Borchardt, *Characterization of the human colon carcinoma cell line (Caco-2) as a model system for intestinal epithelial permeability*. Gastroenterology, 1989. **96**(3): p. 736-49.
7. Resta-Lenert, S. and K.E. Barrett, *Probiotics and commensals reverse TNF-alpha and IFN-gamma-induced dysfunction in human intestinal epithelial cells*. Gastroenterology, 2006. **130**(3): p. 731-46.
8. Walter, E., et al., *HT29-MTX/Caco-2 cocultures as an in vitro model for the intestinal epithelium: in vitro-in vivo correlation with permeability data from rats and humans*. J Pharm Sci, 1996. **85**(10): p. 1070-6.
9. Sambuy, Y., et al., *The Caco-2 cell line as a model of the intestinal barrier: influence of cell and culture-related factors on Caco-2 cell functional characteristics*. Cell Biol Toxicol, 2005. **21**(1): p. 1-26.
10. Artursson, P., K. Palm, and K. Luthman, *Caco-2 monolayers in experimental and theoretical predictions of drug transport*. Adv Drug Deliv Rev, 2001. **46**(1-3): p. 27-43.
11. Bock, U., Kottke, T., Gindorf, C., Haltner, E. *Validation of the Caco-2 cell monolayer system for determining the permeability of drug substances according to the Biopharmaceutics Classification System (BCS)*. 2003 [cited; Available from: www.acrossbarriers.de].
12. Engle, M.J., G.S. Goetz, and D.H. Alpers, *Caco-2 cells express a combination of colonocyte and enterocyte phenotypes*. J Cell Physiol, 1998. **174**(3): p. 362-9.
13. Lodish, H., Berk, A., Kaiser, C., Scott, M., Bretscher, A., Ploegh, H., Matsudaira, P., *Molecular Cell Biology*. Sixth Edition ed. 2007, New York: W.H. Freeman and Company.
14. Schreider, C., et al., *Integrin-mediated functional polarization of Caco-2 cells through E-cadherin-actin complexes*. J Cell Sci, 2002. **115**(Pt 3): p. 543-52.
15. Haltner, E., et al., *[In vitro permeability studies as a substitute for in vivo studies--which requirements have to be met?]*. ALTEX, 2001. **18**(1): p. 81-7.

16. Ligumsky, M., et al., *Role of interleukin 1 in inflammatory bowel disease--enhanced production during active disease*. Gut, 1990. **31**(6): p. 686-9.
17. Rogler, G. and T. Andus, *Cytokines in inflammatory bowel disease*. World J Surg, 1998. **22**(4): p. 382-9.
18. Stallmach, A., et al., *Cytokine/chemokine transcript profiles reflect mucosal inflammation in Crohn's disease*. Int J Colorectal Dis, 2004. **19**(4): p. 308-15.
19. Al-Sadi, R.M. and T.Y. Ma, *IL-1beta causes an increase in intestinal epithelial tight junction permeability*. J Immunol, 2007. **178**(7): p. 4641-9.
20. Ma, T.Y., et al., *Mechanism of TNF- α modulation of Caco-2 intestinal epithelial tight junction barrier: role of myosin light-chain kinase protein expression*. Am J Physiol Gastrointest Liver Physiol, 2005. **288**(3): p. G422-30.
21. Utech, M., et al., *Mechanism of IFN-gamma-induced endocytosis of tight junction proteins: myosin II-dependent vacuolarization of the apical plasma membrane*. Mol Biol Cell, 2005. **16**(10): p. 5040-52.
22. Cobrin, G.M. and M.T. Abreu, *Defects in mucosal immunity leading to Crohn's disease*. Immunol Rev, 2005. **206**: p. 277-95.
23. Ko, J.S., et al., *Lactobacillus plantarum inhibits epithelial barrier dysfunction and interleukin-8 secretion induced by tumor necrosis factor-alpha*. World J Gastroenterol, 2007. **13**(13): p. 1962-5.
24. Ma, T.Y., et al., *TNF-alpha-induced increase in intestinal epithelial tight junction permeability requires NF-kappa B activation*. Am J Physiol Gastrointest Liver Physiol, 2004. **286**(3): p. G367-76.
25. Basuroy, S., et al., *MAPK interacts with occludin and mediates EGF-induced prevention of tight junction disruption by hydrogen peroxide*. Biochem J, 2006. **393**(Pt 1): p. 69-77.
26. Rao, R., R.D. Baker, and S.S. Baker, *Inhibition of oxidant-induced barrier disruption and protein tyrosine phosphorylation in Caco-2 cell monolayers by epidermal growth factor*. Biochem Pharmacol, 1999. **57**(6): p. 685-95.
27. Cario, E., G. Gerken, and D.K. Podolsky, *"For whom the bell tolls!" -- innate defense mechanisms and survival strategies of the intestinal epithelium against luminal pathogens*. Z Gastroenterol, 2002. **40**(12): p. 983-90.
28. Herbst, R.S., *Review of epidermal growth factor receptor biology*. Int J Radiat Oncol Biol Phys, 2004. **59**(2 Suppl): p. 21-6.
29. Zwick, E., J. Bange, and A. Ullrich, *Receptor tyrosine kinase signalling as a target for cancer intervention strategies*. Endocr Relat Cancer, 2001. **8**(3): p. 161-73.
30. Cell-Signalling-Technology. *PhosphoSitePlus*. 2011 [cited 2011 16.08.2011]; Available from: <http://www.phosphosite.org>.
31. Schulze, W.X., L. Deng, and M. Mann, *Phosphotyrosine interactome of the ErbB-receptor kinase family*. Mol Syst Biol, 2005. **1**: p. 2005 0008.
32. Mizoguchi, A. and E. Mizoguchi, *Inflammatory bowel disease, past, present and future: lessons from animal models*. J Gastroenterol, 2008. **43**(1): p. 1-17.
33. Nakamura, M., et al., *Cytokine production in patients with inflammatory bowel disease*. Gut, 1992. **33**(7): p. 933-7.

34. Cavaillon, J.M., et al., *Cytokine cascade in sepsis*. Scand J Infect Dis, 2003. **35**(9): p. 535-44.
35. Lubberts, E. and W.B. van den Berg, *Cytokines in the pathogenesis of rheumatoid arthritis and collagen-induced arthritis*. Adv Exp Med Biol, 2003. **520**: p. 194-202.
36. Tedgui, A. and Z. Mallat, *Cytokines in atherosclerosis: pathogenic and regulatory pathways*. Physiol Rev, 2006. **86**(2): p. 515-81.
37. Murphy, K., Travers, P., Walport, M., *Janeway's Immunobiology*. 7 ed. 2008, New York: Garland Science. 885.
38. Budhu, A. and X.W. Wang, *The role of cytokines in hepatocellular carcinoma*. J Leukoc Biol, 2006. **80**(6): p. 1197-213.
39. Ono, S.J., et al., *Chemokines: roles in leukocyte development, trafficking, and effector function*. J Allergy Clin Immunol, 2003. **111**(6): p. 1185-99; quiz 1200.
40. Yoshie, O., *Role of chemokines in trafficking of lymphocytes and dendritic cells*. Int J Hematol, 2000. **72**(4): p. 399-407.
41. Zlotnik, A. and O. Yoshie, *Chemokines: a new classification system and their role in immunity*. Immunity, 2000. **12**(2): p. 121-7.
42. Heaney, M.L. and D.W. Golde, *Soluble receptors in human disease*. J Leukoc Biol, 1998. **64**(2): p. 135-46.
43. Levine, S.J., *Mechanisms of soluble cytokine receptor generation*. J Immunol, 2004. **173**(9): p. 5343-8.
44. Hull, K.M., et al., *The TNF receptor-associated periodic syndrome (TRAPS): emerging concepts of an autoinflammatory disorder*. Medicine (Baltimore), 2002. **81**(5): p. 349-68.
45. Lemmers, A., et al., *An inhibitor of interleukin-6 trans-signalling, sgp130, contributes to impaired acute phase response in human chronic liver disease*. Clin Exp Immunol, 2009. **156**(3): p. 518-27.
46. Junghans, R.P. and T.A. Waldmann, *Metabolism of Tac (IL2Ralpha): physiology of cell surface shedding and renal catabolism, and suppression of catabolism by antibody binding*. J Exp Med, 1996. **183**(4): p. 1587-602.
47. Boldt, J., et al., *Do plasma levels of circulating soluble adhesion molecules differ between surviving and nonsurviving critically ill patients?* Chest, 1995. **107**(3): p. 787-92.
48. Klimiuk, P.A., et al., *Soluble cell adhesion molecules (sICAM-1, sVCAM-1, and sE-selectin) in patients with early rheumatoid arthritis*. Scand J Rheumatol, 2007. **36**(5): p. 345-50.
49. Ridker, P.M., et al., *Plasma concentration of soluble intercellular adhesion molecule 1 and risks of future myocardial infarction in apparently healthy men*. Lancet, 1998. **351**(9096): p. 88-92.
50. Jones, S.C., et al., *Adhesion molecules in inflammatory bowel disease*. Gut, 1995. **36**(5): p. 724-30.
51. Tokuhira, M., et al., *Soluble vascular cell adhesion molecule 1 mediation of monocyte chemotaxis in rheumatoid arthritis*. Arthritis Rheum, 2000. **43**(5): p. 1122-33.

-
52. Abe, Y., et al., *Soluble cell adhesion molecules in hypertriglyceridemia and potential significance on monocyte adhesion*. *Arterioscler Thromb Vasc Biol*, 1998. **18**(5): p. 723-31.
 53. Bloemena, E., et al., *Whole-blood lymphocyte cultures*. *J Immunol Methods*, 1989. **122**(2): p. 161-7.
 54. Swaak, A.J., H.G. van den Brink, and L.A. Aarden, *Cytokine production in whole blood cell cultures of patients with rheumatoid arthritis*. *Ann Rheum Dis*, 1997. **56**(11): p. 693-5.
 55. Schmolz, M., Eisinger, D. *Truiculture: a simple whole blood collection and culture system for quantifying physiological interactions of the human immunesystem in the clinic*. **Volume**,
 56. Sato, M., et al., *Direct binding of Toll-like receptor 2 to zymosan, and zymosan-induced NF-kappa B activation and TNF-alpha secretion are down-regulated by lung collectin surfactant protein A*. *J Immunol*, 2003. **171**(1): p. 417-25.
 57. Sanguedolce, M.V., et al., *Zymosan-stimulated tumor necrosis factor-alpha production by human monocytes. Down-modulation by phorbol ester*. *J Immunol*, 1992. **148**(7): p. 2229-36.
 58. Underhill, D.M., et al., *The Toll-like receptor 2 is recruited to macrophage phagosomes and discriminates between pathogens*. *Nature*, 1999. **401**(6755): p. 811-5.
 59. Ezekowitz, R.A., et al., *Interaction of human monocytes, macrophages, and polymorphonuclear leukocytes with zymosan in vitro. Role of type 3 complement receptors and macrophage-derived complement*. *J Clin Invest*, 1985. **76**(6): p. 2368-76.
 60. Muzio, M., et al., *Toll-like receptor family and signalling pathway*. *Biochem Soc Trans*, 2000. **28**(5): p. 563-6.
 61. Pugin, J., et al., *Lipopolysaccharide activation of human endothelial and epithelial cells is mediated by lipopolysaccharide-binding protein and soluble CD14*. *Proc Natl Acad Sci U S A*, 1993. **90**(7): p. 2744-8.
 62. Beutler, B. and E.T. Rietschel, *Innate immune sensing and its roots: the story of endotoxin*. *Nat Rev Immunol*, 2003. **3**(2): p. 169-76.
 63. Lauw, F.N., et al., *Role of endogenous interleukin-12 in immune response to staphylococcal enterotoxin B in mice*. *Infect Immun*, 2001. **69**(9): p. 5949-52.
 64. Krakauer, T., *Coordinate suppression of superantigen-induced cytokine production and T-cell proliferation by a small nonpeptidic inhibitor of class II major histocompatibility complex and CD4 interaction*. *Antimicrob Agents Chemother*, 2000. **44**(4): p. 1067-9.
 65. Krakauer, T., *Induction of CC chemokines in human peripheral blood mononuclear cells by staphylococcal exotoxins and its prevention by pentoxifylline*. *J Leukoc Biol*, 1999. **66**(1): p. 158-64.
 66. Gandhi, R., et al., *Influence of poly I:C on sickness behaviors, plasma cytokines, corticosterone and central monoamine activity: moderation by social stressors*. *Brain Behav Immun*, 2007. **21**(4): p. 477-89.
 67. Lundberg, A.M., et al., *Key differences in TLR3/poly I:C signaling and cytokine induction by human primary cells: a phenomenon absent from murine cell systems*. *Blood*, 2007. **110**(9): p. 3245-52.

68. Irving, P.M., et al., *Review article: appropriate use of corticosteroids in Crohn's disease*. *Aliment Pharmacol Ther*, 2007. **26**(3): p. 313-29.
69. O'Dell, J.R., *Therapeutic strategies for rheumatoid arthritis*. *N Engl J Med*, 2004. **350**(25): p. 2591-602.
70. Morand, E.F. and M. Leech, *Glucocorticoid regulation of inflammation: the plot thickens*. *Inflamm Res*, 1999. **48**(11): p. 557-60.
71. Flower, R.J. and N.J. Rothwell, *Lipocortin-1: cellular mechanisms and clinical relevance*. *Trends Pharmacol Sci*, 1994. **15**(3): p. 71-6.
72. Yao, X.L., et al., *Dexamethasone alters arachidonate release from human epithelial cells by induction of p11 protein synthesis and inhibition of phospholipase A2 activity*. *J Biol Chem*, 1999. **274**(24): p. 17202-8.
73. Ray, A. and K.E. Prefontaine, *Physical association and functional antagonism between the p65 subunit of transcription factor NF-kappa B and the glucocorticoid receptor*. *Proc Natl Acad Sci U S A*, 1994. **91**(2): p. 752-6.
74. Besedovsky, H.O. and A. del Rey, *Regulating inflammation by glucocorticoids*. *Nat Immunol*, 2006. **7**(6): p. 537.
75. Newton, R., *Molecular mechanisms of glucocorticoid action: what is important?* *Thorax*, 2000. **55**(7): p. 603-13.
76. Jonat, C., et al., *Antitumor promotion and antiinflammation: down-modulation of AP-1 (Fos/Jun) activity by glucocorticoid hormone*. *Cell*, 1990. **62**(6): p. 1189-204.
77. Rao, P. and E.E. Knaus, *Evolution of nonsteroidal anti-inflammatory drugs (NSAIDs): cyclooxygenase (COX) inhibition and beyond*. *J Pharm Pharm Sci*, 2008. **11**(2): p. 81s-110s.
78. Laufer, s., Gay, S., Brune, K., ed. *Inflammation and Rheumatic Disease -The molecular basis of novel therapies*. 2003, Thieme: Stuttgart, New York.
79. Shiraishi, Y., et al., *Prostaglandin D2-induced eosinophilic airway inflammation is mediated by CRTH2 receptor*. *J Pharmacol Exp Ther*, 2005. **312**(3): p. 954-60.
80. Hirai, H., et al., *Prostaglandin D2 selectively induces chemotaxis in T helper type 2 cells, eosinophils, and basophils via seven-transmembrane receptor CRTH2*. *J Exp Med*, 2001. **193**(2): p. 255-61.
81. Pablos, J.L., et al., *Cyclooxygenase-1 and -2 are expressed by human T cells*. *Clin Exp Immunol*, 1999. **115**(1): p. 86-90.
82. Simmons, D.L., R.M. Botting, and T. Hla, *Cyclooxygenase isozymes: the biology of prostaglandin synthesis and inhibition*. *Pharmacol Rev*, 2004. **56**(3): p. 387-437.
83. Kunkel, S.L., S.W. Chensue, and S.H. Phan, *Prostaglandins as endogenous mediators of interleukin 1 production*. *J Immunol*, 1986. **136**(1): p. 186-92.
84. Kunkel, S.L., et al., *Regulation of macrophage tumor necrosis factor production by prostaglandin E2*. *Biochem Biophys Res Commun*, 1986. **137**(1): p. 404-10.
85. Betz, M. and B.S. Fox, *Prostaglandin E2 inhibits production of Th1 lymphokines but not of Th2 lymphokines*. *J Immunol*, 1991. **146**(1): p. 108-13.

-
86. Strassheim, D., et al., *Prostacyclin inhibits IFN-gamma-stimulated cytokine expression by reduced recruitment of CBP/p300 to STAT1 in a SOCS-1-independent manner*. J Immunol, 2009. **183**(11): p. 6981-8.
 87. Luttmann, W., et al., *Modulation of cytokine release from mononuclear cells by prostacyclin, IL-4 and IL-13*. Cytokine, 1999. **11**(2): p. 127-33.
 88. Baumgart, D.C., J.K. Macdonald, and B. Feagan, *Tacrolimus (FK506) for induction of remission in refractory ulcerative colitis*. Cochrane Database Syst Rev, 2008(3): p. CD007216.
 89. Baumgart, D.C., et al., *Tacrolimus is safe and effective in patients with severe steroid-refractory or steroid-dependent inflammatory bowel disease--a long-term follow-up*. Am J Gastroenterol, 2006. **101**(5): p. 1048-56.
 90. Hogan, P.G., et al., *Transcriptional regulation by calcium, calcineurin, and NFAT*. Genes Dev, 2003. **17**(18): p. 2205-32.
 91. Liu, J., et al., *Calcineurin is a common target of cyclophilin-cyclosporin A and FKBP-FK506 complexes*. Cell, 1991. **66**(4): p. 807-15.
 92. Tocci, M.J., et al., *The immunosuppressant FK506 selectively inhibits expression of early T cell activation genes*. J Immunol, 1989. **143**(2): p. 718-26.
 93. Kiani, A., A. Rao, and J. Aramburu, *Manipulating immune responses with immunosuppressive agents that target NFAT*. Immunity, 2000. **12**(4): p. 359-72.
 94. Punyadeera, C., et al., *A biomarker panel to discriminate between systemic inflammatory response syndrome and sepsis and sepsis severity*. J Emerg Trauma Shock, 2010. **3**(1): p. 26-35.
 95. Beidler, S.K., et al., *Multiplexed analysis of matrix metalloproteinases in leg ulcer tissue of patients with chronic venous insufficiency before and after compression therapy*. Wound Repair Regen, 2008. **16**(5): p. 642-8.
 96. Zhu, H. and M. Snyder, *Protein chip technology*. Curr Opin Chem Biol, 2003. **7**(1): p. 55-63.
 97. Templin, M.F., et al., *Protein microarrays and multiplexed sandwich immunoassays: what beats the beads?* Comb Chem High Throughput Screen, 2004. **7**(3): p. 223-9.
 98. Kramer, S., T.O. Joos, and M.F. Templin, *Protein microarrays*. Curr Protoc Protein Sci, 2005. **Chapter 23**: p. Unit 23 5.
 99. Schmohl, M., et al., *Protein-protein-interactions in a multiplexed, miniaturized format a functional analysis of Rho GTPase activation and inhibition*. Proteomics. **10**(8): p. 1716-20.
 100. Ekins, R.P., *Multi-analyte immunoassay*. J Pharm Biomed Anal, 1989. **7**(2): p. 155-68.
 101. Ekins, R.P., *Ligand assays: from electrophoresis to miniaturized microarrays*. Clin Chem, 1998. **44**(9): p. 2015-30.
 102. Stoll, D., et al., *Microarray technology: an increasing variety of screening tools for proteomic research*. Targets, 2004. **3**(1): p. 24-31.
 103. Luminex-Corp., *The Luminex Corporation Homepage, 16 June 2008* <<http://www.luminexcorp.com>> (16 June 2008). 2008.

-
104. Gardy, J.L., et al., *Enabling a systems biology approach to immunology: focus on innate immunity*. Trends Immunol, 2009. **30**(6): p. 249-62.
 105. de Jager, W., et al., *Simultaneous detection of 15 human cytokines in a single sample of stimulated peripheral blood mononuclear cells*. Clin Diagn Lab Immunol, 2003. **10**(1): p. 133-9.
 106. Hsu, H.Y., et al., *Suspension microarrays for the identification of the response patterns in hyperinflammatory diseases*. Med Eng Phys, 2008. **30**(8): p. 976-83.
 107. van Erk, M.J., et al., *Insight in modulation of inflammation in response to diclofenac intervention: a human intervention study*. BMC Med Genomics. **3**: p. 5.
 108. Mogensen, T.H., et al., *Mechanisms of dexamethasone-mediated inhibition of Toll-like receptor signaling induced by Neisseria meningitidis and Streptococcus pneumoniae*. Infect Immun, 2008. **76**(1): p. 189-97.
 109. Torrence, A.E., et al., *Serum biomarkers in a mouse model of bacterial-induced inflammatory bowel disease*. Inflamm Bowel Dis, 2008. **14**(4): p. 480-90.
 110. Yamamura, K., et al., *Intracellular protein phosphorylation in eosinophils and the functional relevance in cytokine production*. Int Arch Allergy Immunol, 2009. **149 Suppl 1**: p. 45-50.
 111. Khan, I.H., et al., *Multiplex analysis of intracellular signaling pathways in lymphoid cells by microbead suspension arrays*. Mol Cell Proteomics, 2006. **5**(4): p. 758-68.
 112. Poetz, O., et al., *Sequential multiplex analyte capturing for phosphoprotein profiling*. Mol Cell Proteomics. **9**(11): p. 2474-81.
 113. Yu, X., et al., *Protein microarrays: effective tools for the study of inflammatory diseases*. Methods Mol Biol, 2009. **577**: p. 199-214.
 114. Hsu, H.Y., *Suspension Microarrays For The Identification Of the Response Patterns In Hyperinflammatory Diseases*, in *Faculty of Biology*. 2008, Eberhard Karls University Tübingen: Tübingen. p. 98.
 115. Saeed, A.I., et al., *TM4 microarray software suite*. Methods Enzymol, 2006. **411**: p. 134-93.
 116. Tonseth C. P., D., J., *Guidelines For Validation Of Analytical Methods*. 1993, NYCOMED. p. 35-58.
 117. Countaway, J.L., A.C. Nairn, and R.J. Davis, *Mechanism of desensitization of the epidermal growth factor receptor protein-tyrosine kinase*. J Biol Chem, 1992. **267**(2): p. 1129-40.
 118. Wang, F., et al., *IFN-gamma-induced TNFR2 expression is required for TNF-dependent intestinal epithelial barrier dysfunction*. Gastroenterology, 2006. **131**(4): p. 1153-63.
 119. Wang, F., et al., *Interferon-gamma and tumor necrosis factor-alpha synergize to induce intestinal epithelial barrier dysfunction by up-regulating myosin light chain kinase expression*. Am J Pathol, 2005. **166**(2): p. 409-19.
 120. Henzen, C., *Therapie mit Glucocorticoiden: Risiken und Nebenwirkungen*. Schweiz Med Forum., 2003. **19**(7): p. 442-6.
 121. de Jager, W. and G.T. Rijkers, *Solid-phase and bead-based cytokine immunoassay: a comparison*. Methods, 2006. **38**(4): p. 294-303.

122. Polifke, T., Rauch, P., *Affinity discrimination to avoid interferences in assays*. IVD Technology, 2009. **15**(2).
123. Ma, T.Y., *Intestinal epithelial barrier dysfunction in Crohn's disease*. Proc Soc Exp Biol Med, 1997. **214**(4): p. 318-27.
124. Korzenik, J.R., *Past and current theories of etiology of IBD: toothpaste, worms, and refrigerators*. J Clin Gastroenterol, 2005. **39**(4 Suppl 2): p. S59-65.
125. Bruewer, M., et al., *Proinflammatory cytokines disrupt epithelial barrier function by apoptosis-independent mechanisms*. J Immunol, 2003. **171**(11): p. 6164-72.
126. Han, X., M.P. Fink, and R.L. Delude, *Proinflammatory cytokines cause NO*-dependent and -independent changes in expression and localization of tight junction proteins in intestinal epithelial cells*. Shock, 2003. **19**(3): p. 229-37.
127. Parlesak, A., et al., *Modulation of cytokine release by differentiated CACO-2 cells in a compartmentalized coculture model with mononuclear leucocytes and nonpathogenic bacteria*. Scand J Immunol, 2004. **60**(5): p. 477-85.
128. Saegusa, S., et al., *Cytokine responses of intestinal epithelial-like Caco-2 cells to non-pathogenic and opportunistic pathogenic yeasts in the presence of butyric acid*. Biosci Biotechnol Biochem, 2007. **71**(10): p. 2428-34.
129. Sunil, Y., G. Ramadori, and D. Raddatz, *Influence of NFkappaB inhibitors on IL-1beta-induced chemokine CXCL8 and -10 expression levels in intestinal epithelial cell lines: glucocorticoid ineffectiveness and paradoxical effect of PDTC*. Int J Colorectal Dis. **25**(3): p. 323-33.
130. Schuerer-Maly, C.C., et al., *Colonic epithelial cell lines as a source of interleukin-8: stimulation by inflammatory cytokines and bacterial lipopolysaccharide*. Immunology, 1994. **81**(1): p. 85-91.
131. Warhurst, A.C., S.J. Hopkins, and G. Warhurst, *Interferon gamma induces differential upregulation of alpha and beta chemokine secretion in colonic epithelial cell lines*. Gut, 1998. **42**(2): p. 208-13.
132. Yeruva, S., G. Ramadori, and D. Raddatz, *NF-kappaB-dependent synergistic regulation of CXCL10 gene expression by IL-1beta and IFN-gamma in human intestinal epithelial cell lines*. Int J Colorectal Dis, 2008. **23**(3): p. 305-17.
133. Nishimura, M., et al., *TAK1-mediated serine/threonine phosphorylation of epidermal growth factor receptor via p38/extracellular signal-regulated kinase: NF-{kappa}B-independent survival pathways in tumor necrosis factor alpha signaling*. Mol Cell Biol, 2009. **29**(20): p. 5529-39.
134. Murthy, S., S.N. Mathur, and F.J. Field, *Tumor necrosis factor-alpha and interleukin-1beta inhibit apolipoprotein B secretion in CaCo-2 cells via the epidermal growth factor receptor signaling pathway*. J Biol Chem, 2000. **275**(13): p. 9222-9.
135. McElroy, S.J., et al., *Tumor necrosis factor inhibits ligand-stimulated EGF receptor activation through a TNF receptor 1-dependent mechanism*. Am J Physiol Gastrointest Liver Physiol, 2008. **295**(2): p. G285-93.
136. Bird, T.A. and J. Saklatvala, *IL-1 and TNF transmodulate epidermal growth factor receptors by a protein kinase C-independent mechanism*. J Immunol, 1989. **142**(1): p. 126-33.

137. Downward, J., P. Parker, and M.D. Waterfield, *Autophosphorylation sites on the epidermal growth factor receptor*. Nature, 1984. **311**(5985): p. 483-5.
138. Li, X., et al., *IL-1-induced NFkappa B and c-Jun N-terminal kinase (JNK) activation diverge at IL-1 receptor-associated kinase (IRAK)*. Proc Natl Acad Sci U S A, 2001. **98**(8): p. 4461-5.
139. Huang, J., et al., *Recruitment of IRAK to the interleukin 1 receptor complex requires interleukin 1 receptor accessory protein*. Proc Natl Acad Sci U S A, 1997. **94**(24): p. 12829-32.
140. Ninomiya-Tsuji, J., et al., *The kinase TAK1 can activate the NIK-I kappaB as well as the MAP kinase cascade in the IL-1 signalling pathway*. Nature, 1999. **398**(6724): p. 252-6.
141. Akira, S. and K. Takeda, *Toll-like receptor signalling*. Nat Rev Immunol, 2004. **4**(7): p. 499-511.
142. Enslen, H., J. Raingeaud, and R.J. Davis, *Selective activation of p38 mitogen-activated protein (MAP) kinase isoforms by the MAP kinase kinases MKK3 and MKK6*. J Biol Chem, 1998. **273**(3): p. 1741-8.
143. Shirakabe, K., et al., *TAK1 mediates the ceramide signaling to stress-activated protein kinase/c-Jun N-terminal kinase*. J Biol Chem, 1997. **272**(13): p. 8141-4.
144. Ichijo, H., *From receptors to stress-activated MAP kinases*. Oncogene, 1999. **18**(45): p. 6087-93.
145. Derijard, B., et al., *Independent human MAP-kinase signal transduction pathways defined by MEK and MKK isoforms*. Science, 1995. **267**(5198): p. 682-5.
146. Stein, B., et al., *Cloning and characterization of MEK6, a novel member of the mitogen-activated protein kinase kinase cascade*. J Biol Chem, 1996. **271**(19): p. 11427-33.
147. Tsuchiya, Y., et al., *Nuclear IKKbeta is an adaptor protein for IkappaBalpha ubiquitination and degradation in UV-induced NF-kappaB activation*. Mol Cell. **39**(4): p. 570-82.
148. Adachi, S., et al., *p38 MAP kinase controls EGF receptor downregulation via phosphorylation at Ser1046/1047*. Cancer Lett, 2009. **277**(1): p. 108-13.
149. Adachi, S., et al., *(-)-Epigallocatechin gallate downregulates EGF receptor via phosphorylation at Ser1046/1047 by p38 MAPK in colon cancer cells*. Carcinogenesis, 2009. **30**(9): p. 1544-52.
150. Hatz, H.J., *Glucocorticoide-Immunologische Grundlagen, Pharmakologie und Therapierichtlinien*. Medizinisch-pharmakologisches Kompendium, ed. H. Ammon, Werner, C. Vol. 12. 1998, Stuttgart: Wissenschaftliche Verlagsgesellschaft mbH.
151. Duggan, D.E., et al., *Bioavailability of oral dexamethasone*. Clin Pharmacol Ther, 1975. **18**(2): p. 205-9.
152. Loew, D., O. Schuster, and E.H. Graul, *Dose-dependent pharmacokinetics of dexamethasone*. Eur J Clin Pharmacol, 1986. **30**(2): p. 225-30.
153. Tauber, U., et al., *The pharmacokinetics of fluocortolone and prednisolone after intravenous and oral administration*. Int J Clin Pharmacol Ther Toxicol, 1984. **22**(1): p. 48-55.

154. De Bosscher, K., W. Vanden Berghe, and G. Haegeman, *The interplay between the glucocorticoid receptor and nuclear factor-kappa B or activator protein-1: molecular mechanisms for gene repression*. *Endocr Rev*, 2003. **24**(4): p. 488-522.
155. Mukaida, N., et al., *Novel mechanism of glucocorticoid-mediated gene repression. Nuclear factor-kappa B is target for glucocorticoid-mediated interleukin 8 gene repression*. *J Biol Chem*, 1994. **269**(18): p. 13289-95.
156. Boumpas, D.T., *A novel action of glucocorticoids--NF-kappa B inhibition*. *Br J Rheumatol*, 1996. **35**(8): p. 709-10.
157. Yang-Yen, H.F., et al., *Transcriptional interference between c-Jun and the glucocorticoid receptor: mutual inhibition of DNA binding due to direct protein-protein interaction*. *Cell*, 1990. **62**(6): p. 1205-15.
158. Auphan, N., et al., *Immunosuppression by glucocorticoids: inhibition of NF-kappa B activity through induction of I kappa B synthesis*. *Science*, 1995. **270**(5234): p. 286-90.
159. McKay, L.I. and J.A. Cidlowski, *Molecular control of immune/inflammatory responses: interactions between nuclear factor-kappa B and steroid receptor-signaling pathways*. *Endocr Rev*, 1999. **20**(4): p. 435-59.
160. Rhen, T. and J.A. Cidlowski, *Antiinflammatory action of glucocorticoids--new mechanisms for old drugs*. *N Engl J Med*, 2005. **353**(16): p. 1711-23.
161. Necela, B.M. and J.A. Cidlowski, *Mechanisms of glucocorticoid receptor action in noninflammatory and inflammatory cells*. *Proc Am Thorac Soc*, 2004. **1**(3): p. 239-46.
162. Cippitelli, M., et al., *Negative transcriptional regulation of the interferon-gamma promoter by glucocorticoids and dominant negative mutants of c-Jun*. *J Biol Chem*, 1995. **270**(21): p. 12548-56.
163. Grewe, M., et al., *Regulation of the mRNA expression for tumor necrosis factor-alpha in rat liver macrophages*. *J Hepatol*, 1994. **20**(6): p. 811-8.
164. Collart, M.A., P. Baeuerle, and P. Vassalli, *Regulation of tumor necrosis factor alpha transcription in macrophages: involvement of four kappa B-like motifs and of constitutive and inducible forms of NF-kappa B*. *Mol Cell Biol*, 1990. **10**(4): p. 1498-506.
165. Bendrups, A., et al., *Reduction of tumor necrosis factor alpha and interleukin-1 beta levels in human synovial tissue by interleukin-4 and glucocorticoid*. *Rheumatol Int*, 1993. **12**(6): p. 217-20.
166. Jeon, Y.J., et al., *Dexamethasone inhibits IL-1 beta gene expression in LPS-stimulated RAW 264.7 cells by blocking NF-kappa B/Rel and AP-1 activation*. *Immunopharmacology*, 2000. **48**(2): p. 173-83.
167. Park, S.K., et al., *Dexamethasone regulates AP-1 to repress TNF-alpha induced MCP-1 production in human glomerular endothelial cells*. *Nephrol Dial Transplant*, 2004. **19**(2): p. 312-9.
168. Yang, K., et al., *Inhibitory effect of rapamycin and dexamethasone on production of IL-17 and IFN-gamma in Vogt-Koyanagi-Harada patients*. *Br J Ophthalmol*, 2009. **93**(2): p. 249-53.
169. Momcilovic, M., et al., *Methylprednisolone inhibits interleukin-17 and interferon-gamma expression by both naive and primed T cells*. *BMC Immunol*, 2008. **9**: p. 47.

-
170. Ramirez, F., et al., *Glucocorticoids promote a TH2 cytokine response by CD4+ T cells in vitro*. J Immunol, 1996. **156**(7): p. 2406-12.
 171. Wu, C.Y., et al., *Glucocorticoids suppress the production of interleukin 4 by human lymphocytes*. Eur J Immunol, 1991. **21**(10): p. 2645-7.
 172. Byron, K.A., G. Varigos, and A. Wootton, *Hydrocortisone inhibition of human interleukin-4*. Immunology, 1992. **77**(4): p. 624-6.
 173. Sewell, W.A., et al., *Induction of interleukin-4 and interleukin-5 expression in mast cells is inhibited by glucocorticoids*. Clin Diagn Lab Immunol, 1998. **5**(1): p. 18-23.
 174. Agarwal, S.K. and G.D. Marshall, Jr., *Dexamethasone promotes type 2 cytokine production primarily through inhibition of type 1 cytokines*. J Interferon Cytokine Res, 2001. **21**(3): p. 147-55.
 175. Arzt, E., et al., *Glucocorticoids suppress interleukin-1 receptor antagonist synthesis following induction by endotoxin*. Endocrinology, 1994. **134**(2): p. 672-7.
 176. Sauer, J., et al., *Inhibition of lipopolysaccharide-induced monocyte interleukin-1 receptor antagonist synthesis by cortisol: involvement of the mineralocorticoid receptor*. J Clin Endocrinol Metab, 1996. **81**(1): p. 73-9.
 177. Kovalovsky, D., et al., *Molecular mechanisms and Th1/Th2 pathways in corticosteroid regulation of cytokine production*. J Neuroimmunol, 2000. **109**(1): p. 23-9.
 178. Luster, A.D., J.C. Unkeless, and J.V. Ravetch, *Gamma-interferon transcriptionally regulates an early-response gene containing homology to platelet proteins*. Nature, 1985. **315**(6021): p. 672-6.
 179. Wang, X., et al., *Interferon-inducible protein-10 involves vascular smooth muscle cell migration, proliferation, and inflammatory response*. J Biol Chem, 1996. **271**(39): p. 24286-93.
 180. Sauty, A., et al., *The T cell-specific CXC chemokines IP-10, Mig, and I-TAC are expressed by activated human bronchial epithelial cells*. J Immunol, 1999. **162**(6): p. 3549-58.
 181. Cassatella, M.A., et al., *Regulated production of the interferon-gamma-inducible protein-10 (IP-10) chemokine by human neutrophils*. Eur J Immunol, 1997. **27**(1): p. 111-5.
 182. Tudhope, S.J., et al., *The role of I κ B kinase 2, but not activation of NF- κ B, in the release of CXCR3 ligands from IFN-gamma-stimulated human bronchial epithelial cells*. J Immunol, 2007. **179**(9): p. 6237-45.
 183. Hefner, K., *Untersuchungen zur Interaktion von Arzneistoffen mit immunkompetenten Zellen in komplexen organotypischen Zellkulturmodellen*. 2011, Hochschule Albstadt-Sigmaringen.
 184. *Open Drug Database*. 2011, ywesee GmbH.
 185. Martin, W., et al., *Pharmacokinetics and absolute bioavailability of ibuprofen after oral administration of ibuprofen lysine in man*. Biopharm Drug Dispos, 1990. **11**(3): p. 265-78.
 186. Dewland, P.M., S. Reader, and P. Berry, *Bioavailability of ibuprofen following oral administration of standard ibuprofen, sodium ibuprofen or ibuprofen acid incorporating poloxamer in healthy volunteers*. BMC Clin Pharmacol, 2009. **9**: p. 19.

187. Hinz, B., et al., *Aceclofenac spares cyclooxygenase 1 as a result of limited but sustained biotransformation to diclofenac*. Clin Pharmacol Ther, 2003. **74**(3): p. 222-35.
188. Patrono, C., P. Patrignani, and L.A. Garcia Rodriguez, *Cyclooxygenase-selective inhibition of prostanoid formation: transducing biochemical selectivity into clinical read-outs*. J Clin Invest, 2001. **108**(1): p. 7-13.
189. Hinz, B., et al., *Bioavailability of diclofenac potassium at low doses*. Br J Clin Pharmacol, 2005. **59**(1): p. 80-4.
190. Willis, J.V., et al., *The pharmacokinetics of diclofenac sodium following intravenous and oral administration*. Eur J Clin Pharmacol, 1979. **16**(6): p. 405-10.
191. Kirchheiner, J., et al., *Pharmacokinetics of diclofenac and inhibition of cyclooxygenases 1 and 2: no relationship to the CYP2C9 genetic polymorphism in humans*. Br J Clin Pharmacol, 2003. **55**(1): p. 51-61.
192. Kuroda, E., et al., *Prostaglandin E2 up-regulates macrophage-derived chemokine production but suppresses IFN-inducible protein-10 production by APC*. J Immunol, 2001. **166**(3): p. 1650-8.
193. Sacco, S., et al., *Nonsteroidal anti-inflammatory drugs increase tumor necrosis factor production in the periphery but not in the central nervous system in mice and rats*. J Neurochem, 1998. **71**(5): p. 2063-70.
194. Craig, R., et al., *p38 MAPK and NF-kappa B collaborate to induce interleukin-6 gene expression and release. Evidence for a cytoprotective autocrine signaling pathway in a cardiac myocyte model system*. J Biol Chem, 2000. **275**(31): p. 23814-24.
195. Dwinell, M.B., et al., *Regulated production of interferon-inducible T-cell chemoattractants by human intestinal epithelial cells*. Gastroenterology, 2001. **120**(1): p. 49-59.
196. Shi, S., et al., *MyD88 primes macrophages for full-scale activation by interferon-gamma yet mediates few responses to Mycobacterium tuberculosis*. J Exp Med, 2003. **198**(7): p. 987-97.
197. Sanceau, J., et al., *IL-6 and IL-6 receptor modulation by IFN-gamma and tumor necrosis factor-alpha in human monocytic cell line (THP-1). Priming effect of IFN-gamma*. J Immunol, 1991. **147**(8): p. 2630-7.
198. Khan, M.M., *Regulation of IL-4 and IL-5 secretion by histamine and PGE2*. Adv Exp Med Biol, 1995. **383**: p. 35-42.
199. Napolitani, G., et al., *Prostaglandin E2 enhances Th17 responses via modulation of IL-17 and IFN-gamma production by memory CD4+ T cells*. Eur J Immunol, 2009. **39**(5): p. 1301-12.
200. Dawicki, W. and J.S. Marshall, *New and emerging roles for mast cells in host defence*. Curr Opin Immunol, 2007. **19**(1): p. 31-8.
201. Bachawaty, T., S.L. Washington, and S.W. Walsh, *Neutrophil expression of cyclooxygenase 2 in preeclampsia*. Reprod Sci. **17**(5): p. 465-70.
202. Guslandi, M., *Exacerbation of inflammatory bowel disease by nonsteroidal anti-inflammatory drugs and cyclooxygenase-2 inhibitors: fact or fiction?* World J Gastroenterol, 2006. **12**(10): p. 1509-10.

203. Venkataramanan, R., et al., *Clinical pharmacokinetics of tacrolimus*. Clin Pharmacokinet, 1995. **29**(6): p. 404-30.
204. Vicari-Christensen, M., et al., *Tacrolimus: review of pharmacokinetics, pharmacodynamics, and pharmacogenetics to facilitate practitioners' understanding and offer strategies for educating patients and promoting adherence*. Prog Transplant, 2009. **19**(3): p. 277-84.
205. Venkataramanan, R., et al., *Pharmacokinetics of FK 506 in transplant patients*. Transplant Proc, 1991. **23**(6): p. 2736-40.
206. Staatz, C.E. and S.E. Tett, *Clinical pharmacokinetics and pharmacodynamics of tacrolimus in solid organ transplantation*. Clin Pharmacokinet, 2004. **43**(10): p. 623-53.
207. Rao, A., C. Luo, and P.G. Hogan, *Transcription factors of the NFAT family: regulation and function*. Annu Rev Immunol, 1997. **15**: p. 707-47.
208. Trevillyan, J.M., et al., *Potent inhibition of NFAT activation and T cell cytokine production by novel low molecular weight pyrazole compounds*. J Biol Chem, 2001. **276**(51): p. 48118-26.
209. Andersson, J., et al., *Effects of FK506 and cyclosporin A on cytokine production studied in vitro at a single-cell level*. Immunology, 1992. **75**(1): p. 136-42.
210. Sakuma, S., et al., *Tacrolimus suppressed the production of cytokines involved in atopic dermatitis by direct stimulation of human PBMC system. (Comparison with steroids)*. Int Immunopharmacol, 2001. **1**(6): p. 1219-26.
211. Sakuma, S., et al., *FK506 potently inhibits T cell activation induced TNF-alpha and IL-1beta production in vitro by human peripheral blood mononuclear cells*. Br J Pharmacol, 2000. **130**(7): p. 1655-63.
212. Sakuma, S., et al., *Effects of FK506 and other immunosuppressive anti-rheumatic agents on T cell activation mediated IL-6 and IgM production in vitro*. Int Immunopharmacol, 2001. **1**(4): p. 749-57.
213. Zhang, X.J., et al., *Effects and mechanisms of tacrolimus on development of murine Th17 cells*. Transplant Proc. **42**(9): p. 3779-83.
214. Gonzalez-Alvaro, I., et al., *Inhibition of tumour necrosis factor and IL-17 production by leflunomide involves the JAK/STAT pathway*. Ann Rheum Dis, 2009. **68**(10): p. 1644-50.
215. Jiang, H., et al., *Tacrolimus and cyclosporine differ in their capacity to overcome ongoing allograft rejection as a result of their differential abilities to inhibit interleukin-10 production*. Transplantation, 2002. **73**(11): p. 1808-17.
216. Dumont, F.J., *FK506 enhances IL-13 production by T cells activated through CD3/CD28*. Int Arch Allergy Immunol, 1997. **114**(3): p. 300-1.
217. Dumont, F.J., *FK506, an immunosuppressant targeting calcineurin function*. Curr Med Chem, 2000. **7**(7): p. 731-48.
218. Pahl, A., et al., *Regulation of IL-13 synthesis in human lymphocytes: implications for asthma therapy*. Br J Pharmacol, 2002. **135**(8): p. 1915-26.
219. Kohyama, T., et al., *A potent immunosuppressant FK506 inhibits IL-8 expression in human eosinophils*. Mol Cell Biol Res Commun, 1999. **1**(1): p. 72-7.

220. Sasakawa, Y., et al., *FK506 suppresses neutrophil chemoattractant production by peripheral blood mononuclear cells*. Eur J Pharmacol, 2000. **403**(3): p. 281-8.
221. Okamoto, S., et al., *The interleukin-8 AP-1 and kappa B-like sites are genetic end targets of FK506-sensitive pathway accompanied by calcium mobilization*. J Biol Chem, 1994. **269**(11): p. 8582-9.
222. Duwiejua, M., et al., *Anti-inflammatory activity of Polygonum bistorta, Guaiacum officinale and Hamamelis virginiana in rats*. J Pharm Pharmacol, 1994. **46**(4): p. 286-90.

9. Supplementary Material

Supplementary Table 1: Cross-reactivities in Panel II.

Cross-reactivities between capture and detection antibodies **A**, capture antibodies and analytes **B**, analytes and detection antibodies **C**. Displayed are median fluorescence intensities (MFI). If present analytes were used at 10000 pg/ml. The cut off threshold was set to 40 MFI.

A: all beads, no analyte, separate detection antibodies

detection	capture coated beads			
	IL-4	IL-17A	TSLP	TARC
IL-4	3	2	3	3
IL-17A	2	3	5	3
TSLP	1	5	1	4
TARC	2	5	6	9

B: all beads, separate analytes, all detection antibodies

analyte	capture coated beads			
	IL-4	IL-17A	TSLP	TARC
IL-4	4885	12	8	8
IL-17	5	5201	7	6
TSLP	3	19	6004	6
TARC	3	11	19	12982

C: all beads, all analytes, separate detection antibodies

detection	capture coated beads			
	IL-4	IL-17A	TSLP	TARC
IL-4	4347	3	3	3
IL-17	2	5107	4	3
TSLP	2	4	6170	4
TARC	2	3	4	11142

Supplementary Table 2: Cross reactivities in Panel III.

Crossreactivities between capture and detection antibodies **A**, capture antibodies and analytes **B**, analytes and detection antibodies **C**. Displayed are median fluorescence intensities (MFI). If present analytes were used at 10000 pg/ml. The cut off threshold was set to 40 MFI.

A: all beads, no analyte, separate detection antibodies

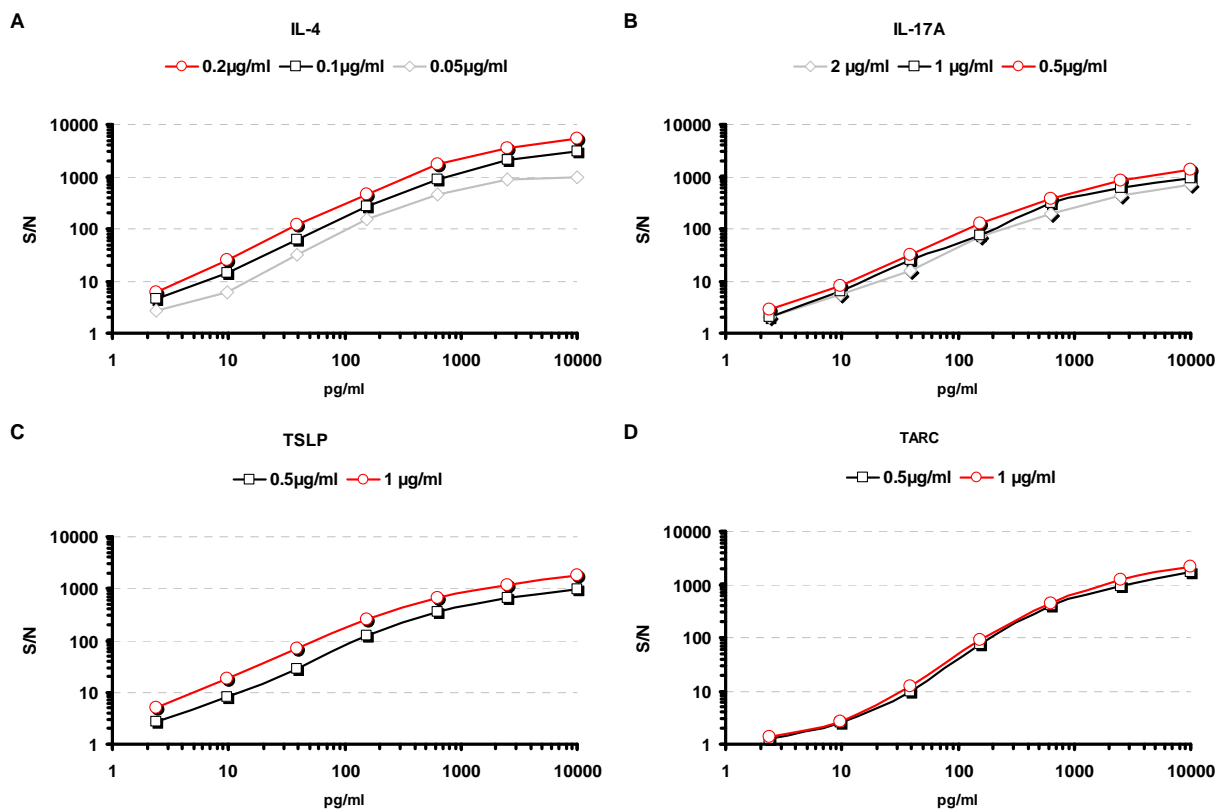
detection	capture coated beads				
	IL-13	IL-1ra	IL-5	IL-10	IL-12p70
IL-13	8	4	3	3	2
IL-1ra	7	3	1.5	2	2
IL-5	7	2	39	2	2
IL-10	8	3	2	2	2
IL-12p70	9	13	3	3	40

B: all beads, separate analytes, all detection antibodies

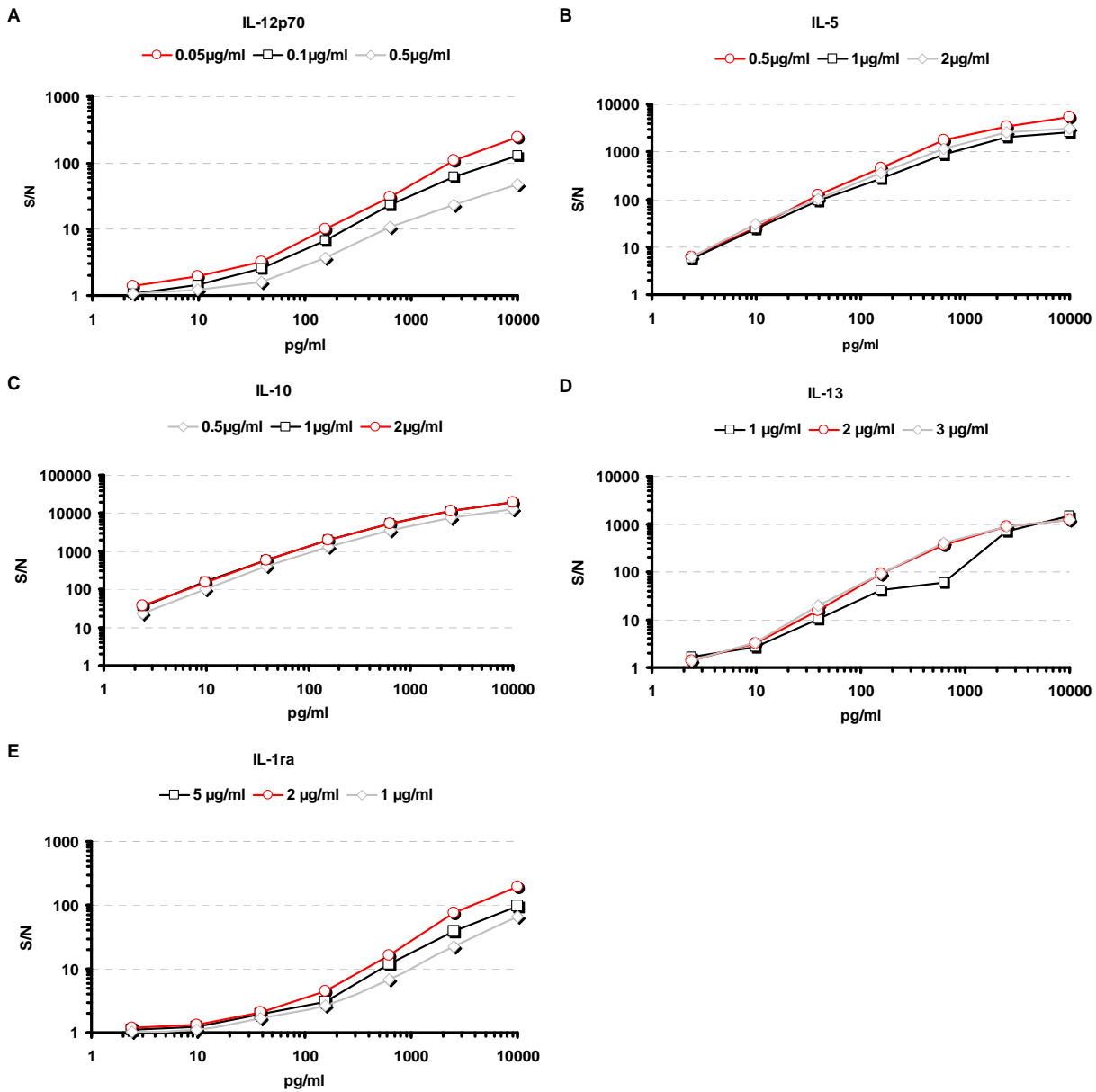
analyte	capture coated beads				
	IL-13	IL-1ra	IL-5	IL-10	IL-12p70
IL-13	2505	6	27	6	8
IL-1ra	11	2171	18	5	7
IL-5	10	6	13760	5	7
IL-10	11	6	12	16169	6
IL-12p70	10	5	15	6	4313

C: all beads, all analytes, separate detection antibodies

detection	capture coated beads				
	IL-13	IL-1ra	IL-5	IL-10	IL-12p70
IL-13	2815	4	5	8	2
IL-1ra	8	2104	5	3	1
IL-5	8	4	14217	4	3
IL-10	9	4	5	14667	2
IL-12p70	9	12	10	8	3677

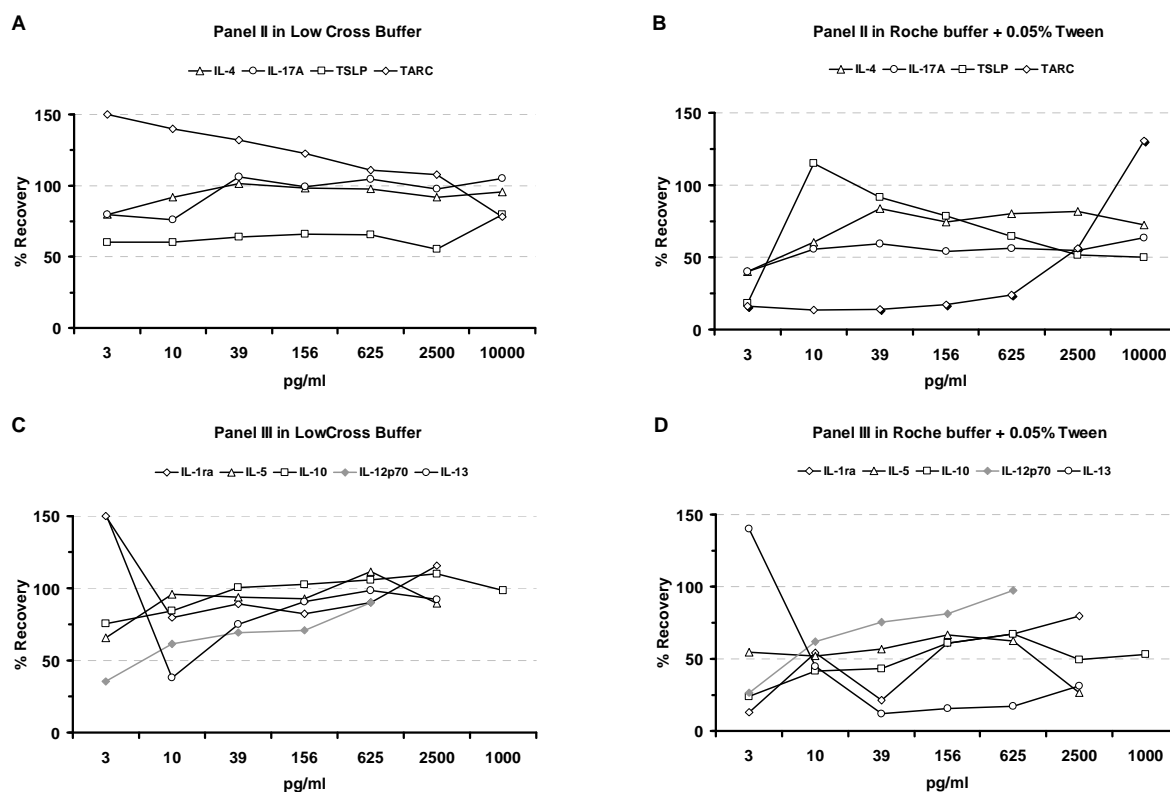


Supplementary Figure 1: Titration of detection antibodies in Panel II. Shown are signal to noise ratios. Curves of the selected concentrations are depicted in red. **A** IL-4, **B** IL-17A, **C** TSLP, **D** TARC.



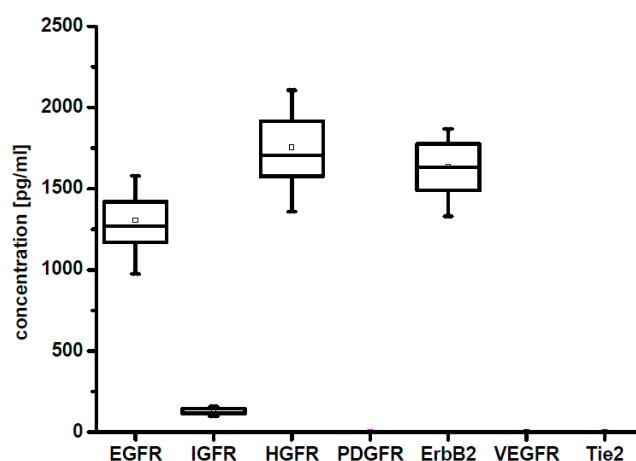
Supplementary Figure 2: Titration of detection antibodies in Panel III.

Shown are signal to noise ratios. Curves of the selected concentrations are depicted in red. **A** IL-12p70, **B** IL-5, **C** IL-10, **D** IL-13, **E** IL-1ra.



Supplementary Figure 3: Optimization of Spike-in recovery for Panel II+III.

Recombinant proteins were spiked into human heparin plasma in the indicated concentrations. In parallel standard curves were determined in LowCross buffer (**A, C**) and Roche buffer + 0,05% Tween (**B, D**). The measured MFI signals in human plasma were converted into concentration values using a 5-parametric fitting of the detected standard curve and percental recovery was determined on the basis of the initially added concentrations. Shown are the results obtained with Low Cross buffer and Roche buffer + 0,05%Tween used as standard dilution matrix.



Supplementary Figure 4: Distribution of concentrations for total RTK proteins in Caco-2 lysates. Caco-2 cells were treated with IL-1 β or EGF (10 ng/ml) for different time periods. Cell lysates were analyzed for total protein expression (Merck/EMD WideScreenTM total RTK 7-plex Kit). Measurements were performed in technical triplicates. Each diagram shows the distribution of mean protein concentrations (pg/ml) derived from the 3 technical replicates across 15 independent cell culture experiments. Boxes indicate the median and the 25th and 75th percentile. Whiskers represent the 5th and 95th percentiles. Additionally the mean (square) and the 1st and 99th percentiles (crosses) are shown. Concentration ranges: EGFR (974-1579 pg/ml), HGFR (1356-2106 pg/ml), ErbB2 (1330-1867 pg/ml), IGFR (98-158 pg/ml) were observed. PDGFR, VEGFR and Tie-2 could not be detected.

Supplementary Table 3: InhibitorSelect™ protein kinase Inhibitors

Nr	Inhibitor	Inhibition Constants (IC ₅₀ , K _i , or K _d)	Human Kinome Branch
		IC ₅₀ values are in vitro, cell-free, unless otherwise stated	
1	Adenosine Kinase Inhibitor	IC ₅₀ = 50.7 nM for AKT	Other
2	Akt Inhibitor XII, Isozyme-Selective, Akti-2	IC ₅₀ = 805 nM for Akt2. IC ₅₀ > 10 μM for Akt1/3.	AGC
3	Arcyriaflavin A, Synthetic	IC ₅₀ = 59 nM for CDK4/D1.	CMGC
4	1-Azakenpaulone	IC ₅₀ = 18 nM for GSK-3β.	CMGC
5	Bisindolylmaleimide III, Hydrochloride	IC ₅₀ = 26 nM for protein kinase C.	AGC
6	Bisindolylmaleimide V	IC ₅₀ > 100 μM for protein kinase C	AGC
7	CR8, (R)-Isomer	IC ₅₀ = 0.09 μM for CDK	CMGC
8	CR8, (S)-Isomer	IC ₅₀ = 0.15 μM for CDK	CMGC
9	CaMKII Inhibitor, CK59	IC ₅₀ < 10 μM for CaMKII.	CAMK
10	Cdk1 Inhibitor IV, RO-3306	K _i = 35 nM for Cdk1/B1. K _i = 110 nM for Cdk1/A.	CMGC
11	Cdc7/Cdk9 Inhibitor	IC ₅₀ = 10 nM for Cdc7. IC ₅₀ = 34 nM for Cdk9.	CMGC
12	Casein Kinase II Inhibitor I	IC ₅₀ = 900 nM for CK2 in rat liver.	CMGC
13	Keratinoocyte Differentiation Inducer	IC ₅₀ = 9 nM for casein kinase II.	CMGC
14	Casein Kinase II Inhibitor IV	IC ₅₀ = 390 nM for casein kinase II.	CMGC
15	Cdk2 Inhibitor II	IC ₅₀ = 60 nM for Cdk2.	CMGC
16	Cdk2/5 Inhibitor	K _i = 2 μM for Cdk5/p25.	CMGC
17	Cdk Inhibitor, p35	IC ₅₀ = 100 nM for Cdk	CMGC
18	Chk2 Inhibitor	IC ₅₀ = 8 nM for Chk2.	CAMK
19	Compound 401	IC ₅₀ = 280 nM for DNA-PK. IC ₅₀ = 5.3 μM for mTOR.	Atypical
20	Cdk2/9 Inhibitor	K _i = 2 nM for Cdk2/E. K _i = 4 nM for Cdk9/T1.	CMGC
21	Cdk9 Inhibitor II	IC ₅₀ = 350 nM for Cdk9.	CMGC
22	4-Cyano-3-methylisoquinoline	IC ₅₀ = 30 nM for protein kinase A.	AGC
23	eEF-2 Kinase Inhibitor, NH125	IC ₅₀ = 60 nM for eEF-2 kinase/CaMKIII.	Atypical
24	GSK-3 Inhibitor IX, Control, MeBIO	IC ₅₀ > 92 μM for Cdk1/B.	CMGC
25	Gö 7874, Hydrochloride	IC ₅₀ = 4 nM for rat brain PKC.	AGC
26	H-8, Dihydrochloride	K _i = 1.2 μM for PKA. K _i = 15 μM for PKC	AGC
27	HA 1004, Dihydrochloride	K _i = 2.3 μM for PKA. K _i = 150 μM for PKC	AGC
28	IKK-2 Inhibitor V	IC ₅₀ = 250 nM for IKK-2	Other
29	IKK-2 Inhibitor VI	IC ₅₀ = 13 nM for IKK-2.	Other
30	IKK Inhibitor VII	IC ₅₀ = 40 nM for IKK-2. IC ₅₀ = 70 nM for IKK complex.	Other
31	IKK-2 Inhibitor VIII	IC ₅₀ = 8.5 nM for IKK-2. IC ₅₀ = 250 nM for IKK-1.	Other
32	IKK-3 Inhibitor IX	IC ₅₀ = 40 nM for IKK-3.	Other
33	IKK Inhibitor X	IC ₅₀ = 88 nM for IKK.	Other
34	IKK-2 Inhibitor XI	IC ₅₀ = 25 nM for IKK-2.	Other
35	Indirubin-3'-monoxime, 5-Iodo-	IC ₅₀ = 9 nM for GSK-3β.	CMGC
36	IP3K Inhibitor	IC ₅₀ = 10.2 μM for IP3-K.	Other
37	5-Iodotubercidin	K _i = 30 nM for Adenosine Kinase A. K _i = 530 nM for ERK2.	Other
38	KT5720	K _i = 56 nM for protein kinase A.	AGC
39	KN-92	Negative control for CaM Kinase II.	NA
40	LY 294002, 4'-NH ₂	IC ₅₀ = 183 nM for p110α. IC ₅₀ = 98 nM for p110β.	Other
41	MEK1/2 Inhibitor II	IC ₅₀ = 8 nM for MEK1/2.	STE
42	MK-2 Inhibitor III	IC ₅₀ = 8.5 nM for MK-2. IC ₅₀ = 81 nM for MK-5.	STE
43	ML-7, Hydrochloride	K _i = 300 nM for myosin light chain kinase.	CAMK
44	Necrostatin-1	IC ₅₀ = 494 nM	TKL
45	Olomoucine II	IC ₅₀ = 20 nM for Cdk1/B.	CMGC
46	p21-Activated Kinase Inhibitor III, IPA-3	IC ₅₀ = 2.5 μM for PAK 1.	STE
47	p38 MAP Kinase Inhibitor IV	IC ₅₀ = 130 nM for p38a MAPK.	STE
48	p38 MAP Kinase Inhibitor VI, JX401	IC ₅₀ = 32 nM for MAPK p38a.	STE
49	p38 MAP Kinase Inhibitor VII, SD-169	IC ₅₀ = 3.2 nM for p38a MAP kinase.	STE
50	p38 MAP Kinase Inhibitor VIII	IC ₅₀ = 40 nM for p38a.	STE
51	PIKfyve Inhibitor	IC ₅₀ = 33 nM for mammalian type III PtdInsP kinase.	Other
52	PIM1 Kinase Inhibitor II	IC ₅₀ = 50 nM for PIM1 kinase.	CAMK
53	PIM1 Kinase Inhibitor IV	K _i = 0.091 μM for PIM1 Kinase.	CAMK
54	PIM1/2 Kinase Inhibitor V	IC ₅₀ = 24 nM for PIM1. IC ₅₀ = 100 nM for PIM2.	CAMK
55	PIM1/2 Kinase Inhibitor VI	IC ₅₀ = 150 nM for PIM1. IC ₅₀ = 20 nM for PIM2.	CAMK
56	PI 3-Ka Inhibitor IV	IC ₅₀ = 2 nM for p110α. IC ₅₀ = 16 nM for p110β.	Other
57	PI 3-Ky/CKII Inhibitor	IC ₅₀ = 20 nM for PI3-Kg. IC ₅₀ = 20 nM for CKII.	Other, CMGC
58	PI 3-Kβ Inhibitor VI, TGX-221	IC ₅₀ = 0.005 μM for PI3-Kb. IC ₅₀ = 0.1 μM for PI3-Kd.	Other
59	PI 3-Ky Inhibitor VII	IC ₅₀ = 0.24 μM for PI3-Ka. IC ₅₀ = 1.45 μM for PI3-Kb.	Other
60	PI 3-Ka Inhibitor VIII	IC ₅₀ = 0.3 nM for p110α. IC ₅₀ = 40 nM for p110γ.	Other
61	Polo-like Kinase Inhibitor I	IC ₅₀ = 126 nM for polo-like kinase 1 (Plk1).	Other
62	Polo-like Kinase Inhibitor II, BTO-1	IC ₅₀ = 8 μM for polo-like kinase 1 (Plk1).	Other
63	UCN-01	IC ₅₀ = 29 nM for PKCα. IC ₅₀ = 34 nM for PKCβ.	AGC, CAMK, CMGC, TK
64	Quercetin	IC ₅₀ = 340 nM for PIM1 Kinase. IC ₅₀ = 3.45 μM for PIM2	CAMK
65	Ras/Rac Transformation Blocker, SCH 51344	N/A	Other
66	Reversine	IC ₅₀ = 8 nM for MEK1.	STE, Other
67	Rho Kinase Inhibitor	K _i = 1.6 nM for G-protein Rho-associated kinase.	AGC
68	Rho Kinase Inhibitor II	IC ₅₀ = 0.2 μM for Rho-associated protein kinase.	AGC
69	Rho Kinase Inhibitor V	IC ₅₀ = 1.5 nM for ROCK-II.	AGC
70	Roscovitine	IC ₅₀ = 650 nM for p34cdk1/cyclin B.	CMGC
71	Roscovitine, (S)-Isomer	IC ₅₀ = 800 nM for p34cdk1/Cyclin B kinase.	CMGC
72	Ro-31-8220	IC ₅₀ = 10 nM for protein kinase C.	AGC, CMGC
73	RSK Inhibitor, SL0101	IC ₅₀ = 89 nM for RSK	AGC
74	SB 203580, Sulfone	IC ₅₀ = 30 nM for p38 MAP kinase.	CMGC
75	SB 239063	IC ₅₀ = 44 nM for MAP kinase p38a. IC ₅₀ = 44 nM for p38b.	CMGC
76	Scytonemin, <i>Lyngbya</i> sp.	IC ₅₀ = 3.4 μM for PKCβ1. IC ₅₀ = 2.7 μM for PKCβ2.	AGC, CAMK, CMGC
77	Stem-Cell Factor/c-Kit Inhibitor, ISCK03	IC ₅₀ < 2.5 μM for blocking c-kit activity	TK
78	Ste11 MAPKKK Activation Inhibitor	IC ₅₀ = 250 nM for inhibiting Src	TK
79	Tpl2 Kinase Inhibitor II	IC ₅₀ = 160 nM for Tpl2.	STE
80	TX-1918	IC ₅₀ = 440 nM for eF2-K.	Atypical
81	WHI-P180, Hydrochloride	IC ₅₀ = 1 μM for Cdk2.	CMGC
82	Wee1/Chk1 Inhibitor	IC ₅₀ = 97 nM for Wee1. IC ₅₀ = 47 nM for Chk1.	Other, CAMK
83	Wee1 Inhibitor	IC ₅₀ = 11 nM for Wee1. IC ₅₀ = 440 nM for Chk1.	Other
84	Wee1 Inhibitor II	IC ₅₀ = 59 nM for Wee1.	Other
85	KN-62	K _i = 900nM for rat brain CAMK II	CAMK
86	KN-93	K _i = 370nM for CAMKII	CAMK

Supplementary Table 4: Concentration data after immune activation. Whole blood of different donors was treated with Zymosan, LPS/SEB/anti-CD28, Zymosan/anti-CD3/anti-CD28, anti-CD3/anti-CD28 or Poly I:C in a co-culture set up with differentiated Caco-2 monolayer. Caco-2 cells were removed after 5 h and the whole blood was further cultivated for 19 h. The whole blood of duplicate wells was pooled and the plasma was analyzed using multiplexed immunoassays. Depicted are the measured analyte concentrations in pg/ml. Values below the lower limit of quantification are replaced by the value of the LOQ and displayed in red. Values exceeding the upper limit of detection are assigned the value of the ULD and marked in blue.

Treatment	Donor ID	concentration [pg/ml]																			
		IL-1β	IL-6	INFγ	MCP-1	IL-8	IP10	TNFα	IL-4	IL-17A	TARC	IL-13	IL-5	IL-10	E-Sele.	Fas	gpi130	TNF-RI	TNF-RII	VCAM-1	ICAM-1
LPS/SEB/aCD28	118	1477	14941	2062	3754	5525	2458	15000	51	287	48	<474	16	807	1757	4263	26762	227	11826	37440	22039
	128	661	22078	880	5320	11280	1830	7738	70	1041	32	2647	73	7280	4929	2667	42894	209	4920	36127	44062
	119	3290	26558	4274	3075	9373	4071	13157	28	715	16	<474	6	6991	965	1282	23046	235	9293	26789	16380
	123	1144	34052	2316	5285	13130	7653	9390	36	165	108	<474	6	1550	3044	1135	26035	218	11395	21474	16750
	134	1375	13644	1969	12630	40214	2962	13637	50	461	65	544	11	1155	1987	6305	30852	349	19020	26288	22088
	120	1767	14927	5331	5195	12650	5279	15000	84	763	63	1605	99	1652	4219	10837	28578	355	16001	20455	65034
aCD3/aCD28	135	2228	30043	643	3089	6296	5346	2840	14	53	233	<474	3	233	4856	3220	13864	237	14788	41562	30478
	143	1542	21961	3510	3183	9244	5481	3797	53	744	62	<474	83	778	13188	14775	18217	548	32683	34467	19748
	124	841	17294	1855	5583	8827	2422	4880	<21.6	155	19	<474	404	1893	1795	18496	136	7755	26178	22399	
	129	1429	20335	488	7513	4091	3712	2778	26	144	42	755	7	839	6486	4832	33263	303	21549	44038	26969
	126	1224	12768	2410	2315	3336	13825	4923	33	164	26	1098	6	677	4552	5598	22731	230	12561	31521	17559
	134	31	61	253	1788	5625	3185	15000	116	45	145	871	41	513	784	1797	30622	192	6360	23519	18836
Zymosan	118	26	76	108	979	533	1261	1936	77	1334	111	744	40	492	1853	6964	13062	290	8968	34132	15422
	123	25	74	96	1308	1244	1948	3915	45	401	357	674	29	272	2427	5217	15366	177	6542	19628	14483
	143	5892	6894	<7.4	799	35284	43	9850	<21.6	<7	26	<474	<2.1	262	2427	5217	15366	177	6542	19628	14483
	119	3883	11305	25	2888	96078	16	14346	<21.6	<7	35	<474	<2.1	114	1162	6493	21997	329	11439	31738	28996
	118	1432	13981	<7.4	2487	45738	24	10558	<21.6	<7	27	<474	3	82	1359	2990	17155	316	9234	30701	24432
	128	4049	42725	3938	18104	400000	151	12682	197	4982	1622	11263	399	143	4753	6829	20907	647	36243	15023	28564
Zymosan/aCD3/aCD28	119	1764	13555	7978	12410	124370	335	15000	75	2279	1085	11666	215	168	973	4396	14903	318	16674	12227	15345
	118	681	20101	8111	19010	400000	264	12175	155	1402	907	15000	554	171	1296	2912	12257	555	23644	16825	17128
	134	7458	44234	7071	8601	400000	236	13732	52	1025	130	3948	67	98	1401	5371	17449	269	15120	16126	13159
	123	2083	67468	1642	30798	400000	249	15000	46	2932	176	3037	33	92	6946	5815	16667	314	21612	23046	13721
	120	<17.7	53	<7.4	1058	11	3992	56	<21.6	<7	16	<226	<2.1	<4.5	7132	9643	8696	574	3104	12972	29713
	128	<17.7	28	<7.4	1247	9	2148	52	<21.6	<7	16	<226	<2.1	<4.5	5281	2979	9087	204	1893	13938	16405
Poly I:C	134	<17.7	22	<7.4	2046	38	3934	107	<21.6	<7	16	<226	<2.1	<4.5	1098	1725	7378	580	1503	8225	6940
	135	<17.7	397	32	689	5	21776	101	<21.6	<7	25	<226	<2.1	<4.5	5953	4533	19663	465	11233	49752	49064
	143	<17.7	136	<7.4	1988	9	14112	<46.3	<21.6	<7	19	<226	<2.1	<4.5	18216	18932	19590	744	21649	38063	24700
	118	<17.7	<6	<7.4	121	6	13	<46.3	<21.6	<7	16	<226	<2.1	<4.5	1577	3957	24596	152	5422	37838	24463
	128	<17.7	<6	<7.4	25	8	15	<46.3	<21.6	<7	16	<226	<2.1	<4.5	4359	2289	38954	159	4358	26708	34212
	119	<17.7	<6	<7.4	<23.7	3	13	<46.3	<21.6	<7	16	<226	<2.1	<4.5	965	1345	25822	188	4317	25597	17031
untreated	123	<17.7	<6	<7.4	35	4	13	<46.3	<21.6	<7	16	<226	<2.1	<4.5	2681	1072	24381	151	3993	16595	13777
	134	<17.7	<6	<7.4	35	4	13	<46.3	<21.6	<7	16	<226	<2.1	<4.5	1427	5335	28254	202	5051	23542	16980
	120	<17.7	<6	<7.4	58	27	22	<46.3	<21.6	<7	16	<226	<2.1	<4.5	3839	9493	25861	241	5790	19188	59368
	135	<17.7	<6	<7.4	32	84	19	<46.3	<21.6	<7	20	<226	<2.1	<4.5	5052	3163	15858	180	6578	30842	35938
	143	<17.7	<6	<7.4	176	40	36	<46.3	<21.6	<7	20	<226	<2.1	<4.5	15345	16800	15389	520	15119	35776	18137
	124	<17.7	<6	<7.4	221	61	76	<46.3	<21.6	<7	16	<226	<2.1	<4.5	1771	1587	17510	79	2989	23000	17091
129	<17.7	<6	<7.4	35	12	13	<46.3	<21.6	<7	16	<226	<2.1	<4.5	7006	4591	35430	210	53445	33839	23962	
126	<17.7	<6	<7.4	66	11	104	<46.3	<21.6	<7	16	<226	<2.1	<4.5	7119	7904	28888	272	8872	43526	21614	

10. List of Publications

Schmohl, M., *et al.*, Protein-protein-interactions in a multiplexed, miniaturized format, a functional analysis of Rho GTPase activation and inhibition. *Proteomics*, 2010. 10(8): p. 1716-20.

Schmohl, M., Rimmele, S., *et al.*, Functional Analysis of Rho GTPase Activation and Inhibition in a Bead-Based Miniaturized Format. *Meth Mol Biol*, 2011. *Submitted*.

11. Akademische Lehrer

Prof. Dr. Bisswanger

Prof. Dr. Probst

Prof. Dr. Rammensee

Prof. Dr. Stehle

Dr. Sarrazin

Prof. Dr. Nordheim

Dr. Bayer

Prof. Dr. Schott

Prof. Dr. Bohley

Prof. Dr. Stevanović

Prof. Dr. Gauglitz

Prof. Dr. Dodt

Prof. Dr. Hambrecht

Prof. Dr. Schwarz

PD Dr. Just

Prof. Dr. Pawelek

Dr. Kalbacher

Prof. Dr. Vallera

Prof. Dr. Klein

Prof. Dr. Maier

Prof. Dr. Kohlbacher

Prof. Dr. Nagel

PD Dr. Maier

Prof. Dr. Wesemann

Prof. Dr. Nürnberger

Prof. Dr. Ziegler

Prof. Dr. Oberhammer

Prof. Dr. Feil

12. Curriculum Vitae

Personal Details

Name	Michael Schmohl
Date of birth	10/10/1979
Place of birth	Nürtingen
Nationality	German

Education/Qualification

Aug. 2010-Sept. 2010	Visiting fellow at the KTH Royal Institute of Technology, Stockholm, in the group of Dr. Jochen Schwenk, Dept. of Proteomics, EMBO Travel Grant Awardee
since Sept. 2008	Dissertation at the NMI-University of Tübingen, Dept. of Biochemistry. Thesis: Quantification of Immunemediators in an in vitro model of the human gut. Supervisors: Dr. T. Joos, Dr. N. Schneiderhan-Marra, Prof. Dr. S. Stevanovic
Nov. 2007- July 2008	Diplomathesis at the NMI-University of Tübingen, Dept. of Biochemistry. Thesis: Effects of Prenylderivatives on Rho-GTPase activity (grade: 1.0). Supervisors: Dr. T. Joos, Dr. N. Schneiderhan-Marra
Aug. 2006-Oct. 2006	Visiting Fellow at the University of Minnesota Cancer Center, in the group of Prof. D. Valleria Ph.D. Division of Radiation Oncology
Oct. 2003 – July 2008	Study of Biochemistry at the University of Tübingen, Dipl. Biochemiker
Oct. 2000 - Sept. 2003	Study of Industrial Management at the Berufsakademie Stuttgart. Diplom Betriebswirt (BA); Bachelor of Arts Open University of London, Thesis: Betriebliche Fehlzeiten
Sept. 1990-June 1999	Max Planck Gymnasium Nürtingen (Allgemeine Hochschulreife).